

# TFT CONSTRUCTION OF RCFT CORRELATORS V: PROOF OF MODULAR INVARIANCE AND FACTORISATION

JENS FJELSTAD, JÜRGEN FUCHS, INGO RUNKEL,  
AND CHRISTOPH SCHWEIGERT

ABSTRACT. The correlators of two-dimensional rational conformal field theories that are obtained in the TFT construction of [FRSI, FRSII, FRSIV] are shown to be invariant under the action of the relative modular group and to obey bulk and boundary factorisation constraints. We present results both for conformal field theories defined on oriented surfaces and for theories defined on unoriented surfaces. In the latter case, in particular the so-called cross cap constraint is included.

## Contents

1	Introduction	1
2	Consistency conditions for CFT correlators	6
3	Proof of modular invariance	20
4	Proof of boundary factorisation	29
5	Proof of bulk factorisation	39
A	Algebras in modular tensor categories	62
B	The assignment $X \mapsto C(X)$	68
C	Two-point correlators	75
D	Some properties of (bimodule) morphisms	82

## 1. Introduction

Quantum field theories have, deservedly, the reputation of being both mathematically rich and difficult to address at a conceptual level. This is, in fact, a major reason for the importance of “exactly solvable” models in quantum field theory. However, the notion of exact solvability needs some reflection: at a naive level, one might aim at computing “all” correlation functions – i.e. for all fields in the theory and on all spaces on which the theory makes sense – explicitly. It is not hard to see that this hope is unrealistic, even for a model apparently as simple as the two-dimensional massless free boson on an arbitrary conformal surface. (In this model one would need, for example, a rather detailed explicit knowledge of higher genus theta functions, and of the dependence of determinants on the moduli of the surface.)

A more realistic aim is to achieve the following:

---

2000 Mathematics Subject Classification: 81T40,18D10,18D35,81T45.

© Jens Fjelstad, Jürgen Fuchs, Ingo Runkel,  
and Christoph Schweigert, 2005. Permission to copy for private use granted.

- To establish the *existence* of a consistent collection of correlation functions, for all fields in the theory and all spaces on which the theory is supposed to make sense.
- To identify those features of correlation functions which at the same time are interesting and can be controlled.

Specifically, one should have at one's disposal sufficiently powerful mathematical tools to establish general properties of these characteristics, and one should be able to set up efficient algorithms for computing them explicitly in specific models.

These are the two goals for which the TFT approach to the correlators of (two-dimensional, euclidean) conformal field theory – the topic of the present series of papers – has been designed. The TFT approach makes it possible to formulate and reach these goals in a purely categorical setting. In particular, all relevant information on the problem is encoded in appropriate category theoretic structures, and thus algebro-geometric and functional-analytic issues that must be dealt with in other approaches to conformal field theory are taken into account by assumptions on these category theoretic structures. Among the interesting and controllable features that can be computed in this approach are in particular the coefficients of the correlation functions in an expansion in a chosen basis of conformal blocks.

Our approach to CFT correlators applies to all chiral conformal field theories for which the representation category of the underlying chiral algebra is a modular tensor category. The structure of a modular tensor category on the representation category arises from the properties of (half-)monodromies of conformal blocks on surfaces of genus zero and one. A modular tensor category, in turn, allows one to construct a three-dimensional topological field theory (TFT), which furnishes a tensor functor from a suitable cobordism category to a category of vector spaces (for some pertinent details about TFT, see appendix A.2). In particular, it provides (projective) representations of the mapping class groups for surfaces of higher genus. A central assumption in the TFT approach, which is known to be met in a large class of models, is that these representations are indeed the ones arising from the monodromies of conformal blocks on these surfaces.

Another essential ingredient in our construction is the principle of holomorphic factorisation: the correlator  $C(X)$  on a two-dimensional world sheet  $X$  is an element of the vector space  $\mathcal{H}(\widehat{X})$  that the TFT assigns to the double  $\widehat{X}$  of  $X$ :

$$C(X) \in \mathcal{H}(\widehat{X}).$$

(Here it should be kept in mind that the vector space  $\mathcal{H}(\widehat{X})$  is actually a space of multi-valued functions of the marked points and of the complex structure of  $\widehat{X}$ .) To this end, the surface  $\widehat{X}$  must come with enough structure so that it indeed constitutes an object in the cobordism category, i.e. an extended surface in the terminology of [Tu]. In the TFT approach, the structure of  $X$  that makes it into a valid world sheet encodes precisely the right amount of information such that its double  $\widehat{X}$  has a canonical structure of an extended surface.

Two different types of local two-dimensional conformal field theories are covered by the TFT approach:

- theories that are defined on oriented world sheets only (the surfaces are allowed to have non-empty boundary); and
- theories that are defined on world sheets without orientation (the surfaces are allowed to have non-empty boundary, and are not required to be orientable).

Apart from a modular tensor category  $\mathcal{C}$ , further input is required, and this additional input is different for the two types of theories. In the oriented case, a *symmetric special Frobenius algebra*  $A$  in  $\mathcal{C}$  contains sufficient information to construct all correlators [FRS0, FRSI]. Morita equivalent algebras yield the same correlators. For unoriented world sheets, as shown in [FRSII], in order to have enough input for constructing all correlators one must require that the algebra is even a *Jandl algebra*  $\tilde{A}$ . (The structure of a Jandl algebra generalises the notion of a complex algebra with involution; relevant information about algebras in monoidal categories is collected in appendix A.3.)

With regard to the two aims for understanding a quantum field theory formulated above, the objectives of the papers in this series are the following:

- In the papers [FRSI], [FRSII] and [FRSIV], crucial quantities of conformal quantum field theories – partition functions [FRSI, FRSII] and operator products [FRSIV] – were extracted and algorithms for computing them were presented.
- The purpose of the paper [FRSIII] was to establish a systematic procedure, based on abelian group cohomology, to obtain symmetric special Frobenius algebras, and to specialise results from [FRSI, FRSIV] to the conformal field theories that are obtained by this procedure.
- The aim of the present paper is to prove that the correlators obtained by our prescription satisfy the relevant consistency conditions, and thereby to establish the existence of a consistent set of correlators.

Let us describe the consistency conditions for correlators in some detail. First of all, correlators must obey the so-called chiral Ward identities. In the present approach, these are taken into account by the postulate that the correlation function on  $X$  is an element of the space  $\mathcal{H}(\hat{X})$  of conformal blocks on the double. (For the construction of such spaces of multivalued functions from a conformal vertex algebra, see e.g. [FB].)

There are, however, also two other requirements that must be imposed:

$$\textit{modular invariance} \quad \text{and} \quad \textit{factorisation}.$$

By the axioms of TFT, the space  $\mathcal{H}(\hat{X})$  of conformal blocks carries a projective representation of the mapping class group  $\text{Map}(\hat{X})$  of  $\hat{X}$  [Tu, chap. IV:5]. The double  $\hat{X}$  comes with an orientation reversing involution  $\tau$  such that  $X$  is the quotient of  $\hat{X}$  by the action of the group  $\langle \tau \rangle$  generated by  $\tau$ . The mapping class group  $\text{Map}(X)$  of  $X$  can be identified with the subgroup of  $\text{Map}(\hat{X})$  that commutes with  $\tau$ . The latter group – termed *relative modular group* in [BS] – acts genuinely on the vector space  $\mathcal{H}(\hat{X})$ . The requirement of

modular invariance is the postulate that  $C(X)$  should be invariant under the action of this group. (For the precise statements see section 2.1. Actually, modular invariance can be generalised to a covariance property of correlation functions, see the theorems 2.2 and 2.4.)

The modular invariance property not only implies that the torus partition function is modular invariant in the ordinary sense. It also implies that the correlator  $C(X)$  (a vector in the space  $\mathcal{H}(\widehat{X})$  of multivalued functions) is in fact a single-valued function, both of the insertion points and (up to the Weyl anomaly) of the conformal structure of  $X$ . This is indeed the motivation to impose this constraint.

As emphasised above, we distinguish between two different types of conformal field theories, depending on whether oriented or unoriented surfaces are considered. This difference, too, is relevant for the issue of modular invariance: in the oriented case, only orientation preserving maps from  $X$  to  $X$  are admitted, while for the unoriented theory this requirement is dropped. As a consequence, modular invariance for the oriented torus without field insertions is invariance of the torus partition function under the action of  $SL(2, \mathbb{Z})$ , whereas in the unoriented case, in addition the symmetry of the partition function under exchange of left- and right-movers is implied.

Up to now we have only discussed constraints that involve a single world sheet  $X$ . Factorisation constraints relate world sheets of different topology, and are thus more subtle and more powerful. There are two types of factorisation constraints, boundary factorisation (present when  $\partial X \neq \emptyset$ ) and bulk factorisation. We formulate boundary factorisation as follows: Consider an interval in  $X$  with end points on the boundary  $\partial X$ . Cut  $X$  along this interval, and glue to the two newly created boundary segments the chords of two semi-disks with one boundary field insertion each. This yields a new world sheet with two additional boundary insertions. Boundary factorisation relates the correlator for this new world sheet and (the inverse of) the two-point function on the disk to the correlator for the original world sheet. (For the precise statements, see section 2.7, in particular theorems 2.9 and 2.10.)

Bulk factorisation works in a similar manner. Consider a circle  $S^1$  embedded in  $X$  admitting an oriented neighbourhood. Cut  $X$  along this circle, and glue to the two newly created boundary circles the equators of two hemispheres with one bulk field insertion each. This yields a new world sheet with two additional bulk insertions. Bulk factorisation relates the correlator for this new world sheet and (the inverse of) the two-point function on the sphere to the correlator of the original world sheet. (For the precise statements, see section 2.11, in particular theorems 2.13 and 2.14.)

For unoriented world sheets  $X$ , it can happen that an embedded circle  $S^1 \subset X$  does not admit an oriented neighbourhood. Cutting along such a circle and gluing in a hemisphere produces a world sheet with just a single additional bulk field insertion. We deduce from the previous results that there is an identity relating the correlator for this new world sheet, (the inverse of) the two-point function on the sphere and the one-point function on the cross cap  $\mathbb{R}P^2$  to the correlator of the original world sheet. As a particular case, this implies the cross cap constraint studied in [FPS].

As an important consequence of the factorisation constraints, one can cut every world sheet into a few simple building blocks and reconstruct the correlators from a few fundamental correlators on these particular surfaces. This explains on the one hand the importance of the correlators considered in [FRSIV], and on the other hand it proves that they indeed solve the sewing constraints that were formulated in [S1, S2, CL, Le].

Factorisation constraints can be motivated by a Hamiltonian formulation of the theory: locally around the circle or interval along which  $X$  is cut, the world sheet looks like  $S^1 \times (-\epsilon, \epsilon)$  and as  $[-1, 1] \times (-\epsilon, \epsilon)$ , respectively. In a Hamiltonian description, one would like to associate dual topological vector spaces  $\mathcal{H}_{\text{bulk}}^\pm$  to circles  $S^1$  with opposite orientations, and  $\mathcal{H}_{\text{bnd}}^\pm$  to intervals  $[-1, 1]$  with opposite orientations. Very much like when defining a path integral for a particle using a Wiener measure, one should then be allowed to insert a complete system of states at a fixed “time”  $t \in (-\epsilon, \epsilon)$  and sum over it, without changing the result.

Summing over intermediate states is closely related to the concept of an operator product expansion: Suppose that two insertions, say in the bulk of  $X$ , are close. Then they can be encircled by an  $S^1$  along which we apply bulk factorisation. This way, the situation is related to a world sheet with one insertion less and to the three-point correlator on the sphere, which determines the OPE coefficients. This statement can be regarded as the best possible counterpart in the TFT approach of the fact that the OPE controls the short distance behaviour in all situations.

This paper is organised as follows. Section 2 contains precise statements of our main results: invariance under the mapping class group, and bulk and boundary factorisation. In sections 3–5 detailed proofs of these three types of consistency conditions are presented, both for oriented and for unoriented world sheets. In appendix A some basic information about modular tensor categories, about algebras in monoidal categories, and about topological field theory is recalled. Appendix B is devoted to the definition of the vector  $C(X) \in \mathcal{H}(\widehat{X})$  assigned to the correlator for a world sheet  $X$ , using suitable cobordisms from  $\emptyset$  to  $\widehat{X}$ . Non-degeneracy of the two-point correlators on a disk and on a sphere enters crucially in the formulation of boundary and bulk factorisation, respectively; it is established in appendix C. Finally, appendix D provides a few specific properties of certain morphisms which are employed in the proofs.

When referring to [FRSI, FRSII, FRSIII, FRSIV], we use the numbering of sections, theorems, equations etc. as in those papers, preceded by a prefix “I:” for [FRSI], “II:” for [FRSII], etc.; thus e.g. “lemma IV:2.2” refers to lemma 2.2 in [FRSIV], while (II:2.26) stands for equation (2.26) in [FRSII].

**Acknowledgements.** We are indebted to N. Potylitsina-Kube for her skillful help with the illustrations. J.Fu. is supported by VR under project no. 621–2003–2385, and C.S. is supported by the DFG project SCHW 1162/1-1.

## 2. Consistency conditions for CFT correlators

Let us select once and for all a modular tensor category  $\mathcal{C}$  as well as the following data:

- a symmetric special Frobenius algebra  $A$  in  $\mathcal{C}$ ;
- a symmetric special Frobenius algebra with reversion (a Jandl algebra)  $\tilde{A}$  in  $\mathcal{C}$ .

An explanation of these terms can e.g. be found in definitions I:3.3, I:3.4 and II:2.1; for convenience, we repeat these definitions in appendix A. Also note that, by omitting the reversion, every Jandl algebra provides us with a symmetric special Frobenius algebra, but not every symmetric special Frobenius algebra admits a reversion.

The structure of a symmetric special Frobenius algebra is needed to study correlators on oriented world sheets, while the structure of a Jandl algebra is needed to investigate correlators on unoriented world sheets. More specifically, the TFT construction of correlation functions that was proposed in [FRS0] and developed in [FRSI, FRSII, FRSIV] provides us with assignments

$$C_A : X \mapsto C_A(X) \quad \text{and} \quad C_{\tilde{A}} : \tilde{X} \mapsto C_{\tilde{A}}(\tilde{X}) \quad (2.1)$$

which take an oriented world sheet  $X$  to a vector  $C_A(X) \in \mathcal{H}(\widehat{X})$  in the space of blocks on the double  $\widehat{X}$  of  $X$ , and an unoriented world sheet  $\tilde{X}$  to a vector  $C_{\tilde{A}}(\tilde{X}) \in \mathcal{H}(\widehat{\tilde{X}})$ . The precise definition of oriented and unoriented world sheets that is to be used here, as well as the notion of the double of a world sheet, is recalled in appendix B.1. The assignments (2.1) are summarised in appendix B.3. When we want to describe ‘one and the same conformal field theory’ both on oriented and on unoriented world sheets, then the relevant symmetric special Frobenius algebra  $A$  is the one obtained from the Jandl algebra  $\tilde{A}$  by forgetting the reversion, so that if an unoriented world sheet  $\tilde{X}$  is obtained from an oriented world sheet  $X$  by forgetting the orientation, then  $C_{\tilde{A}}(\tilde{X}) = C_A(X)$ .

In the present section we formulate the assertions that the systems of correlators  $C_A$  and  $C_{\tilde{A}}$  are invariant under the action of the mapping class groups and that they are consistent with factorisation. The proofs of these claims are presented in sections 3–5.

To be precise, we consider here correlators with any number of bulk and boundary field insertions, and with arbitrary boundary conditions preserving the underlying chiral symmetry. On the other hand, the formalism of [FRSI, FRSII, FRSIII, FRSIV] allows in addition for the treatment of conformal defects and defect fields. While the proofs given here are for correlators without such defects, our methods allow one to establish the consistency of correlators in the presence of defects as well, albeit various aspects of the consistency conditions and their proofs become a lot more involved. In particular, one must introduce defect fields (in the bulk and on the boundary) from which an arbitrary number of defect lines is emanating – see the discussion at the beginning of section IV:3.4, and in particular figure (IV:3.31) – and introduce bases for these fields, as well as compute their two-point functions.

The tensor unit  $\mathbf{1}$  in any modular tensor category  $\mathcal{C}$  is a Jandl algebra (and thus in particular a symmetric special Frobenius algebra). The CFT obtained from  $A = \mathbf{1}$ , or from  $\tilde{A} = \mathbf{1}$ , has as its torus partition function the charge conjugation modular invariant. This

CFT is often referred to as the ‘Cardy case’. In the Cardy case, the TFT formulation of correlators was accomplished in [FFFS1, FFFS2], where also consistency with factorisation and the action of the mapping class group was established. The corresponding statements and proofs for the general case given in the present paper simplify considerably when setting  $A = \mathbf{1}$  (respectively,  $\tilde{A} = \mathbf{1}$ ), and then indeed reduce to those given in [FFFS1, FFFS2].

### 2.1. INVARIANCE UNDER THE MAPPING CLASS GROUP.

We will now formulate the statements concerning covariance properties of correlators, and in particular invariance under the action of the mapping class group of the world sheet.

Let  $E$  and  $E'$  be extended surfaces (for the notion of an extended surface, see appendix B.1). To an isomorphism  $f: E \rightarrow E'$  of extended surfaces,<sup>1</sup> we associate a cobordism  $M_f$  from  $E$  to  $E'$  as

$$M_f := \left( E \times [-1, 0] \sqcup E' \times [0, 1] \right) / \sim, \quad (2.2)$$

where ‘ $\sim$ ’ is an equivalence relation that relates boundary points in the two components  $E_{<} := E \times [-1, 0]$  and  $E_{>} := E' \times [0, 1]$  of the disjoint union  $E_{<} \sqcup E_{>}$ . Denoting points in  $E_{<}$  and  $E_{>}$  by  $(p, t)_{<}$  and  $(p, t)_{>}$ , respectively, the equivalence relation is given by

$$(p, 0)_{<} \sim (f(p), 0)_{>}. \quad (2.3)$$

We abbreviate the homomorphism that the TFT assigns to the cobordism by  $f_{\sharp}$ ,

$$f_{\sharp} := Z(M_f, E, E') : \mathcal{H}(E) \rightarrow \mathcal{H}(E'). \quad (2.4)$$

For  $E = E'$ , the assignment

$$[f] \mapsto f_{\sharp} \quad (2.5)$$

furnishes a projective action of the mapping class group  $\text{Map}_{\text{or}}(E)$  on  $\mathcal{H}(E)$  (see e.g. chapter IV.5 of [Tu]).

Let now  $X$  and  $Y$  be unoriented world sheets and  $[f] \in \text{Map}(X, Y)$ , i.e.  $[f]$  is a homotopy class of homeomorphisms  $f: X \rightarrow Y$  that map each marked arc of  $X$  to an arc of  $Y$  with the same marking, and map each boundary segment of  $X$  to a boundary segment of  $Y$  with the same boundary condition. Denote by  $\pi_X$  the canonical projection from  $\hat{X}$  to  $X$ , and by  $\pi_Y$  the one from  $\hat{Y}$  to  $Y$ . The homeomorphism  $f$  has a unique lift  $\hat{f}: \hat{X} \rightarrow \hat{Y}$  such that  $\hat{f}$  is an orientation preserving homeomorphism and  $\pi_Y \circ \hat{f} = f \circ \pi_X$ .

For oriented world sheets, invariance of the correlators under the action of the mapping class group is then formulated as follows.

**2.2. THEOREM.** *Covariance of oriented correlators: For any two oriented world sheets  $X$  and  $Y$ , and any orientation preserving  $[f] \in \text{Map}(X, Y)$  we have*

$$C_A(Y) = \hat{f}_{\sharp}(C_A(X)). \quad (2.6)$$

---

<sup>1</sup> An isomorphism  $f: E \rightarrow E'$  of extended surfaces is an orientation preserving homeomorphism  $f$  such that for the respective Lagrangian subspaces we have  $f_*(\lambda_E) = \lambda_{E'}$ , and such that each marked point  $(p, [\gamma], U, \varepsilon)$  of  $E$  gets mapped to a marked point  $(f(p), [f \circ \gamma], U, \varepsilon)$  of  $E'$ .

2.3. COROLLARY. Modular invariance of oriented correlators: *For any oriented world sheet  $X$  and any  $[f] \in \text{Map}_{\text{or}}(X)$  we have*

$$C_A(X) = \hat{f}_{\#}(C_A(X)). \quad (2.7)$$

For unoriented world sheets, the corresponding statements are:

2.4. THEOREM. Covariance of unoriented correlators: *For any two unoriented world sheets  $X$  and  $Y$ , and any  $[f] \in \text{Map}(X, Y)$ , we have*

$$C_{\tilde{A}}(Y) = \hat{f}_{\#}(C_{\tilde{A}}(X)). \quad (2.8)$$

2.5. COROLLARY. Modular invariance of unoriented correlators: *For any unoriented world sheet  $X$  and any  $[f] \in \text{Map}(X)$  we have*

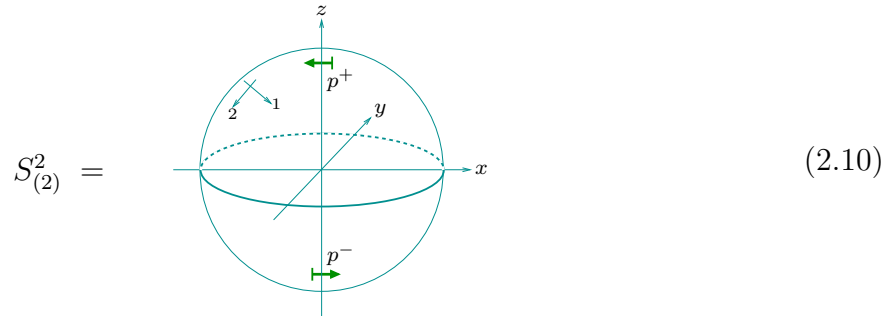
$$C_{\tilde{A}}(X) = \hat{f}_{\#}(C_{\tilde{A}}(X)). \quad (2.9)$$

For the partition function (i.e., zero-point correlator)  $C_A(\mathbb{T}; \emptyset)$  on an oriented torus, the assertion of corollary 2.3 is just what is usually referred to as modular invariance of the torus partition function. When the torus is unoriented, then this is replaced by corollary 2.5 for  $C_{\tilde{A}}(\mathbb{T}; \emptyset)$ ; the fact that  $\tilde{A}$  is a Jandl algebra implies that the torus partition function is symmetric, compare remark II:2.5(i).

## 2.6. CUTTING AND GLUING OF EXTENDED SURFACES.

To discuss the factorisation properties of correlators, we must first analyse the corresponding cutting and gluing procedures at the chiral level, i.e. for extended surfaces.

Let  $S^2$  be the unit sphere embedded in  $\mathbb{R}^3$  with Cartesian coordinates  $(x, y, z)$ , oriented by the inward pointing normal. Denote by  $S^2_{(2)}$  the unit sphere  $S^2$  with two embedded arc germs  $[\gamma^{\pm}]$  that are centered at the points  $p^+ = (0, 0, 1)$  and  $p^- = (0, 0, -1)$ , with arcs given by  $\gamma^+(t) = (-\sin t, 0, \cos t)$  and  $\gamma^-(t) = -\gamma^+(t)$ . Pictorially,



Further, let

$$A_\varepsilon := \{(x, y, z) \in S^2 \mid |z| < \varepsilon\} \quad (2.11)$$

be an open annulus around the equator, and understand by  $S^1 \subset A_\varepsilon$  the unit circle in the  $x$ - $y$ -plane. Given an extended surface  $E$ , a continuous orientation preserving embedding  $f: A_\varepsilon \rightarrow E$  and an object  $U \in \text{Obj}(\mathcal{C})$ , we will define another extended surface, to be

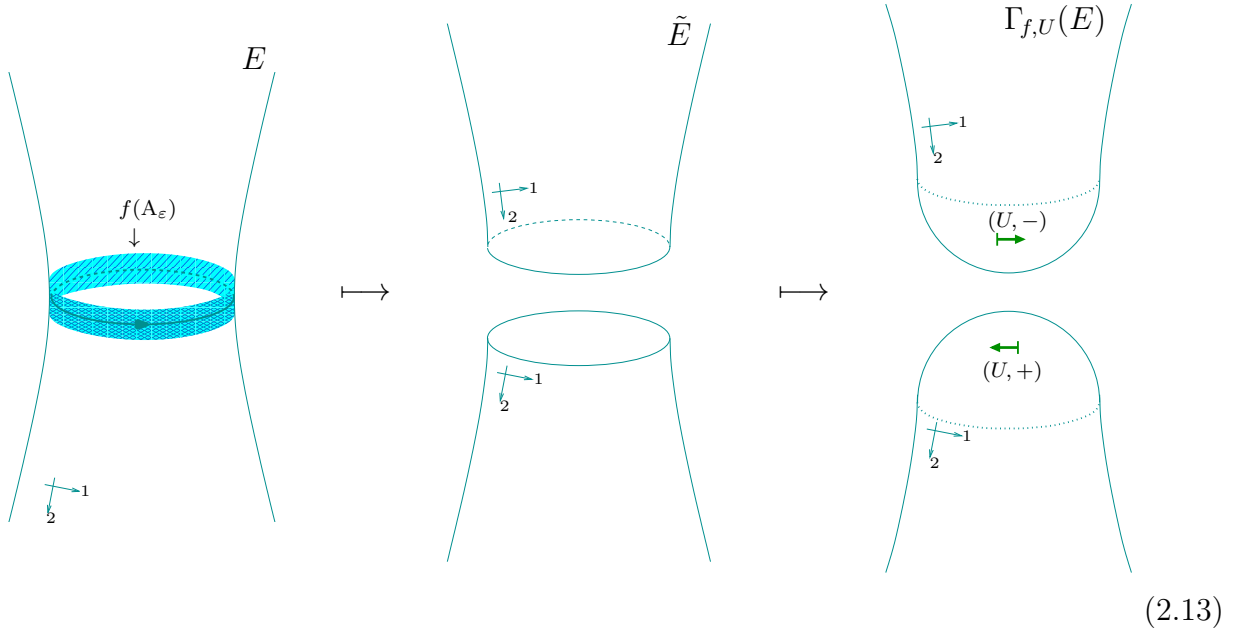


denoted by  $\Gamma_{f,U}(E)$ . In brief,  $\Gamma_{f,U}(E)$  is obtained by cutting  $E$  along  $f(S^1)$  and then closing the resulting holes by gluing two half-spheres with marked points  $(U, +)$  and  $(U, -)$ , respectively. In the case of unoriented world sheets, an additional datum is necessary, namely a prescription to which part of the cut surface the upper and lower hemispheres are to be glued. The procedure of first embedding the ‘collar’  $A_\varepsilon$  and then cutting along the circle  $f(S^1) \subset f(A_\varepsilon)$  provides a natural choice of this additional datum.

In more detail,  $\Gamma_{f,U}(E)$  is constructed as follows. For  $U \in \mathcal{Obj}(\mathcal{C})$ , let  $P_U$  be the extended surface given by  $S^2_{(2)}$  with the arc germ  $[\gamma^+]$  marked by  $(U, +)$  and  $[\gamma^-]$  marked by  $(U, -)$ . We denote by  $P_{U,\varepsilon}^+$  and  $P_{U,\varepsilon}^-$  the two hemispheres of  $P_U$  consisting of those points of  $P_U$  for which  $z \geq -\varepsilon$  and  $z \leq \varepsilon$ , respectively, so that  $A_\varepsilon = P_{U,\varepsilon}^+ \cap P_{U,\varepsilon}^-$ . Also, let  $\tilde{E} := E \setminus f(S^1)$ ; then we set

$$\Gamma_{f,U}(E) := (\tilde{E} \sqcup P_{U,\varepsilon}^+ \sqcup P_{U,\varepsilon}^-) / \sim, \quad (2.12)$$

where the lower hemisphere  $P_{U,\varepsilon}^-$  is joined to  $\tilde{E}$  via  $f(q) \sim q$  for  $q \in \{(x, y, z) \in P_{U,\varepsilon}^- \mid z > 0\}$ , while the upper hemisphere  $P_{U,\varepsilon}^+$  is joined via  $f(q) \sim q$  for  $q \in \{(x, y, z) \in P_{U,\varepsilon}^+ \mid z < 0\}$ . This procedure is illustrated in the following figure:



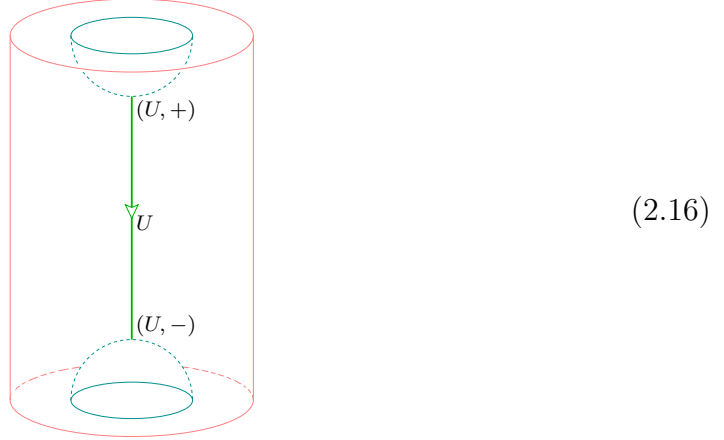
To turn the two-manifold  $\Gamma_{f,U}(E)$  into an extended surface we must also specify a Lagrangian subspace  $\lambda \subset H_1(\Gamma_{f,U}(E), \mathbb{R})$ . To this end we employ the cobordism  $M_{f,U}(E): \Gamma_{f,U}(E) \rightarrow E$  that is obtained by taking the cylinder over  $\Gamma_{f,U}(E)$  and identifying points on its boundary:

$$M_{f,U}(E) = (\Gamma_{f,U}(E) \times [0, 1]) / \sim. \quad (2.14)$$

The equivalence relation is given by

$$(\iota^+(p), 1) \sim (\iota^-(\tau(p)), 1) \quad \text{for } p \in \{(x, y, z) \in S^2 \mid z \geq 0\}, \quad (2.15)$$

where  $\tau: S^2 \rightarrow S^2$  is the involutive map  $\tau(x, y, z) := (x, y, -z)$ , while  $\iota^\pm: P_{U,\varepsilon}^\pm \rightarrow \Gamma_{f,U}(E)$  are the natural embeddings implied by the construction of  $\Gamma_{f,U}(E)$ . Close to the images of  $P_{U,\varepsilon}^-$  and  $P_{U,\varepsilon}^+$ , the manifold  $M_{f,U}(E)$  looks as follows<sup>2</sup>



Here the inner boundary components (which are connected by the  $U$ -ribbon) are part of  $\Gamma_{f,U}(E) \times \{0\}$ , while the outer boundary is part of  $\{[p, 1] \in \partial M_{f,U}(E)\} \cong E$ . Given the cobordism  $M_{f,U}(E): \Gamma_{f,U}(E) \rightarrow E$  we obtain the Lagrangian subspace  $\lambda$  of the extended surface  $\Gamma_{f,U}(E)$  from the Lagrangian subspace  $\lambda_E$  of  $E$  as  $\lambda := M_{f,U}(E)^* \lambda_E$ , i.e. as the set of those cycles  $x$  in  $\Gamma_{f,U}(E)$  for which there exists an  $x' \in \lambda(E)$  such that  $x - x'$  is homologous to zero in the three-manifold  $M_{f,U}(E)$ ; as shown in section IV.4.2 of [Tu], this yields indeed a Lagrangian subspace of  $H_1(\Gamma_{f,U}(E), \mathbb{R})$ .

The TFT assigns to  $M_{f,U}(E)$  a linear map

$$g_{f,U}(E) := Z(M_{f,U}(E), \Gamma_{f,U}(E), E) : \mathcal{H}(\Gamma_{f,U}(E)) \rightarrow \mathcal{H}(E). \quad (2.17)$$

Morphisms obtained from gluing constructions similar to the above will be referred to as *gluing homomorphisms*.

For the description of cutting and gluing world sheets further on, it is helpful to iterate the above procedure, thus giving rise to an operation of *cutting twice*, and to restrict one's attention to simple objects  $U$ . This is done as follows. Given an extended surface  $E$ , a map  $f: A_\varepsilon \rightarrow E$ , and a label  $k \in \mathcal{I}$  of a simple object of  $\mathcal{C}$ , let  $\tilde{f}: A_\varepsilon \rightarrow \Gamma_{f,U_k}(E)$  be the map  $\tilde{f}(x, y, z) := \iota^-(-x, y, -z)$ .

Then we define a new extended surface  $\hat{\Gamma}_{f,k}(E)$  as

$$\hat{\Gamma}_{f,k}(E) := \Gamma_{\tilde{f},U_k}(\Gamma_{f,U_k}(E)). \quad (2.18)$$

<sup>2</sup> That  $(U, \pm)$  occur at opposite places in (2.13) and (2.16) is due to the fact that it is  $-\Gamma_{f,U}(E)$  rather than  $\Gamma_{f,U}(E)$  that appears in  $\partial M_{f,U}(E) = E \sqcup (-\Gamma_{f,U}(E))$ .

In pictures we have

(2.19)

Analogously as for  $\Gamma_{f,U}(E)$  we define a cobordism  $\hat{M}_{f,k}: \hat{\Gamma}_{f,k}(E) \rightarrow E$  by composing the cobordism  $M_{\tilde{f},U_{\bar{k}}}: \hat{\Gamma}_{f,k}(E) \rightarrow \Gamma_{f,U_k}(E)$  with  $M_{f,U_k}: \Gamma_{f,U_k}(E) \rightarrow E$ . The part of the cobordism  $\hat{M}_{f,k}$  that is analogous to (2.16) looks as

(2.20)

We also set

$$\hat{g}_{f,k}(E) := Z(\hat{M}_{f,k}(E), \hat{\Gamma}_{f,k}(E), E) : \mathcal{H}(\hat{\Gamma}_{f,k}(E)) \rightarrow \mathcal{H}(E). \quad (2.21)$$

This linear map is another example of a gluing homomorphism.

This finishes our discussion of cutting and gluing operations at the chiral level.

## 2.7. BOUNDARY FACTORISATION.

TWO-POINT FUNCTION ON THE DISK. Denote by  $D \equiv D(M_l, M_r, k, \psi^+, \psi^-)$  the world sheet for the standard two-point function on the unit disk, i.e. (see definition B.2 for the conventions regarding the world sheet and boundary labels)

$$D(M_l, M_r, k, \psi^+, \psi^-) = \text{img} \quad (2.22)$$

Here the boundary and bulk are oriented as indicated, the boundary condition is  $M_l$  and  $M_r$  for  $x < 0$  and  $x > 0$ , respectively, and  $k \in \mathcal{I}$  is the label of a simple object. The two field insertions are

$$\begin{aligned} \Psi^+ &= (M_l, M_r, U_k, \psi^+, p^+, [\gamma^+]) \quad \text{and} \\ \Psi^- &= (M_r, M_l, U_{\bar{k}}, \psi^-, p^-, [\gamma^-]), \end{aligned} \quad (2.23)$$

respectively, where  $p^+ = (0, 1)$  and the arc germ  $[\gamma^+]$  is given by  $\gamma^+(t) = (-\sin t, \cos t)$ , while  $p^- = -p^+$  and  $\gamma^-(t) = -\gamma^+(t)$ . Accordingly, the morphisms  $\psi^\pm$  are elements of the spaces  $\text{Hom}_A(M_l \otimes U_k, M_r)$  and  $\text{Hom}_A(M_r \otimes U_{\bar{k}}, M_l)$ , respectively.

The double  $\hat{D}$  of  $D$  can be identified with  $S^2_{(2)}$ , where  $[\gamma^+]$  is now marked by  $(U_k, +)$  and  $[\gamma^-]$  by  $(U_{\bar{k}}, +)$ . The corresponding space  $\mathcal{H}(\hat{D})$  of conformal blocks is one-dimensional; a basis is given by applying  $Z$  to the cobordism  $B_{k\bar{k}}^+ : \emptyset \rightarrow \hat{D}$  that is given by

$$B_{k\bar{k}}^+ := \text{img} \quad (2.24)$$

(with the black side of the ribbons facing the reader). The morphism  $\lambda_{k\bar{k}} \in \text{Hom}(U_k \otimes U_{\bar{k}}, \mathbf{1})$  is the non-zero morphism introduced in (I:2.29), where it was denoted by  $\lambda_{(k, \bar{k}), 0}$  instead. For the morphism dual to  $\lambda_{i\bar{i}}$ , which was denoted by  $\Upsilon^{(i, \bar{i}), 0}$  in [FRSI], we use here an abbreviated notation, too, namely  $\bar{\lambda}^{i\bar{i}}$ . Also, in the sequel, when drawing pictures in

blackboard framing (using lines in place of ribbons), these morphisms will be represented graphically as

$$\begin{aligned}
\lambda_{i\bar{i}} &= \begin{array}{c} \text{---} \\ | \\ \text{---} \\ | \\ U_i \quad U_{\bar{i}} \\ | \\ \text{---} \\ | \\ \text{---} \\ | \\ U_i \quad U_{\bar{i}} \\ | \\ \text{---} \\ | \\ \text{---} \\ | \\ \text{---} \end{array} \\
\bar{\lambda}^{i\bar{i}} &= \begin{array}{c} \text{---} \\ | \\ \text{---} \\ | \\ U_i \quad U_{\bar{i}} \\ | \\ \text{---} \\ | \\ \text{---} \\ | \\ \text{---} \end{array}
\end{aligned} \tag{2.25}$$

The normalisation of  $\lambda_{k\bar{k}}$ , and hence the choice of basis (2.24), is arbitrary, but will be kept fixed throughout the paper.

In the chosen basis the structure constant  $c^{\text{bnd}} \in \mathbb{C}$  of the two-point function on the disk is defined by

$$C(D(M_l, M_r, k, \psi^+, \psi^-)) =: c_{M_l, M_r, k; \psi^+, \psi^-}^{\text{bnd}} B_{k\bar{k}}^+. \tag{2.26}$$

Here  $C$  stands for either  $C_A$  or  $C_{\bar{A}}$ . In the first case,  $D$  is understood as an oriented world sheet, in the latter case as an unoriented world sheet, i.e. the 2-orientation of the disk is omitted. Given bases  $\{\psi_\alpha^+\}$  of  $\text{Hom}_A(M_l \otimes U_k, M_r)$  and  $\{\psi_\beta^-\}$  of  $\text{Hom}_A(M_r \otimes U_{\bar{k}}, M_l)$ , we define a complex-valued matrix  $c_{M_l, M_r, k}^{\text{bnd}}$  by

$$(c_{M_l, M_r, k}^{\text{bnd}})_{\alpha\beta} := c_{M_l, M_r, k; \psi_\alpha^+, \psi_\beta^-}^{\text{bnd}}. \tag{2.27}$$

It is shown in appendix C.1 that the boundary two-point function is non-degenerate, in the sense that the matrix  $c_{M_l, M_r, k}^{\text{bnd}}$  is invertible for fixed  $M_l$ ,  $M_r$  and  $k$ .

CUTTING WORLD SHEETS ALONG AN INTERVAL. In the sequel we use several subsets of  $D$ , in particular the strip

$$R_\varepsilon := \{(x, y) \in D \mid |y| < \varepsilon\}, \tag{2.28}$$

as well as

$$\begin{aligned}
D_\varepsilon^+ &:= \{(x, y) \in D \mid y > -\varepsilon\} \quad \text{and} \\
D_\varepsilon^- &:= \{(x, y) \in D \mid y < \varepsilon\},
\end{aligned} \tag{2.29}$$

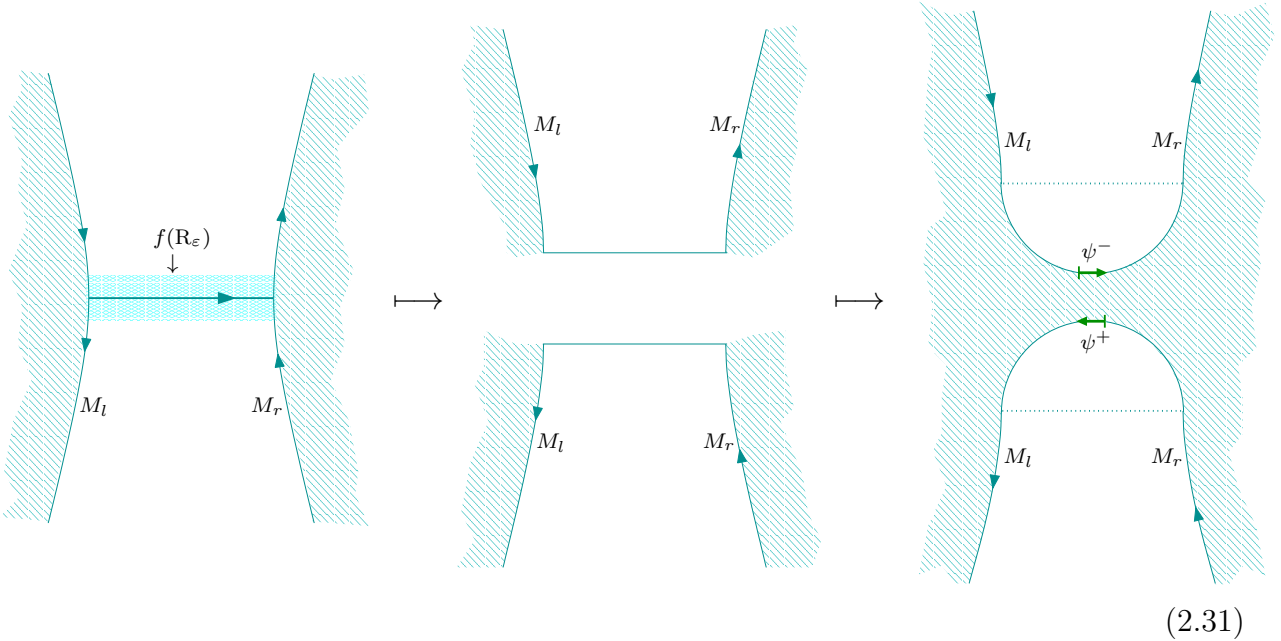
such that  $R_\varepsilon = D_\varepsilon^+ \cap D_\varepsilon^-$ . The boundary of  $R_\varepsilon$  satisfies  $\partial R_\varepsilon \cap R_\varepsilon = R_\varepsilon \cap \partial D$ . Let  $X$  be a world sheet (oriented or unoriented) with non-empty boundary. Suppose we are given a continuous injection  $f: R_\varepsilon \rightarrow X$  such that  $f(\partial R_\varepsilon \cap R_\varepsilon) \subset \partial X$ , and such that its restriction  $f: \partial R_\varepsilon \cap R_\varepsilon \rightarrow \partial X$  is orientation preserving, and  $f(1, 0)$  lies on a boundary segment of  $X$  labelled by  $M_r$ , while  $f(-1, 0)$  lies on a (not necessarily different) boundary segment labelled by  $M_l$ . We define a new world sheet  $\Gamma_{f, k, \psi^+, \psi^-}^{\text{bnd}}(X)$ , which is obtained from  $X$

by cutting along the image of  $[-1, 1] \times \{0\}$  under  $f$  and gluing half disks with boundary insertions  $\psi^+$ ,  $\psi^-$  to the cuts. This procedure is used to formulate the boundary factorisation of correlators in theorems 2.9 and 2.10.

In more detail, to obtain  $\Gamma_{f,k,\psi^+,\psi^-}^{\text{bnd}}(X)$  we start from  $\tilde{X} = X \setminus f([-1, 1] \times \{0\})$  and define

$$\Gamma_{f,k,\psi^+,\psi^-}^{\text{bnd}}(X) := \left( \tilde{X} \sqcup D_\varepsilon^+ \sqcup D_\varepsilon^- \right) / \sim, \quad (2.30)$$

where the lower half disk gets joined to  $\tilde{X}$  via  $f(p) \sim p$  for  $p \in \{(x, y) \in D_\varepsilon^- \mid y > 0\}$ , while the upper half disk gets joined via  $f(p) \sim p$  for  $p \in \{(x, y) \in D_\varepsilon^+ \mid y < 0\}$ . This procedure is illustrated in the following figure:



(2.31)

If  $X$  is an oriented world sheet then so is  $\Gamma_{f,k,\psi^+,\psi^-}^{\text{bnd}}(X)$ . If  $X$  is an unoriented world sheet, then so is  $\Gamma_{f,k,\psi^+,\psi^-}^{\text{bnd}}(X)$ .

**2.8. REMARK.** Note that  $R_\varepsilon$  has two boundary components, both of which are oriented by the inward pointing normal, i.e. the orientation of  $\partial R_\varepsilon \cap R_\varepsilon = R_\varepsilon \cap \partial D$  is inherited from  $\partial D$ .

To show that a system of correlators is consistent with boundary factorisation we have to prove a factorisation rule for every way to cut a world sheet  $X$  along a non-selfintersecting curve  $\gamma$  connecting two points on the boundary  $\partial X$ . For oriented world sheets, this cutting procedure is directly implemented by the construction of  $\Gamma_{f,k,\psi^+,\psi^-}^{\text{bnd}}(X)$  just described, because for any  $\gamma$  we can find an orientation preserving embedding  $f$  of  $R_\varepsilon$  into  $X$  such that the image of  $[-1, 1] \times \{0\}$  is  $\gamma$ . Since  $\partial X$  and  $\partial R_\varepsilon$  are oriented by the inward pointing normals,  $f$  is automatically consistent with the boundary orientation.

In the unoriented case, on the other hand, one can still find an embedding  $f$  of  $R_\varepsilon$  into  $X$  such that  $f([-1, 1] \times \{0\})$  is equal to  $\gamma$ , but now  $f$  need not preserve the boundary orientation. However, we are free to choose an equivalent labelling of boundary conditions

with possibly different orientation of  $\partial X$  (see appendix B.4), and we can use this freedom to ensure that  $f$  is orientation preserving on the left boundary component (the one with negative  $x$ -values) of  $R_\varepsilon$ . Afterwards, instead of  $R_\varepsilon$  we consider  $R'_\varepsilon$ , defined to be equal to  $R_\varepsilon$  except that the orientation of the right boundary component of  $R'_\varepsilon$  is reversed as compared to  $R_\varepsilon$ . Given an embedding  $f: R'_\varepsilon \rightarrow X$  preserving the boundary orientation, we can again construct a new world sheet  $\Gamma_{f,k,\psi^+,\psi^-}^{\text{bnd}}(X)$  obtained by cutting  $X$  along  $f([-1,1] \times \{0\})$  and gluing half disks. However, owing to our labelling conventions for boundary conditions, the details of the construction of  $\Gamma_{f,k,\psi^+,\psi^-}^{\text{bnd}}(X)$  are slightly more involved than in the situation described above; the details are given in section 4.5 below.

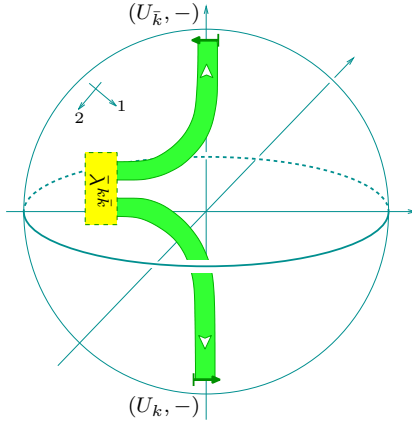
GLUING HOMOMORPHISM BETWEEN SPACES OF BLOCKS. We abbreviate

$$X'_k := \Gamma_{f,k,\psi^+,\psi^-}^{\text{bnd}}(X). \quad (2.32)$$

To compare the correlators for the world sheets  $X'_k$  and  $X$ , we need to construct a map between the spaces of blocks on their doubles. This is again provided by an appropriate gluing homomorphism

$$G_{f,k}^{\text{bnd}}: \mathcal{H}(\widehat{X}'_k) \rightarrow \mathcal{H}(\widehat{X}), \quad (2.33)$$

which we proceed to define. Let the extended surface  $H_{\bar{k}k}^-$  be given by  $S_{(2)}^2$  with  $[\gamma^+]$  marked by  $(U_{\bar{k}}, -)$  and  $[\gamma^-]$  marked by  $(U_k, -)$ . Consider the cobordism  $B_{\bar{k}k}^-: \emptyset \rightarrow H_{\bar{k}k}^-$  given by



$$B_{\bar{k}k}^- := \quad (2.34)$$

where  $\bar{\lambda}^{k\bar{k}} \in \text{Hom}(\mathbf{1}, U_k \otimes U_{\bar{k}})$  is the morphism introduced in figure (2.25).

Given  $f: R_\varepsilon \rightarrow X$ , we can construct an embedding  $\hat{f}: A_\varepsilon \rightarrow \widehat{X}$ . On a point  $(x, y, z) \in A_\varepsilon$  it is defined as

$$\hat{f}(x, y, z) := \begin{cases} [f(x, z), -\text{or}_2(X)] & \text{for } y \leq 0, \\ [f(x, z), \text{or}_2(X)] & \text{for } y \geq 0. \end{cases} \quad (2.35)$$

(Note that for points with  $y=0$  we have  $(x, z) \in \partial D$ , so that by construction of the double  $\widehat{X}$  we have the equality  $[f(x, z), -\text{or}_2(X)] = [f(x, z), \text{or}_2(X)]$ .) Comparing (2.19) and (2.31), it is not difficult to see that there is a canonical isomorphism between the extended

surfaces  $\widehat{X}'_k \sqcup H_{\bar{k}k}^-$  and  $\widehat{\Gamma}_{\hat{f},k}(\widehat{X})$ . Thus the gluing homomorphism (2.21) provides us with a map

$$\hat{g}_{\hat{f},k}(\widehat{X}) : \mathcal{H}(\widehat{X}') \otimes_{\mathbb{C}} \mathcal{H}(H_{\bar{k}k}^-) \rightarrow \mathcal{H}(\widehat{X}). \quad (2.36)$$

Using the basis element  $B_{\bar{k}k}^- \in \mathcal{H}(H_{\bar{k}k}^-)$  we finally define the gluing morphism (2.33) by

$$G_{f,k}^{\text{bnd}}(v) := \hat{g}_{\hat{f},k}(\widehat{X})(v \otimes B_{\bar{k}k}^-). \quad (2.37)$$

for  $v \in \mathcal{H}(\widehat{X}'_k)$ . Note that, strictly speaking, in (2.37) we should write  $Z(B_{\bar{k}k}^-)$  instead of  $B_{\bar{k}k}^-$ . However, to simplify notation we will use the same symbol for a cobordism and its invariant when the meaning is clear from the context.

THE BOUNDARY FACTORISATION. We are now ready to formulate the statements about boundary factorisation of the correlators.

2.9. THEOREM. Boundary factorisation for oriented world sheets: *Let  $X$  be an oriented world sheet with non-empty boundary, and let  $f: R_\varepsilon \rightarrow X$  be injective, continuous and 2-orientation preserving and satisfy  $f(\partial R_\varepsilon \cap R_\varepsilon) \subset \partial X$ . Let the boundary components containing  $f(1,0)$  and  $f(-1,0)$  be labelled by  $M_r$  and  $M_l$ , respectively. Then*

$$C_A(X) = \sum_{k \in \mathcal{I}} \sum_{\alpha, \beta} \dim(U_k) (c_{M_l, M_r, k}^{\text{bnd}})^{-1}_{\beta\alpha} G_{f,k}^{\text{bnd}}(C_A(\Gamma_{f,k,\alpha,\beta}^{\text{bnd}}(X))), \quad (2.38)$$

where  $\alpha$  and  $\beta$  run over bases of  $\text{Hom}_A(M_l \otimes U_k, M_r)$  and of  $\text{Hom}_A(M_r \otimes U_{\bar{k}}, M_l)$ , respectively.

2.10. THEOREM. Boundary factorisation for unoriented world sheets: *Let  $X$  be an unoriented world sheet with non-empty boundary. Suppose we are given either of the following data:*

(i) *A map  $f: R_\varepsilon \rightarrow X$  that is injective and continuous, such that  $f(\partial R_\varepsilon \cap R_\varepsilon) \subset \partial X$ ,  $f$  preserves the boundary orientation, and the boundary components containing  $f(1,0)$  and  $f(-1,0)$  are labelled by  $M_r$  and  $M_l$ , respectively.*

(ii) *A map  $f: R'_\varepsilon \rightarrow X$  that is injective and continuous, such that  $f(\partial R'_\varepsilon \cap R'_\varepsilon) \subset \partial X$ ,  $f$  preserves the boundary orientation, and the boundary components containing  $f(1,0)$  and  $f(-1,0)$  are labelled by  $M_r^\sigma$  and  $M_l$ , respectively.*

Then we have

$$C_{\tilde{A}}(X) = \sum_{k \in \mathcal{I}} \sum_{\alpha, \beta} \dim(U_k) (c_{M_l, M_r, k}^{\text{bnd}})^{-1}_{\beta\alpha} G_{f,k}^{\text{bnd}}(C_{\tilde{A}}(\Gamma_{f,k,\alpha,\beta}^{\text{bnd}}(X))), \quad (2.39)$$

where  $\alpha$  and  $\beta$  run over bases of  $\text{Hom}_{\tilde{A}}(M_l \otimes U_k, M_r)$  and of  $\text{Hom}_{\tilde{A}}(M_r \otimes U_{\bar{k}}, M_l)$ , respectively.

Here  $R'_\varepsilon$  is as introduced in remark 2.8 above, and  $M_r^\sigma$  denotes the  $\tilde{A}$ -module conjugate to  $M_r$ , as described in definition II:2.6.



### 2.11. BULK FACTORISATION.

**TWO-POINT FUNCTION ON THE SPHERE.** Denote by  $S(i, j, \phi^+, \phi^-)$  the world sheet for the standard two-point correlator on the unit sphere, given by  $S_{(2)}^2$  with field insertions

$$\begin{aligned}\Phi^+ &= (i, j, \phi^+, p^+, [\gamma^+], \text{or}_2) \quad \text{and} \\ \Phi^- &= (\bar{i}, \bar{j}, \phi^-, p^-, [\gamma^-], \text{or}_2).\end{aligned}\tag{2.40}$$

Here  $\text{or}_2$  denotes the orientation of  $S_{(2)}^2$ , and  $\phi^\pm$  are bimodule morphisms  $\phi^+ \in \text{Hom}_{A|A}(U_i \otimes^+ A \otimes^- U_j, A)$  and  $\phi^- \in \text{Hom}_{A|A}(U_{\bar{i}} \otimes^+ A \otimes^- U_{\bar{j}}, A)$  (see formula (IV:2.17) for the definition of  $\otimes^\pm$ ).

The double  $\hat{S}$  of  $S$  can be identified with  $S_{(2)}^2 \sqcup S_{(2)}^2$  by taking  $p \mapsto (p, \text{or}_2)$  for the first copy and  $p \mapsto (\tau'(p), -\text{or}_2)$  for the second copy, where  $\tau'(x, y, z) := (x, -y, z)$ . Note that this identification respects the orientation and is compatible with the embedded arcs. On the first copy, to be denoted by  $S_i$ , we mark  $[\gamma^+]$  and  $[\gamma^-]$  by  $(U_i, +)$  and  $(U_{\bar{i}}, +)$ , while on the second copy, to be denoted by  $S_j$ , we mark the two arcs by  $(U_j, +)$  and  $(U_{\bar{j}}, +)$ , respectively. The corresponding space  $\mathcal{H}(\hat{S}) \cong \mathcal{H}(S_i) \otimes_{\mathbb{C}} \mathcal{H}(S_j)$  of conformal blocks is one-dimensional; a basis is given by  $B_{i\bar{i}}^+ \otimes B_{j\bar{j}}^+$ , with  $B_{k\bar{k}}^+$  as defined in (2.24). Accordingly, the structure constant  $c^{\text{bulk}} \in \mathbb{C}$  of the two-point correlator on the sphere is defined by

$$C(S(i, j, \phi^+, \phi^-)) =: c_{i,j,\phi^+,\phi^-}^{\text{bulk}} B_{i\bar{i}}^+ \otimes B_{j\bar{j}}^+.\tag{2.41}$$

Given bases  $\{\phi_\alpha^+\}$  of  $\text{Hom}_{A|A}(U_i \otimes^+ A \otimes^- U_j, A)$  and  $\{\phi_\beta^-\}$  of  $\text{Hom}_{A|A}(U_{\bar{i}} \otimes^+ A \otimes^- U_{\bar{j}}, A)$ , we use the two-point function on the sphere to define a matrix  $c_{i,j}^{\text{bulk}}$  by

$$(c_{i,j}^{\text{bulk}})_{\alpha\beta} := c_{i,j,\phi_\alpha^+,\phi_\beta^-}^{\text{bulk}}.\tag{2.42}$$

As shown in appendix C.2, the bulk two-point function is non-degenerate, in the sense that for fixed  $i, j$  the matrix  $c_{i,j}^{\text{bulk}}$  is invertible.

**CUTTING WORLD SHEETS ALONG A CIRCLE.** Let  $A_\varepsilon$  be the equatorial annulus on the sphere that we introduced in section 2.6, and denote by  $S_\varepsilon^\pm$  the subsets of  $S \equiv S(i, j, \phi^+, \phi^-)$  given by

$$\begin{aligned}S_\varepsilon^+ &:= \{(x, y, z) \in S \mid z > -\varepsilon\} \quad \text{and} \\ S_\varepsilon^- &:= \{(x, y, z) \in S \mid z < \varepsilon\},\end{aligned}\tag{2.43}$$

such that  $A_\varepsilon = S_\varepsilon^+ \cap S_\varepsilon^-$ .

Let  $X$  be an (oriented or unoriented) world sheet and  $f: A_\varepsilon \rightarrow X$  an injective, continuous map. Further, let  $i, j \in \mathcal{I}$  be labels of simple objects, and let  $\phi^\pm$  be bimodule morphisms  $\phi^+ \in \text{Hom}_{A|A}(U_i \otimes^+ A \otimes^- U_j, A)$ ,  $\phi^- \in \text{Hom}_{A|A}(U_{\bar{i}} \otimes^+ A \otimes^- U_{\bar{j}}, A)$ . Similar to the procedure described in section 2.7, we define a new world sheet  $\Gamma_{f,i,j,\phi^+,\phi^-}^{\text{bulk}}(X)$ , which is obtained from  $X$  by cutting along  $f(S^1)$  and gluing hemispheres with bulk insertions  $\phi^+, \phi^-$  to the cuts. We set  $\tilde{X} := X \setminus f(S^1)$  and define

$$\Gamma_{f,i,j,\phi^+,\phi^-}^{\text{bulk}}(X) := (\tilde{X} \sqcup S_\varepsilon^+ \sqcup S_\varepsilon^-) / \sim.\tag{2.44}$$

Here the lower hemisphere gets joined to  $\tilde{X}$  via  $f(p) \sim p$  for  $p \in \{(x, y, z) \in S_\varepsilon^- \mid z > 0\}$ , while the upper hemisphere gets joined via  $f(p) \sim p$  for  $p \in \{(x, y, z) \in S_\varepsilon^+ \mid z < 0\}$ . Again, if  $X$  is an oriented world sheet, then so is  $\Gamma_{f,i,j,\phi^+,\phi^-}^{\text{bulk}}(X)$ . If  $X$  is an unoriented world sheet, then so is  $\Gamma_{f,i,j,\phi^+,\phi^-}^{\text{bulk}}(X)$ .

2.12. **REMARK.** In theorems 2.13 and 2.14 below we formulate factorisation identities which are obtained when cutting a world sheet  $X$  along a closed curve  $\gamma$  that is obtained as the image  $f(S^1)$  under an embedding  $f: A_\varepsilon \rightarrow X$ .

On the other hand, given a closed non-selfintersecting curve  $\gamma$  in  $X$ , in the spirit of remark 2.8 we can wonder whether there is a factorisation identity associated to cutting  $X$  along  $\gamma$ . For oriented world sheets we can find an embedding  $f: A_\varepsilon \rightarrow X$  such that  $f(S^1)$  is equal to  $\gamma$ , since any small neighbourhood of  $\gamma$  is oriented and hence has the topology of an annulus. In this case we find the identity described in theorem 2.13. For unoriented world sheets, on the other hand, a small neighbourhood of  $\gamma$  can have either the topology of an annulus or of a Möbius strip. In the former case, there is again an embedding  $f: A_\varepsilon \rightarrow X$  such that  $f(S^1)$  is equal to  $\gamma$ , and one obtains the identity given in theorem 2.14.

Regarding the second case, let  $h: \text{Mö}_\varepsilon \rightarrow X$  be an embedding of a Möbius strip  $\text{Mö}_\varepsilon$  of width  $\varepsilon$  into  $X$ , such that  $h(S^1) = \gamma$  (where  $S^1$  is the circle forming the ‘middle’ of the Möbius strip). Note that cutting  $X$  along  $\gamma$  introduces only a single additional boundary component. Accordingly, cutting along  $\gamma$  does not locally decompose the world sheet into two disconnected parts, as is the case for any embedding  $A_\varepsilon \rightarrow X$ .

Nonetheless it turns out that an embedding  $h: \text{Mö}_\varepsilon \rightarrow X$  leads to an identity for correlators, too, even though it is not a factorisation identity because, as just described, the world sheet is not cut into two locally disconnected parts. In words, one can recover the correlator  $C(X)$  by gluing a hemisphere with one bulk insertion to the cut boundary of  $X \setminus \gamma$ , and summing over a basis of bulk fields, weighting each term with the one-point function on the cross cap  $\mathbb{RP}^2$  (multiplied by the inverse of the two-point function on the sphere). In this way one obtains in particular the *cross cap constraint* that has been studied in [FPS]. In slightly more detail, given an embedding  $h: \text{Mö}_\varepsilon \rightarrow X$ , consider the curve  $\gamma'$  that is given by the boundary  $\partial h(\text{Mö}_\varepsilon)$ . For small  $\varepsilon$ , the curve  $\gamma'$  is running close to  $\gamma$  and has a small neighbourhood with the topology of an annulus. Thus for  $\gamma'$  we can find an embedding  $f: A_\varepsilon \rightarrow X$  such that  $f(S^1) = \gamma'$ . The world sheet cut along  $\gamma'$  and with the half-spheres  $S_\varepsilon^\pm$  glued to the holes is then given by  $\Gamma_{f,i,j,\phi^+,\phi^-}^{\text{bulk}}(X)$ . Note that gluing a half-sphere to the component of  $X \setminus f(S^1)$  that contains  $\gamma$  produces a cross cap. The above mentioned identity for correlators is now obtained by applying theorem 2.14 to the embedding  $f$ .

**GLUING HOMOMORPHISM BETWEEN SPACES OF BLOCKS.** We abbreviate

$$X'_{ij} := \Gamma_{f,i,j,\phi^+,\phi^-}^{\text{bulk}}(X). \quad (2.45)$$

To formulate the bulk factorisation constraint, we need a map  $G_{f,ij}^{\text{bulk}}$  between the spaces of conformal blocks on the doubles of  $X'_{ij}$  and  $X$ . The embedding  $f: A_\varepsilon \rightarrow X$  gives rise to

two embeddings  $f_i$  and  $f_j$  of  $A_\varepsilon$  into the double  $\widehat{X}$ , given by

$$\begin{aligned} f_i(x, y, z) &= [f(x, y, z), \text{or}_2] \quad \text{and} \\ f_j(x, y, z) &= [f(x, -y, z), -\text{or}_2] \end{aligned} \quad (2.46)$$

for  $(x, y, z) \in A_\varepsilon$ . We can now apply the ‘cutting twice’ procedure (2.19) to both embeddings  $f_i$  and  $f_j$ . This results in an extended surface

$$Y_{ij} := \widehat{\Gamma}_{f_i, i}(\widehat{\Gamma}_{f_j, j}(\widehat{X})). \quad (2.47)$$

This extended surface comes together with an isomorphism  $Y_{ij} \cong \widehat{X}'_{ij} \sqcup H_{ii}^- \sqcup H_{jj}^-$ , with  $H_{kk}^-$  as defined after formula (2.33), so that the gluing homomorphism  $\widehat{g}$  provides a map

$$\widehat{g}_{f_i, i} \circ \widehat{g}_{f_j, j} : \mathcal{H}(\widehat{X}'_{ij}) \otimes_{\mathbb{C}} \mathcal{H}(H_{ii}^-) \otimes_{\mathbb{C}} \mathcal{H}(H_{jj}^-) \rightarrow \mathcal{H}(\widehat{X}). \quad (2.48)$$

We use this map to obtain the desired map  $G_{f, ij}^{\text{bulk}}: \mathcal{H}(\widehat{X}'_{ij}) \rightarrow \mathcal{H}(\widehat{X})$  as

$$G_{f, ij}^{\text{bulk}}(v) := \widehat{g}_{f_i, i} \circ \widehat{g}_{f_j, j}(v \otimes B_{ii}^- \otimes B_{jj}^-). \quad (2.49)$$

**THE BULK FACTORISATION.** We have now gathered all the ingredients to formulate the consistency of the assignment of correlators  $X \mapsto C(X)$  with bulk factorisation.

**2.13. THEOREM.** Bulk factorisation for oriented world sheets: *Let  $X$  be an oriented world sheet and let  $f: A_\varepsilon \rightarrow X$  be injective, continuous and orientation preserving. Then*

$$C_A(X) = \sum_{i, j \in \mathcal{I}} \sum_{\alpha, \beta} \dim(U_i) \dim(U_j) (c_{i, j}^{\text{bulk}^{-1}})_{\beta\alpha} G_{f, ij}^{\text{bulk}}(C_A(\Gamma_{f, i, j, \alpha, \beta}^{\text{bulk}}(X))), \quad (2.50)$$

where  $\alpha$  and  $\beta$  run over bases of  $\text{Hom}_{A|A}(U_i \otimes^+ A \otimes^- U_j, A)$  and  $\text{Hom}_{A|A}(U_{\bar{i}} \otimes^+ A \otimes^- U_{\bar{j}}, A)$ , respectively.

**2.14. THEOREM.** Bulk factorisation for unoriented world sheets: *Let  $X$  be an unoriented world sheet and let  $f: A_\varepsilon \rightarrow X$  be injective and continuous. Then*

$$C_{\tilde{A}}(X) = \sum_{i, j \in \mathcal{I}} \sum_{\alpha, \beta} \dim(U_i) \dim(U_j) (c_{i, j}^{\text{bulk}^{-1}})_{\beta\alpha} G_{f, ij}^{\text{bulk}}(C_{\tilde{A}}(\Gamma_{f, i, j, \alpha, \beta}^{\text{bulk}}(X))), \quad (2.51)$$

where  $\alpha$  and  $\beta$  run over bases of  $\text{Hom}_{\tilde{A}|\tilde{A}}(U_i \otimes^+ \tilde{A} \otimes^- U_j, \tilde{A})$  and  $\text{Hom}_{\tilde{A}|\tilde{A}}(U_{\bar{i}} \otimes^+ \tilde{A} \otimes^- U_{\bar{j}}, \tilde{A})$ , respectively.

### 3. Proof of modular invariance

This section presents the proof that the oriented correlators  $C_A(X)$  are invariant under the action of the mapping class group  $\text{Map}_{\text{or}}(X)$ , and that the unoriented correlators  $C_{\bar{A}}(X)$  are invariant under the action of  $\text{Map}(X)$ . To this end, we will prove the more general covariance results in theorems 2.2 and 2.4 which, when specialised to  $X = Y$ , imply invariance under the action of the mapping class group via the corollaries 2.3 and 2.5.

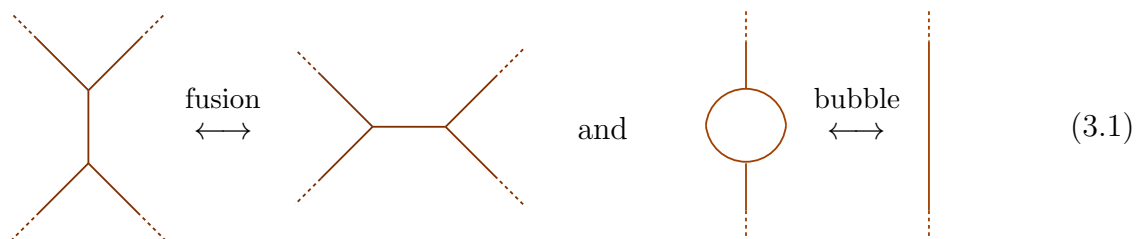
Our strategy is to reduce the covariance property to the statement that the construction of the correlators is independent of the choice of triangulation.<sup>3</sup> We will treat the case of oriented world sheets in detail and then point out the differences in the unoriented case.

#### 3.1. ORIENTED WORLD SHEETS.

Let us first establish the independence of our prescription of the choice of triangulation:

**3.2. PROPOSITION.** *Let  $X$  be an oriented world sheet. The correlator  $C_A(X)$  given by the prescription in appendix B does not depend on the particular choice of triangulation of the embedded world sheet  $\iota_X(X) \subset M_X$ .*

The proof of this statement is contained in the lemmas 3.3–3.6 that will be established below. To prepare the stage for these lemmas, we first recall that any two triangulations of a surface can be connected by a series of only two types of moves, the *bubble* move and the (2,2) or *fusion* move (also known as the two-dimensional Matveev moves), see e.g. [TV, FHK, KM]. These look as follows:

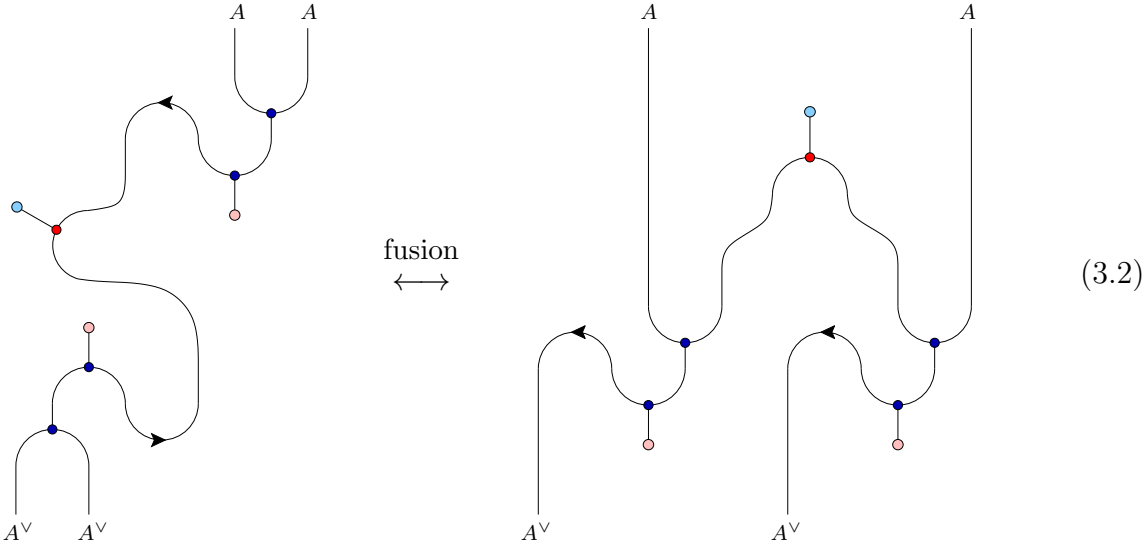


Now as described in the appendix, the construction of the ribbon graph for the correlator  $C_A(X)$  requires to place  $A$ -ribbons along the interior edges of a chosen triangulation of the world sheet  $X$  and to connect them suitably at the vertices of the triangulation. This procedure involves several arbitrary choices. The correlator, which is the invariant of the ribbon graph, does, however, not depend on these choices (see again the appendix), so that it is sufficient to consider just one specific possibility for each choice involved. Concretely, at each vertex of the triangulation that lies in the interior of  $X$ , there are three different possibilities of joining the three outgoing  $A$ -ribbons (either using the ribbon graph fragment displayed in figure (B.8), or using the graphs obtained from that

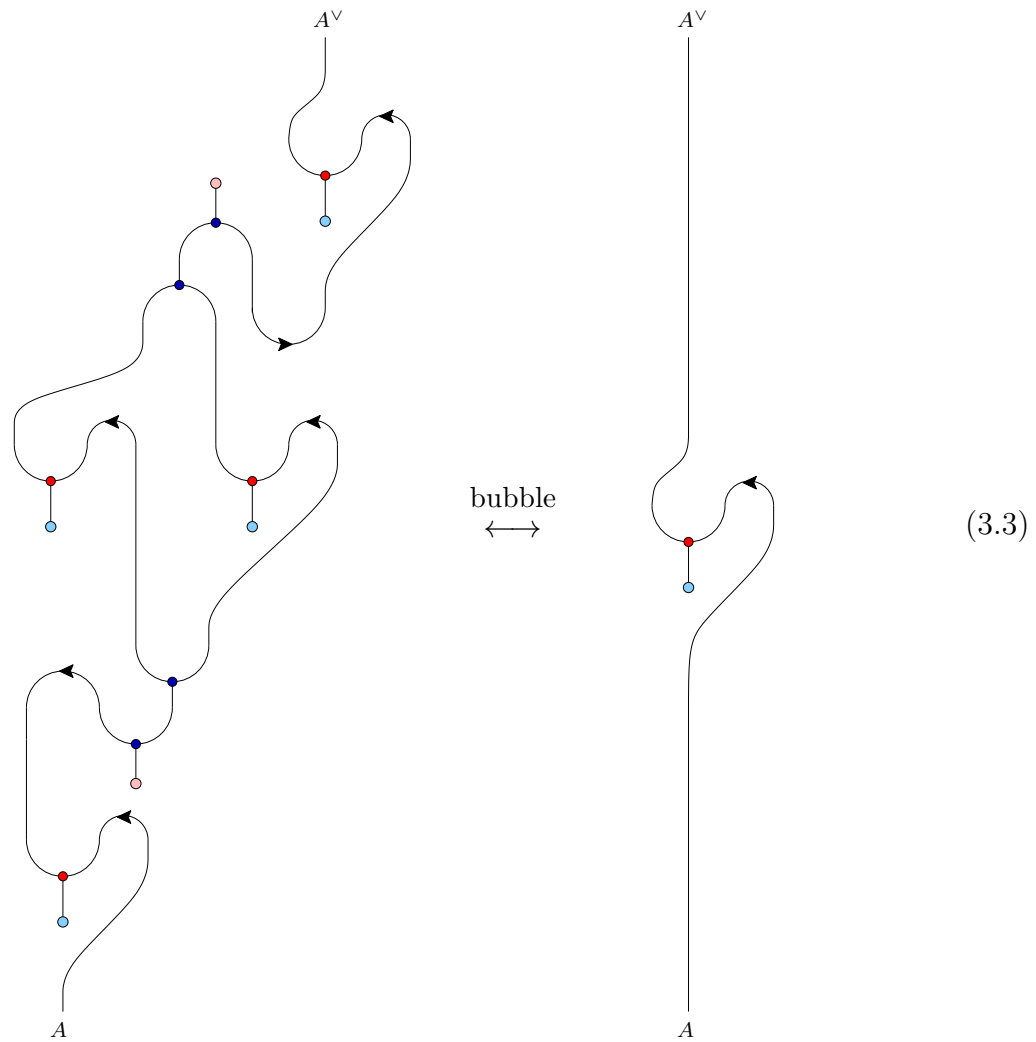
<sup>3</sup> As in appendix B.3, by a triangulation we shall mean a cell decomposition in which each vertex is three-valent and a face can have arbitrarily many edges.

figure by a  $2\pi/3$ - or  $4\pi/3$ -rotation of the part contained in the dashed circle), and we choose any one of them. Similarly, for joining two incoming  $A$ -ribbons along an edge that connects two interior vertices we select one of the two possibilities to insert the left ribbon graph fragment in figure (B.9). Finally, any boundary segment is covered by a ribbon labelled by an  $A$ -module  $M$ ; at a vertex of the triangulation lying on that segment of  $\partial X$ , we place the graph (B.10).

When we want to make the ribbon graph  $R$  embedded in a cobordism  $M$  explicit, we will use the notation  $M[R]$ . For a given triangulation  $T$  of  $X$ , let  $R_T$  be the ribbon graph in  $M_X$  constructed as above. To show that  $Z(M_X[R_T]) = Z(M_X[R_{T'}])$  for any two triangulations  $T$  and  $T'$  of  $X$ , it suffices to consider triangulations  $T$  and  $T'$  that differ only by a single move, either a fusion or a bubble move. Let us start with the fusion move. We cut out a three-ball in the three-manifold  $M_X$  that contains the part in which  $T$  and  $T'$  differ. We can project the ribbon graph fragment contained in that three-ball in a non-singular manner to a plane (for instance, to a plane patch of  $\iota(X)$ ). The resulting graph can then be interpreted as a morphism in the category  $\mathcal{C}$ . Let us for the moment restrict our attention to the case that only interior vertices of the triangulation are involved. Then from  $M_X[R_T]$  and  $M_X[R_{T'}]$  we arrive at the two sides of the picture



Similarly, in the case of the bubble move we obtain



We now proceed to prove that the two sides of (3.2), as well as those of (3.3), are actually equal.

**3.3. LEMMA.** *The two sides of the fusion move (3.2) coincide.*

PROOF. We start by noticing that

Diagrammatic equation (3.4) showing three stages of simplification of a graph with  $A$  and  $A^\vee$  strands. The first graph is a complex structure with multiple crossings and colored dots (blue, red, orange). The second graph is a simplified version of the first, and the third graph is the final simplified form. The strands are labeled  $A$  and  $A^\vee$ .

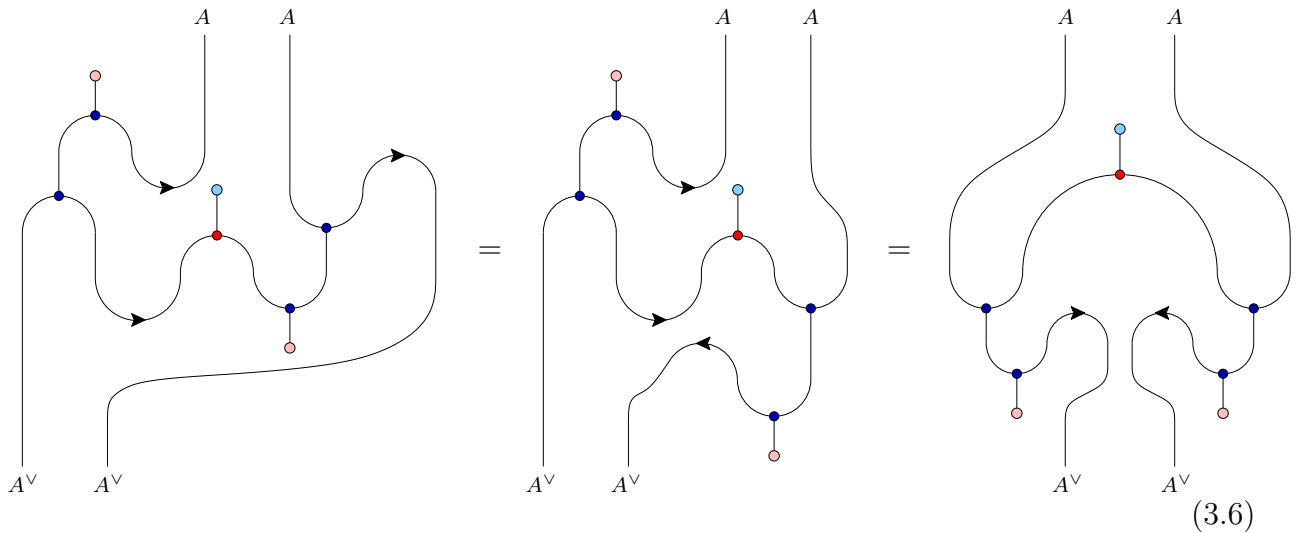
Here the first equality is a simple deformation of the graph, while in the second equality the Frobenius property, together with the unit and counit properties, is used.

Next we perform again a slight deformation so as to arrive at the first graph in the following sequence of equalities:

Diagrammatic equation (3.5) showing three stages of simplification of a graph with  $A$  and  $A^\vee$  strands. The first graph is a complex structure with multiple crossings and colored dots (orange, blue, red). The second graph is a simplified version of the first, and the third graph is the final simplified form. The strands are labeled  $A$  and  $A^\vee$ .

Here the first equality follows by using coassociativity twice, while the second is again a direct consequence of the Frobenius, unit and counit properties. The last graph of the

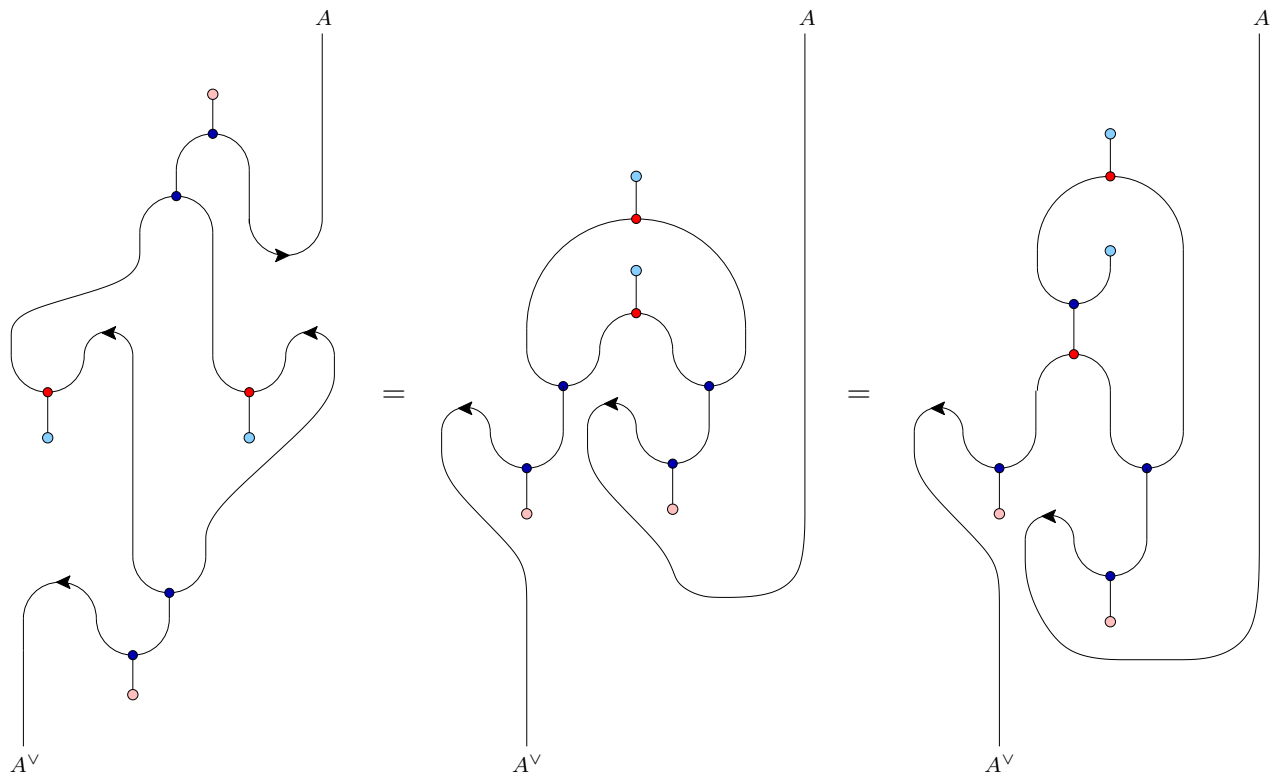
previous picture can be deformed to equal the first graph in



The first of these equalities follows by coassociativity and the symmetry property (compare (I:5.9)), and the second by coassociativity together with another deformation of the graph. Finally, from the last picture in (3.6), the right hand side of the fusion move (3.2) is obtained by use of the symmetry property of  $A$ . ■

3.4. LEMMA. *The two sides of the bubble move (3.3) coincide.*

PROOF. Consider the following moves.





(3.7)

The first equality is a simple deformation of the graph; the second equality follows by the Frobenius property, while the third requires Frobenius, symmetry and the counit property; the next-to-last step follows by specialness and the Frobenius property, and the last by the symmetry property.

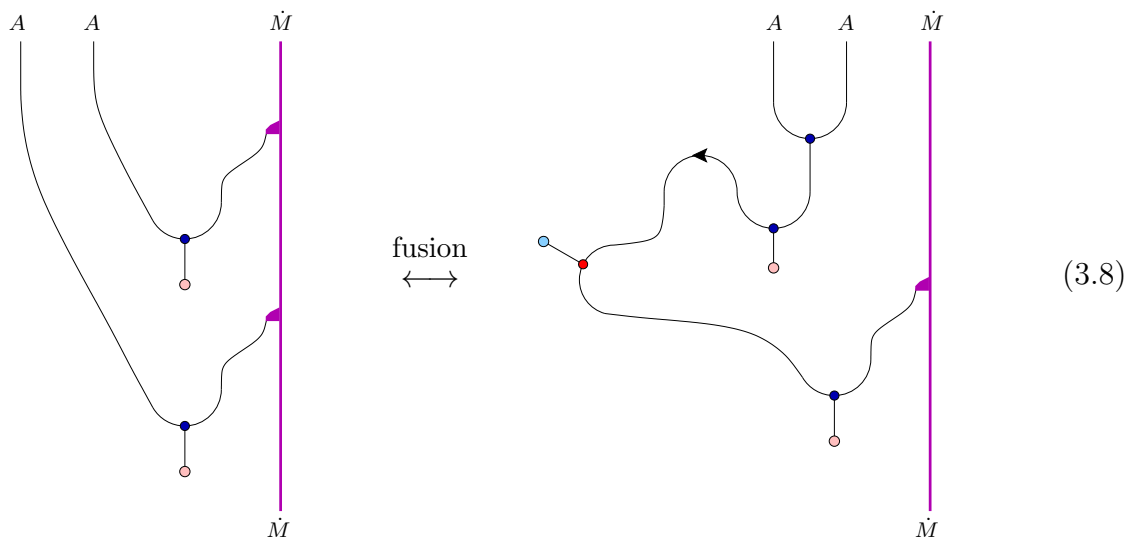
Finally, by composing the first and last graph in this sequence both from the bottom and from the top with the right hand side of (3.3)<sup>4</sup> after a few simple manipulations we arrive at the graphs on the two sides of the bubble move (3.3), respectively. ■

When also vertices of the triangulation that lie on  $\partial X$  are involved, then instead of

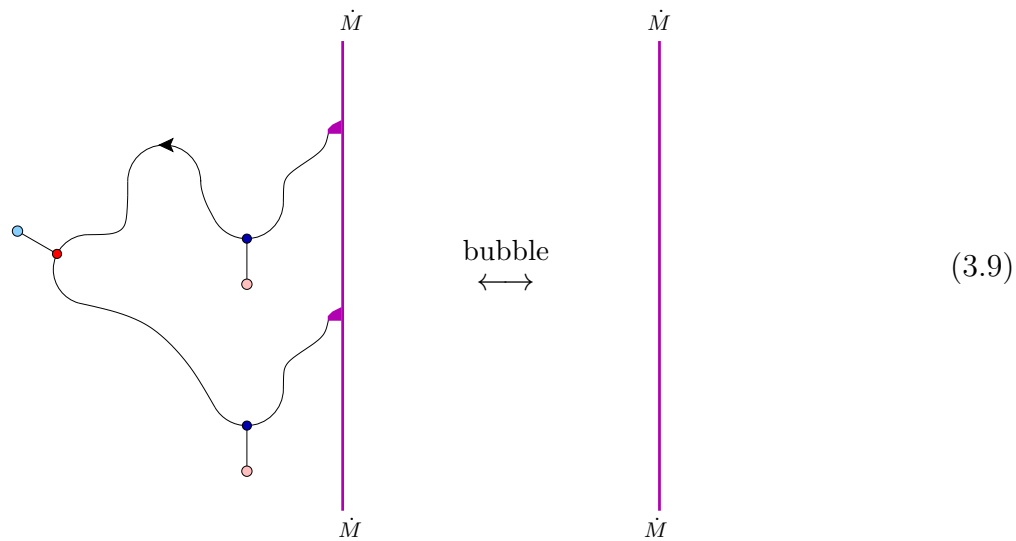
---

<sup>4</sup> When starting directly with the left hand side of (3.3), rather than with the left hand side of (3.7), it is actually convenient to perform the various manipulations in a slightly different order from what we have done here.

(3.2) and (3.3) the fusion and bubble move amount to



and to



respectively.

3.5. LEMMA. *The two sides of the fusion move (3.8) coincide.*

PROOF. Invoking the module property, the left hand side of the fusion move (3.8) becomes the left hand side of the following sequence of equalities:

(3.10)

The first equality uses just the Frobenius, unit and coassociativity properties, and the second follows by the Frobenius, unit and counit properties. The right hand side of (3.10), in turn, is just a deformation of the ribbon graph on the right hand side of the fusion move (3.8). ■

3.6. LEMMA. *The two sides of the bubble move (3.9) coincide.*

PROOF. A deformation of the left hand side of the bubble move (3.9) results in the left hand side of

(3.11)

The first equality employs the Frobenius, unit and counit properties, while the second uses the module property and specialness. That the right hand side of (3.11) is equal to the right hand side of the bubble move (3.3) is a direct consequence of the (unit) module property. ■

This completes the proof of proposition 3.2. Proving theorem 2.2 is now straightforward.

**PROOF OF THEOREM 2.2.** We are given two oriented world sheets  $X$  and  $Y$  and an orientation preserving homeomorphism  $f: X \rightarrow Y$ . To obtain the correlator  $C_A(X)$  via the construction of appendix B we need to choose a triangulation  $T_X$  of the world sheet  $X$ , i.e. an embedding  $T_X: K \rightarrow X$  for some simplicial complex  $K$ . Similarly, to obtain  $C_A(Y)$  we have to choose a triangulation  $T_Y$  of the world sheet  $Y$ . By definition, we have  $C_A(X) = Z(M_X[R_{T_X}])$  and  $C_A(Y) = Z(M_Y[R_{T_Y}])$ , and by proposition 3.2 this definition is independent of the choice of  $T_X$  and  $T_Y$ . On  $Y$  we can define a second triangulation in terms of the triangulation on  $X$  and the map  $f$  as  $T'_Y := f \circ T_X$ . By construction, we have the relation

$$M_{\hat{f}} \circ M_X[R_{T_X}] \cong M_Y[R_{T'_Y}], \quad (3.12)$$

where the notation ‘ $\cong$ ’ indicates that there exists a homeomorphism between the two cobordisms that acts as the identity on the boundary, and where  $\hat{f}$  is the map that was defined in section 2.1. We can then compute

$$\begin{aligned} \hat{f}_\# \circ C_A(X) &= Z(M_{\hat{f}}) \circ Z(M_X[R_{T_X}]) \\ &= Z(M_Y[R_{T'_Y}]) = Z(M_Y[R_{T_Y}]) = C_A(Y), \end{aligned} \quad (3.13)$$

where the first equality is the definition of  $\hat{f}_\#$  and  $C_A(X)$ , in the second step we use functoriality<sup>5</sup> of  $Z$  and (3.12), the third step is triangulation invariance as established in proposition 3.2, and the last step is just the definition of  $C(Y)$ . ■

**3.7. REMARK.** Given a world sheet  $X$  and homeomorphisms  $f, g: X \rightarrow X$ , by the argument of footnote 5 we have  $Z(M_{\hat{f}} \circ M_{\hat{g}}) = Z(M_{\hat{f}}) \circ Z(M_{\hat{g}})$ , i.e. the anomaly factor in the functoriality relation vanishes in this case. Thus we obtain a genuine (non-projective) representation of  $\text{Map}_{\text{or}}(X)$  (and of  $\text{Map}(X)$  in the unoriented case) on  $\mathcal{H}(\hat{X})$ .

This situation for the subgroup  $\text{Map}(X) \subset \text{Map}(\hat{X})$  should be contrasted to the situation for the whole mapping class group  $\text{Map}(\hat{X})$ . For that group, one only obtains (see formula (2.5)) a projective representation on  $\mathcal{H}(\hat{X})$ .

### 3.8. UNORIENTED WORLD SHEETS.

For the construction of correlators on unoriented world sheets the following statement holds.

**3.9. PROPOSITION.** *Let  $X$  be an unoriented world sheet. The correlator  $C_{\hat{A}}(X)$  given by the prescription in appendix B does not depend on the particular choice of triangulation of the embedded world sheet  $\iota_X(X) \subset M_X$ .*

---

<sup>5</sup> By construction, the push-forward  $\hat{f}_\#$  of the Lagrangian subspace  $\lambda(\hat{X}) \in H_1(\hat{X}, \mathbb{R})$  for  $\hat{X}$  gives the Lagrangian subspace for  $\hat{Y}$ . It is not hard to convince oneself that, as a consequence, in the present situation the Maslov indices in the anomaly factor of the functoriality relation for  $Z$  vanish.

The proof of proposition 3.9 proceeds analogously to that of proposition 3.2. The main difference is that one has to choose a triangulation  $T$  of  $X$  together with a local orientation of  $X$  at every vertex of  $T$ . (And there is the obvious modification that in all pictures the algebra ribbons are now labelled by  $\tilde{A}$ .) Changing these local orientations does not affect  $C_{\tilde{A}}(X)$ , as has been demonstrated in section II:3.1. To show that  $C_{\tilde{A}}(X)$  does not depend on the triangulation, one shows independence under the fusion and bubble move by choosing the local orientations at the two vertices involved to be equal and copying the argument of the previous section.

The proof of theorem 2.4 is analogous to the oriented case, too, the main difference being that  $X$  and  $Y$  are not oriented, and as a consequence the homeomorphism  $f: X \rightarrow Y$  can in general not be required to be orientation preserving. However, it can still be used to obtain a triangulation of  $Y$  with local orientations at its vertices from a triangulation of  $X$  with local orientations at its vertices. The proof then proceeds as the proof of theorem 2.2 above.

## 4. Proof of boundary factorisation

In this section we present the proof of theorems 2.9 and 2.10, which describe boundary factorisation. We first develop some ingredients to be used; there are two main aspects, a geometric and an algebraic one. A crucial feature of the geometric aspect of factorisation, indeed the very feature that allows for a general proof of this property, is that it is of local nature. Here the qualification ‘local’ is used to indicate that factorisation only involves a neighbourhood of the interval along which the world sheet is cut, i.e. the image of the set  $R_\epsilon$  in the notation of section 2.7.

### 4.1. GEOMETRIC SETUP OF BOUNDARY FACTORISATION.

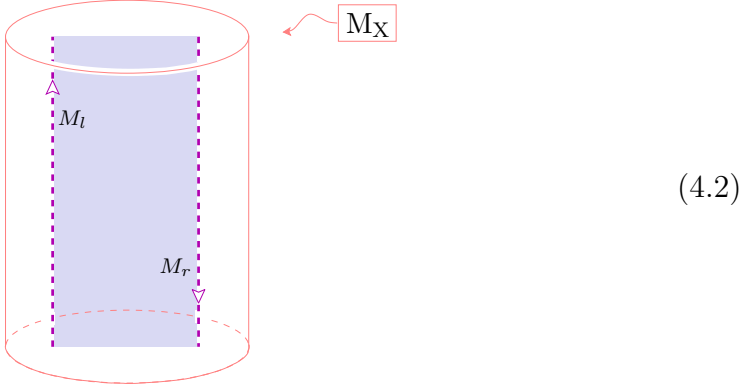
The construction of this subsection applies both to oriented and to unoriented world sheets. Accordingly, below  $C$  stands for  $C_A$  or  $C_{\tilde{A}}$ . The reason that at this point no distinction between the two cases is necessary is that the part of the world sheet that is of interest to us – the image of  $R_\epsilon$  – inherits an orientation from  $R_\epsilon$ . It is this local orientation of the world sheet that is used in the construction.

Let  $X$  and  $f$  be as in theorem 2.9. The first step is to make explicit the geometry of both sides of formulas (2.38) and (2.39), i.e. of  $C(X)$  and of the summands

$$\dim(U_k) (c_{M_l, M_r, k}^{\text{bnd}})^{-1}_{\beta\alpha} G_{f, k}^{\text{bnd}} (C(\Gamma_{f, k, \alpha, \beta}^{\text{bnd}}(X))). \quad (4.1)$$

Consider a strip-shaped region in  $X$  in the neighbourhood of which the ‘cutting twice’ operation (2.19) is going to be performed. The image of that neighbouring region in  $M_X$  can be drawn, as a subset of  $\mathbb{R}^3$ , as a solid cylinder  $Z$  containing two straight ribbons labelled  $M_r$  and  $M_l$ , as shown in the following figure (the shaded region shows the embedding of

the strip-shaped region of  $X$  in  $M_X$ ):



The cylindrical part of  $\partial Z$  is part of the double  $\widehat{X} = \partial M_X$ , and the rest of  $M_X$ , which is not shown here, is attached to the top and bottom bounding disks that make up the remaining part of  $\partial Z$ . With suitable choice of coordinates, the former part of  $\partial Z$  is given by

$$\{(x, y, z) \in \mathbb{R}^3 \mid x^2 + z^2 = 2, y \in [-3, 3]\} \subset \widehat{X} \subset M_X, \tag{4.3}$$

with orientation induced by the inward pointing normal, and the corresponding part of the embedded world sheet is the strip

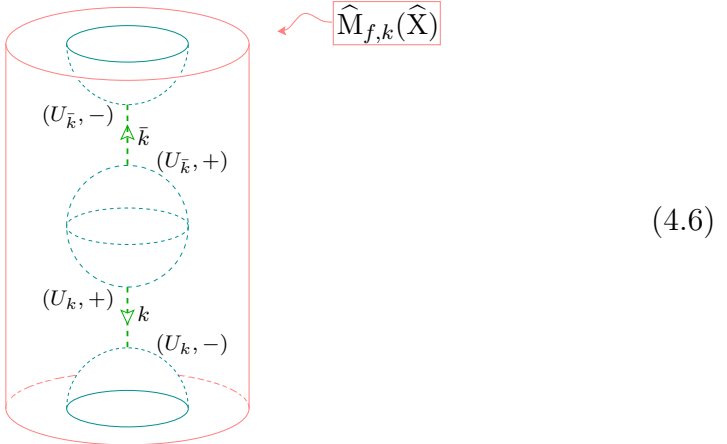
$$\{[-1, 1] \times [-3, 3] \times \{0\}\} \subset \iota(X) \subset M_X. \tag{4.4}$$

The two ribbons, which touch  $\iota(\partial X)$ , are then the strips

$$\{[-1, -\frac{9}{10}] \times [-3, 3] \times \{0\}\} \quad \text{and} \quad \{[\frac{9}{10}, 1] \times [-3, 3] \times \{0\}\} \tag{4.5}$$

in the  $z=0$ -plane, with orientation opposite to that inherited from the local orientation of  $\iota(X)$ , and core-orientation opposite to the orientation of  $\iota(\partial X)$ . The left ribbon is labelled by the  $A$ -module  $M_l$ , and the right one is labelled by  $M_r$ .

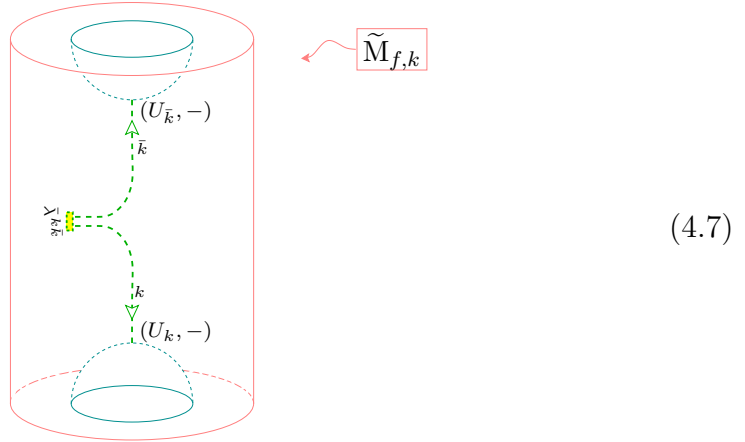
Next consider the gluing homomorphism  $G_{f,k}^{\text{bnd}}$  introduced in (2.37). This is obtained using the gluing homomorphism  $\hat{g}_{f,k}$  defined in equation (2.21), with  $E = \widehat{X}$ . We identify part of  $\widehat{M}_{f,k}(\widehat{X})$  (as defined above (2.20)) with the following region embedded in  $\mathbb{R}^3$ :



This region is a solid cylinder with some parts cut out, and with two vertical ribbons labelled  $k$  and  $\bar{k}$ , respectively. The outer boundary, which is part of  $\widehat{X}$ , is as in figure (4.2) above, while the inner boundary has three disconnected components, two of them being hemispheres and the third a sphere  $s$ . The two hemispheres are part of the boundary component isomorphic to the double of  $\Gamma_{f,k,\alpha,\beta}^{\text{bnd}}(X)$  with opposite orientation, which we denote by  $-\Upsilon_{f,k,\alpha,\beta}^{\text{bnd}}(X)$ . The top and bottom bounding annuli of the solid cylinder are attached to the rest of  $\widehat{M}_{f,k}$ .

The sphere  $s$  is a unit sphere centered at  $(0, 0, 0)$ , while the hemispheres are centered at  $(0, 3, 0)$  and at  $(0, -3, 0)$ , respectively, and have unit radius, too. The two ribbons lie both in the  $z=0$ -plane, and are centered about the line  $x=0$ , with width  $1/10$ . The upper ribbon, labelled by  $\bar{k}$ , ends on marked arcs at  $y=2$  and  $y=1$ , labelled by  $(U_{\bar{k}}, -)$  and by  $(U_{\bar{k}}, +)$ , respectively, while the lower ribbon is labelled by  $k$  and ends on marked arcs at  $y=-1$  and  $y=-2$ , labelled  $(U_k, +)$  and  $(U_k, -)$ . The orientation of the arcs is in the  $+x$ -direction at  $y=1$  and at  $y=-2$ , while it is in the  $-x$ -direction at  $y=-1$  and at  $y=2$ ; the core of the upper and lower ribbon is oriented in the  $+y$ - and  $-y$ -direction, respectively.

From  $\widehat{M}_{f,k}$  we now construct a new cobordism  $\widetilde{M}_{f,k}$  by gluing the cobordism  $B_{\bar{k}k}^-$  to  $s$ . There is a canonical isomorphism between the extended surfaces  $\partial B_{\bar{k}k}^-$  and  $-s$ , and we use this isomorphism for identification. The result, shown in figure (4.7), differs from  $\widehat{M}_{f,k}$  in the central region, where now the two ribbons are joined by a coupon that is labelled by the morphism  $\bar{\lambda}^{k\bar{k}}$ :



Now we have the equality

$$G_{f,k}^{\text{bnd}} = Z(\widetilde{M}_{f,k}, \Upsilon_{f,k,\alpha,\beta}^{\text{bnd}}(X), \widehat{X}), \quad (4.8)$$

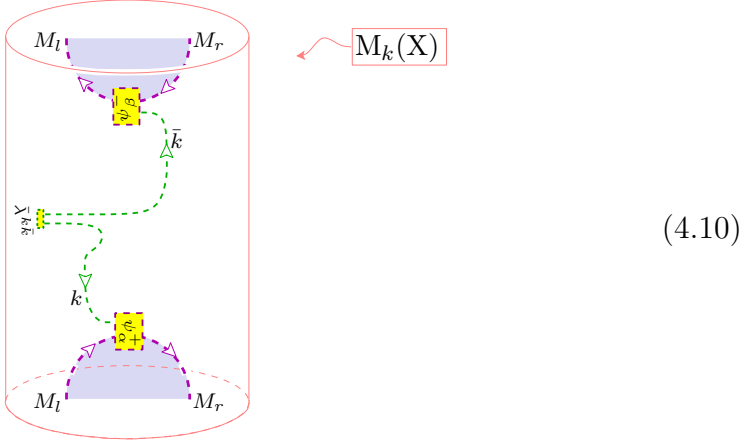
and can therefore write

$$G_{f,k}^{\text{bnd}}(C(\Gamma_{f,k,\alpha,\beta}^{\text{bnd}}(X))) = Z(\widetilde{M}_{f,k}, \Upsilon_{f,k,\alpha,\beta}^{\text{bnd}}(X), \widehat{X}) \circ Z(M_{\Gamma_{f,k,\alpha,\beta}^{\text{bnd}}(X)}, \emptyset, \Upsilon_{f,k,\alpha,\beta}^{\text{bnd}}(X))1. \quad (4.9)$$

By functoriality the latter invariant can be replaced by  $Z(M_k(X), \emptyset, \widehat{X})$ , where the cobordism  $M_k(X)$  is defined by gluing  $M_{\Gamma_{f,k,\alpha,\beta}^{\text{bnd}}(X)}$  to the inside of  $\widetilde{M}_{f,k}$ , using the canonical

identification. Furthermore, both Maslov indices relevant for the functoriality formula vanish (by the formula for the Maslov index in section 2.7 of [FFFS2]) since, by construction, two of the Lagrangian subspaces in their argument coincide.

The relevant part of  $M_k(X)$  has the form



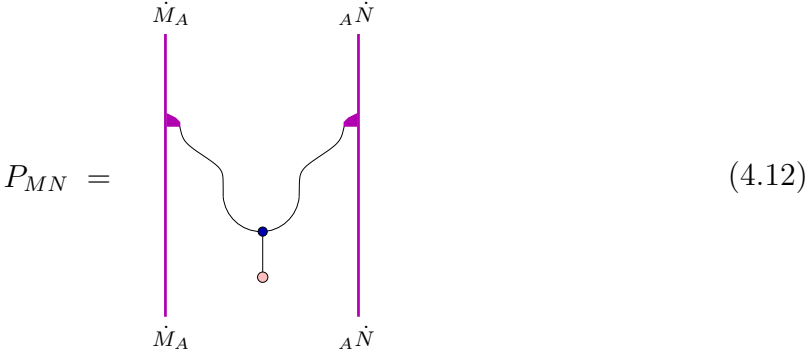
This contains half-annular ribbons in the  $z=0$ -plane, with unit radius, piercing the top and bottom boundary disks, respectively, as well as two additional coupons labelled by the morphisms  $\psi_\alpha^+ \in \text{Hom}_A(M_l \otimes U_k, M_r)$  and  $\psi_\beta^- \in \text{Hom}_A(M_r \otimes U_{\bar{k}}, M_l)$ . The shaded regions in (4.10) show the embedding of the world sheet  $\Gamma_{f,k,\alpha,\beta}^{\text{bnd}}(X)$  in  $M_k(X)$  (compare to the rightmost figure in (2.31)).

4.2. SOME ALGEBRAIC IDENTITIES.

The second ingredient to be used in the proof of boundary factorisation are some algebraic identities for certain morphism spaces; they are needed to transform the ribbon graph in (4.10). Consider a symmetric special Frobenius algebra  $A$  in a tensor category  $\mathcal{C}$  together with left and right  $A$ -modules,  ${}_A N$  and  $M_A$ , respectively. We can define a tensor product over  $A$  of the ordered pair consisting of  $M_A$  and  ${}_A N$  as

$$M_A \otimes_A {}_A N := \text{Im}(P_{MN}), \tag{4.11}$$

with  $P_{MN}$  the idempotent  $(\rho_r \otimes \rho_l) \circ (id_{\dot{M}_A} \otimes (\Delta \circ \eta) \otimes id_{\dot{A}\dot{N}}) \in \text{End}_{\mathcal{C}}(\dot{M} \otimes \dot{N})$ . Here  $\rho_{r/l}$  denote the right and left action of  $A$  on the respective modules; graphically,





Next we note that the dual  $\dot{M}^\vee$  of the object underlying a left  $A$ -module  $M$  carries a natural structure of a right  $A$ -module via

(4.13)

What we will use is that the intertwiner space  $\text{Hom}_A(M \otimes U, N)$  is canonically isomorphic to  $\text{Hom}^{(P)}(U, M^\vee \otimes N) := \{f \in \text{Hom}(U, M^\vee \otimes N) \mid P \circ f = f\}$  for  $P \equiv P_{M^\vee N}$ . The latter space is relevant because  $\text{Hom}^{(P)}(U, M^\vee \otimes N) \cong \text{Hom}(U, M^\vee \otimes_A N)$ , see lemma 2.4 in [FFRS]. An isomorphism  $\text{Hom}_A(M \otimes U, N) \rightarrow \text{Hom}^{(P)}(U, M^\vee \otimes N)$  is given by the map

(4.14)

(for the first equality, see lemma I:4.4(ii)), with inverse

(4.15)

That these two mappings are indeed each others' inverses follows directly from the properties of the duality in  $\mathcal{C}$ . For a simple object  $U_k$  we define an isomorphism  $\text{Hom}_A(N \otimes U_k, M)$

$\rightarrow \text{Hom}^{(P)}(M^\vee \otimes N, U_{\bar{k}})$ ,  $\psi \mapsto e_\psi$ , by

$$\begin{array}{c} U_{\bar{k}} \\ \downarrow \\ \boxed{e_\psi} \\ \downarrow \downarrow \\ M^\vee \quad \dot{N} \end{array} \quad := \quad \begin{array}{c} U_{\bar{k}} \\ \downarrow \\ \boxed{\psi} \\ \downarrow \downarrow \\ M^\vee \quad \dot{N} \end{array} \quad \begin{array}{c} \downarrow \\ \boxed{\bar{\lambda}^{k\bar{k}}} \\ \downarrow \end{array} \quad (4.16)$$

where  $\bar{\lambda}^{k\bar{k}} \in \text{Hom}(\mathbf{1}, U_k \otimes U_{\bar{k}})$  is the basis vector introduced in (2.25). This mapping is indeed an isomorphism; its inverse is a similar composition, using a coevaluation instead of the evaluation morphism, and  $\lambda_{k\bar{k}}$  instead of  $\bar{\lambda}^{k\bar{k}}$ .

Given a basis  $\{\psi_\alpha\}$  of  $\text{Hom}_A(N \otimes U_k, M)$ , the isomorphism (4.16) maps it to a basis  $\{e_\alpha\}$  of  $\text{Hom}^{(P)}(M^\vee \otimes N, U_{\bar{k}})$ . We also use two bases of  $\text{Hom}^{(P)}(U_{\bar{k}}, M^\vee \otimes N)$ : the basis  $\{\bar{e}_\alpha\}$  dual to  $\{e_\alpha\}$ , and the basis  $\{f_\beta\}$  induced from  $\psi_\beta \in \text{Hom}_A(M \otimes U_{\bar{k}}, N)$  by (4.14).

Now let  $M = M_r$  and  $N = M_l$ . As shown in (C.9), the matrix of structure constants for the boundary two-point function is given by

$$(c_{M_l, M_r, k}^{\text{bnd}})_{\alpha\beta} = \dim(U_k) L_{\alpha\beta}, \quad (4.17)$$

where  $L \equiv L(M_l, M_r, k)$  is the invertible matrix affording the basis transformation, according to  $f_\beta = \sum_\gamma L_{\gamma\beta} \bar{e}_\gamma$  (see (C.8)).

We also use the following

**4.3. LEMMA.** *For  $\{e_\alpha\}$  a basis of  $\text{Hom}^{(P)}(M^\vee \otimes N, U_{\bar{k}})$ , and  $\{\bar{e}_\alpha\}$  a dual basis of  $\text{Hom}^{(P)}(U_{\bar{k}}, M^\vee \otimes N)$ , the equality*

$$\sum_{k \in \mathcal{I}} \sum_{\alpha} \bar{e}_\alpha \circ e_\alpha = P_{M^\vee N} \quad (4.18)$$

holds.

Graphically,

$$\sum_{k \in \mathcal{I}} \sum_{\alpha} \begin{array}{c} M^\vee \quad \dot{N} \\ \downarrow \downarrow \\ \boxed{\bar{e}_\alpha} \\ \downarrow \\ U_{\bar{k}} \\ \downarrow \\ \boxed{e_\alpha} \\ \downarrow \downarrow \\ M^\vee \quad \dot{N} \end{array} \quad = \quad \begin{array}{c} M^\vee \quad \dot{N} \\ \downarrow \quad \downarrow \\ \text{cup} \\ \downarrow \quad \downarrow \\ M^\vee \quad \dot{N} \end{array} \quad (4.19)$$

PROOF. The statement is a consequence of dominance in  $\mathcal{C}$ , and of  $A$  being special and Frobenius. Starting from the right hand side, we proceed as follows:

$$(4.20)$$

where  $\tau^a \equiv \tau_{(M^\vee \dot{N})\bar{k}}^a$  and  $\bar{\tau}_a \equiv \bar{\tau}_a^{(M^\vee \dot{N})\bar{k}}$ . In the first step we use the fact that  $P_{M^\vee N}$  is an idempotent. Next, by dominance the identity morphism is decomposed as

$$id_{M^\vee \otimes \dot{N}} = \sum_{k \in \mathcal{I}} \sum_a \bar{\tau}_a^{(M^\vee, \dot{N})\bar{k}} \circ \tau_{(M^\vee, \dot{N})\bar{k}}^a \quad (4.21)$$

with dual bases  $\{\tau_{(M^\vee, \dot{N})\bar{k}}^a\}$  and  $\{\bar{\tau}_a^{(M^\vee, \dot{N})\bar{k}}\}$  of  $\text{Hom}(M^\vee \otimes \dot{N}, U_{\bar{k}})$  and  $\text{Hom}(U_{\bar{k}}, M^\vee \otimes \dot{N})$ , respectively. Now we may choose the former basis in such a way that each basis vector is an eigenvector of  $P_{M^\vee N}$ . Denote the index subset labelling the basis vectors with eigenvalue 1 as  $\{\alpha\}$ . By definition, the basis vectors indexed by  $\{\alpha\}$  provide a basis for  $\text{Hom}^{(P)}(U_{\bar{k}}, M^\vee \otimes N)$ , which we can choose to coincide with the basis  $e_\alpha$  defined above. The basis dual to  $\{\tau^a\}$  then has the same decomposition, so that the effect of the idempotents  $P_{M^\vee N}$  in (4.20) is to restrict the sum from the index set  $\{a\}$  to the subset  $\{\alpha\}$ . ■

#### 4.4. ORIENTED WORLD SHEETS.

We are now ready to prove theorem 2.9, that is, boundary factorisation for oriented world sheets.

PROOF OF THEOREM 2.9. Our task is to establish the equality (2.38). To this end we express both sides of (2.38) through cobordisms and prove that these two cobordisms give the same vector in  $\mathcal{H}(\widehat{X})$ . The relevant part of the cobordism for the left hand side has been displayed in (4.2), while the one for the right hand side is shown in (4.10). Note that as three-manifolds, the two cobordisms coincide, they only differ in the embedded ribbon graph.

In fact, instead of using the fragment of  $M_X[R_T]$  shown in (4.2), which is obtained by applying the construction of appendix B for the triangulation  $T$  of  $X$ , we use the ribbon graph  $R_{T'}$  obtained from a different triangulation  $T'$  that is given by adding one edge to  $T$ . The additional edge covers the interval along which  $X$  is to be cut. The ribbon graph  $R_{T'}$

differs from  $R_T$  by an idempotent  $P_{M^V N}$  inserted in (4.2). By proposition 3.2, changing the triangulation does not affect the vector in  $\mathcal{H}(\widehat{X})$ , i.e.  $Z(M_X[R_T]) = Z(M_X[R_{T'}])$ . Projecting the ribbon graphs to the plane (and looking upon them from the ‘white side’) we see that in order to establish the theorem it is sufficient to prove the following equality for morphisms in  $\text{End}(\dot{M}_r^V \otimes \dot{M}_l)$ :

$$= \sum_{k \in \mathcal{I}} \sum_{\alpha, \beta} \dim(U_k) (c_{M_l, M_r, k}^{\text{bnd}})^{-1}_{\beta\alpha} \quad (4.22)$$

To see that this equality holds, start from the right hand side, apply the isomorphisms (4.16) and (4.14) to  $\psi_\alpha^+$  and  $\psi_\beta^-$ , respectively, and expand the latter in terms of the basis  $\{\bar{e}_\gamma\}$ ; this gives

$$\sum_{k \in \mathcal{I}} \sum_{\alpha, \beta} \dim(U_k) (c_{M_l, M_r, k}^{\text{bnd}})^{-1}_{\beta\alpha} \sum_{\gamma} L_{\gamma\beta} \quad (4.23)$$

Using the inverse of the relation (4.17), carrying out the sum over the bases of intertwiner spaces and isomorphism classes of simple objects, and applying (4.19), we can rewrite (4.23) as the left hand side of

$$\sum_{k \in \mathcal{I}} \sum_{\alpha, \beta, \gamma} L_{\gamma\beta} L_{\beta\alpha}^{-1} \quad (4.24)$$

which is equal to the left hand side of (4.22). This establishes the equality (4.22).  $\blacksquare$

#### 4.5. UNORIENTED WORLD SHEETS.

The proof of theorem 2.10 for the case that the map  $f$  satisfies condition (i) of the theorem is identical to the argument given above for oriented world sheets. Before we can outline the proof for  $f$  satisfying condition (ii) instead, we need to present the details on how to obtain the world sheet  $\Gamma_{f,k,\alpha,\beta}^{\text{bnd}}(\mathbb{X})$  in that case.

CONSTRUCTION OF  $\Gamma_{f,k,\alpha,\beta}^{\text{bnd}}(\mathbb{X})$  FOR  $f: R'_\varepsilon \rightarrow \mathbb{X}$ . The reason to present these details only here is a technical complication in the labelling of boundary conditions which makes the description somewhat lengthy. To construct  $\Gamma_{f,k,\alpha,\beta}^{\text{bnd}}(\mathbb{X})$  for a given map  $f: R'_\varepsilon \rightarrow \mathbb{X}$  we distinguish two cases:

- $f(1)$  and  $f(-1)$  lie on different connected components of  $\partial\mathbb{X}$ . Then we choose an equivalent labelling of the boundary component containing  $f(1)$  with opposite orientation (as explained in section B.4). The map  $f$  is then orientation preserving as a map from  $R'_\varepsilon$  to  $\mathbb{X}$ , and the procedure of section 2.7 can be applied to obtain  $\Gamma_{f,k,\alpha,\beta}^{\text{bnd}}(\mathbb{X})$ .  
In fact, this procedure reduces the proof of theorem 2.10 in case (ii) to the proof of case (i), so that the only situation requiring a special treatment is the next one.
- $f(1)$  and  $f(-1)$  lie on the same connected component of  $\partial\mathbb{X}$ . This happens for example when cutting the Möbius strip along an interval.

The rest of this section deals with the case that  $f(1)$  and  $f(-1)$  lie on the same connected component of  $\partial\mathbb{X}$ .

Let us again start from a situation analogous to that displayed in figure (2.31). Let as in section B.4  $(M_1, \dots, M_{n'}; \Psi_1, \dots, \Psi_n; \text{or}_1)$  be the boundary data labelling the boundary component shown in the leftmost picture of (2.31), such that  $\text{or}_1$  assigns to both boundary intervals an orientation downwards, and the left component is labelled by  $M_1$  while the right is labelled by  $M_m$  for some  $1 \leq m \leq n'$ . We then glue the half disks  $D_\varepsilon^\pm$  as in (2.30). Next we must provide labels  $(M'_1, \dots, M'_{n'+2}; \Psi'_1, \dots, \Psi'_{n'+2}; \text{or}'_1)$  for the resulting boundary component. Choose  $\text{or}'_1$  to be the orientation induced by  $\text{or}_1$  on the left boundary component above the cut. Start on the segment to the left, above the cut, and move along the boundary in the direction opposite to  $\text{or}'_1$ , and label the segments between boundary insertions with  $M'_j := M_j$  for  $1 \leq j \leq m$ . We then end up on the right segment, below the cut. Switch to the left segment below the cut and again move along the boundary in the direction opposite to  $\text{or}'_1$ , labelling the segments with  $M'_{m+1} := M_1^\sigma$  (with  $M^\sigma$  the  $\tilde{A}$ -module defined in (A.16)), and  $M'_j := M_{n'+m+2-j}^\sigma$  for  $m+2 \leq j \leq n'+2$ . For the field insertions we perform the same manipulations again, starting on the left segment above the cut and defining  $\Psi'_j := \Psi_j$  for  $1 \leq j \leq m-1$ .

Next, define

$$\Psi'_m := (M'_m, M'_{m+1}, U_k, s(\psi_\alpha^+) \circ (id_{M'_{m+1}} \otimes \theta_{U_k}^{-1}), p^+, [\gamma^+]) \quad (4.25)$$

and, for  $m+1 \leq j \leq n'+1$ ,

$$\Psi'_j := (M'_j, M'_{j+1}, V_{n'+m+2-j}, \psi'_j, [\gamma_{n'+m+2-j}]) \quad (4.26)$$

with

$$\psi'_j = \begin{cases} s(\psi_{n'+m+2-j}) & \text{if } \text{or}'_1 = \text{or}(\gamma'_j), \\ s(\psi_{n'+m+2-j}) \circ (id_{M'_j} \otimes \theta_{V_{n'+m+2-j}}^{-1}) & \text{if } \text{or}'_1 = -\text{or}(\gamma'_j), \end{cases} \quad (4.27)$$

and finally

$$\Psi'_{n+2} := (M'_{n'+2}, M'_1, U_{\bar{k}}, \psi_{\bar{\beta}}^-, [\gamma^-]). \quad (4.28)$$

Adopting all other data from  $X$ , this defines the new world sheet  $\Gamma_{f,k,\alpha,\beta}^{\text{bnd}}(X)$ .

**BOUNDARY FACTORISATION FOR  $f: R'_\varepsilon \rightarrow X$ .** For the proof in case (ii) of theorem 2.10, let us proceed as in case (i) and first consider the geometric setup.

The part of the world sheet  $X$  containing the image of  $R'_\varepsilon$  under  $f$  is given by the leftmost figure in (2.31), with both boundary fragments oriented downward, and with the right fragment labelled by  $M_r^\sigma$  instead of  $M_r$ . The corresponding part of the world sheet  $\Gamma_{f,k,\alpha,\beta}^{\text{bnd}}(X)$  obtained after cutting is given by the rightmost figure in (2.31), with the lower boundary fragment having opposite orientation and the labels being  $M_l^\sigma$ ,  $M_r^\sigma$  and  $s(\psi^+) \circ (id_{M_r} \otimes \theta_{U_k}^{-1})$  instead of  $M_l$ ,  $M_r$  and  $\psi^+$ .

The left hand side of (2.39) is given by the invariant of the cobordism  $M_X$ , of which the relevant part is, similar to figure (4.2)

Here we used a triangulation of  $X$  with an edge lying on the interval along which  $X$  is to be cut. In the second representation we inserted definitions (II:3.4) and (II:2.26) and slightly deformed the resulting ribbon graph. (Also, unlike in figure (4.2), here we refrain from explicitly indicating the location of the world sheet by a shading.)

Expressing the right hand side of (2.39) via cobordisms leads to

$$\sum_{k,\alpha,\beta} \dim(U_k) (c_{M_l, M_r, k}^{\text{bnd}})^{-1}_{\beta\alpha} \quad = \quad \sum_{k,\alpha,\beta} L_{\beta\alpha}^{-1} \quad (4.30)$$

where, like in the corresponding figure (4.10) in the oriented case, only the relevant fragment of the cobordism for  $G_{f,k}^{\text{bnd}}(C_{\hat{A}}(\Gamma_{f,k,\alpha,\beta}^{\text{bnd}}(\mathbf{X})))$  is shown. Also, in the first figure we have set  $\psi = s(\psi_\alpha^+) \circ (id_{M_r^\sigma} \otimes \theta_{U_k}^{-1})$ , while in the second figure the definition (B.13) of  $s$  has been inserted.

One can now follow the argument in section 4.4 to show that (4.29) and (4.30) describe the same vector in  $\mathcal{H}(\hat{\mathbf{X}})$ . Note that to this end one needs to push the half-twist on the top-right module ribbon in (4.29) further along the boundary component (not shown in the figure) until it emerges at the bottom left module ribbon. That this is the place where it reappears when following the boundary leaving figure (4.29) at the top right corner follows from the choice of orientations and the fact that by assumption both module ribbons in (4.29) lie on the same connected component of  $\iota(\partial\mathbf{X})$ .

## 5. Proof of bulk factorisation

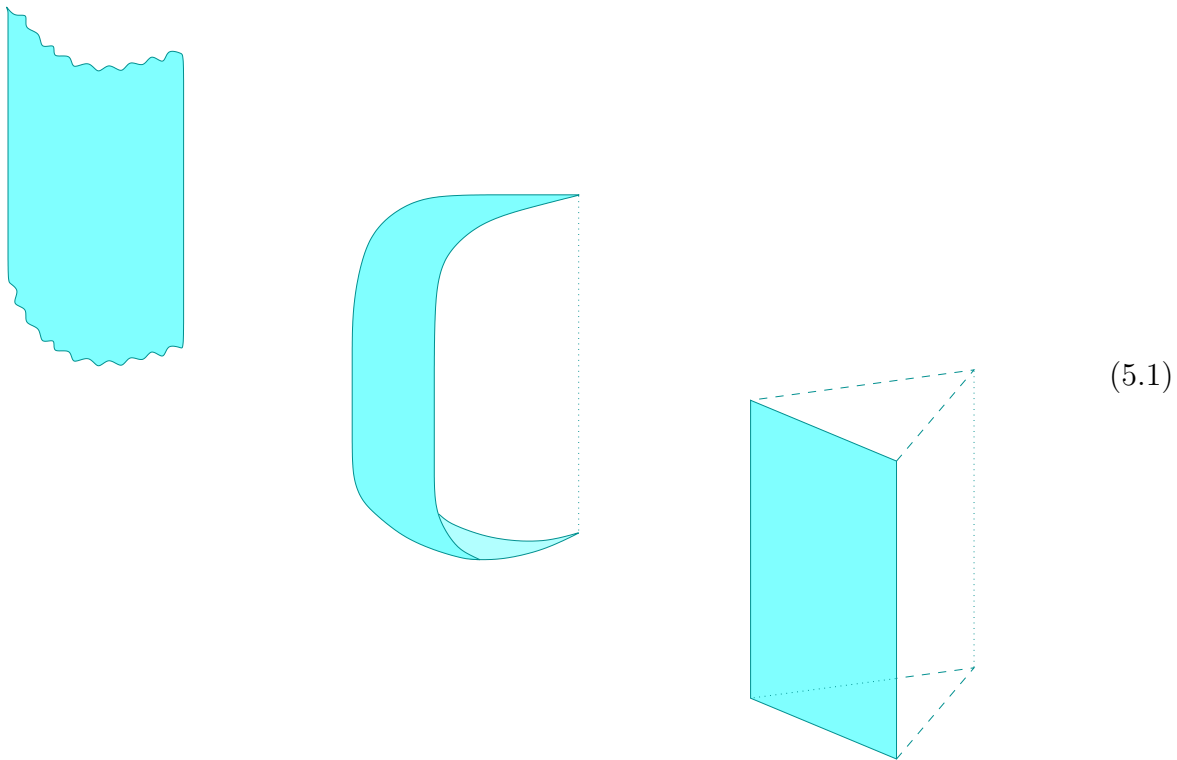
In this section we present the proof of factorisation for bulk correlators, theorem 2.13. Similarly to the case of boundary factorisation, we must first clarify the geometry underlying the two sides of the equalities (2.50) and (2.51), and then establish some algebraic identities to be used in the proof.

### 5.1. GEOMETRIC SETUP OF BULK FACTORISATION.

The construction in this section applies to both oriented and unoriented world sheets. Like in section 4.1, the reason is that the embedding  $f: A_\varepsilon \rightarrow \mathbf{X}$  induces a local orientation on the relevant part of the world sheet  $\mathbf{X}$ .

We are interested in the geometry of the relevant surfaces and three-manifolds in a neighbourhood of the region to which the ‘cutting twice’ procedure (2.19) is applied. Throughout this section we will make use of a ‘wedge presentation’ of surfaces and three-manifolds to illustrate the geometry. By this we mean that a horizontal disk is drawn

as a disk *sector*, with identification of the legs of the sector implied (compare also e.g. picture (II:A.81)). Further, curly lines indicate interfaces at which the displayed piece is connected to other parts of the manifold. To give an example, in this presentation the pictures

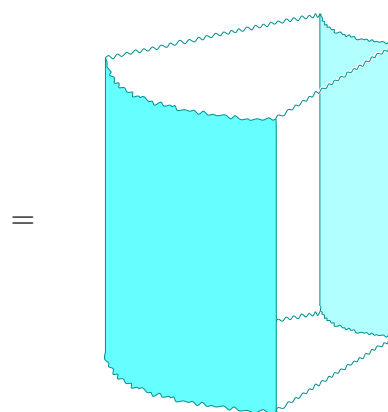
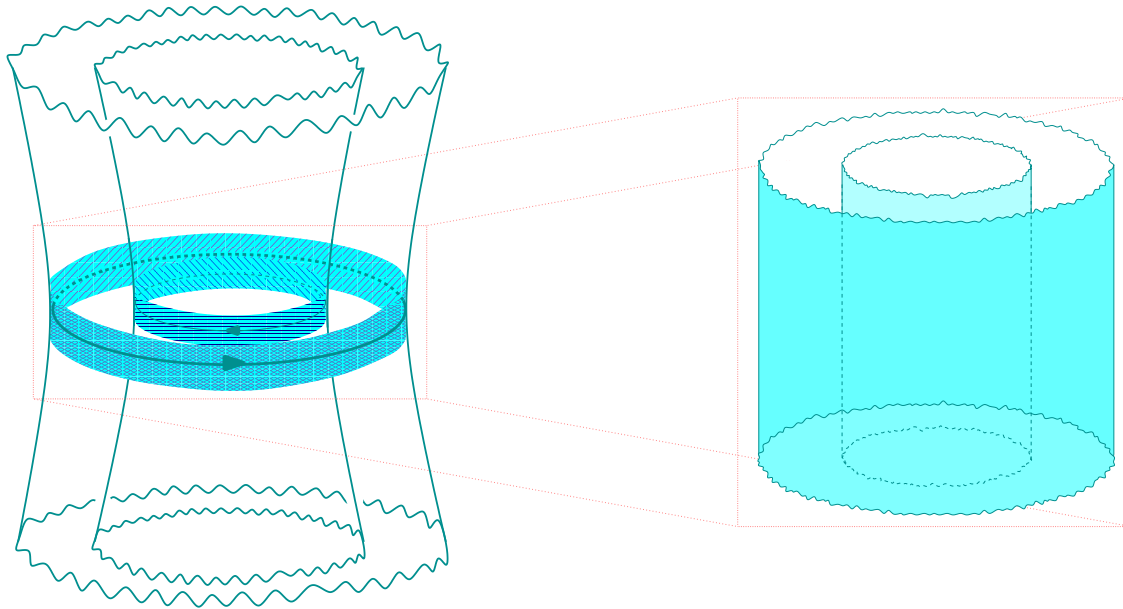


stand for a cylindrical part of a two-manifold, for a solid three-ball, and for a solid torus, respectively; in the latter case, the additional identification of top and bottom faces is indicated by drawing the corresponding legs as dashed lines. Also, it is implied that whenever top and bottom or two vertical faces of a wedge are identified, this is to be performed without any additional rotation or reflection. (For instance, in the middle picture the boundary of the three-manifold is a sphere rather than a cross cap.)

The left hand side of formula (2.50) concerns the connecting manifold  $M_X$ . Let  $N_X \subset M_X$  consist of all points that are mapped to  $f(A_\varepsilon)$  via the canonical projection  $\pi: M_X \rightarrow X$ .  $N_X$  has the topology of a solid cylinder with a solid cylinder cut out, and it contains  $A$ -ribbons which cover the part of a triangulation of  $\iota(X)$  that lies in  $N_X$ . Accordingly, the boundary  $\partial N_X$  has two annular connected components  $\partial N_X^{(1)}$  and  $\partial N_X^{(2)}$ . Let  $\partial N_X^{(1)}$  be the component for which (the restriction to  $\partial N_X$  of) the projection  $\pi$  is orientation preserving. With suitable choice of coordinates,  $\partial N_X^{(2)}$  is a cylinder of radius 2 and  $\partial N_X^{(1)}$  a cylinder of radius 1, and the common axis of  $\partial N_X^{(2)}$  and  $\partial N_X^{(1)}$  is the  $z$ -axis. In this description, the rest of  $M_X$  is connected to the annular top and bottom parts of



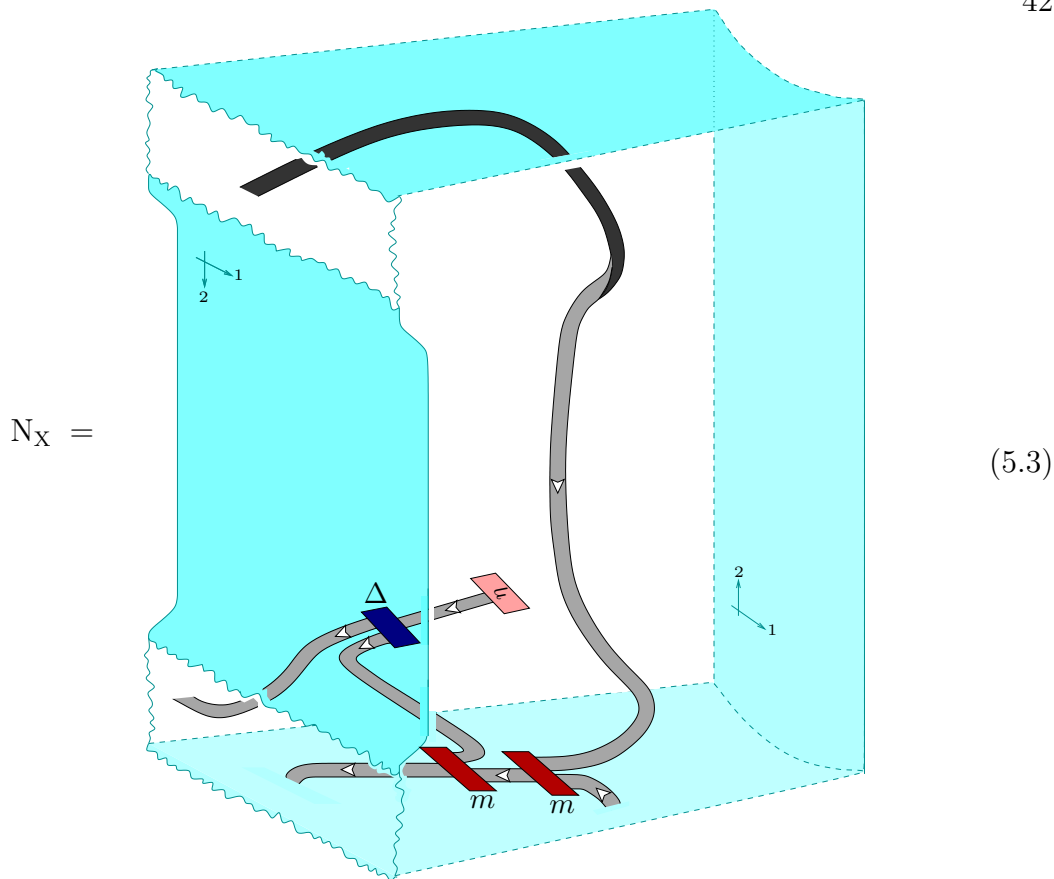
$\partial N_X$ . This situation is illustrated in the following picture:



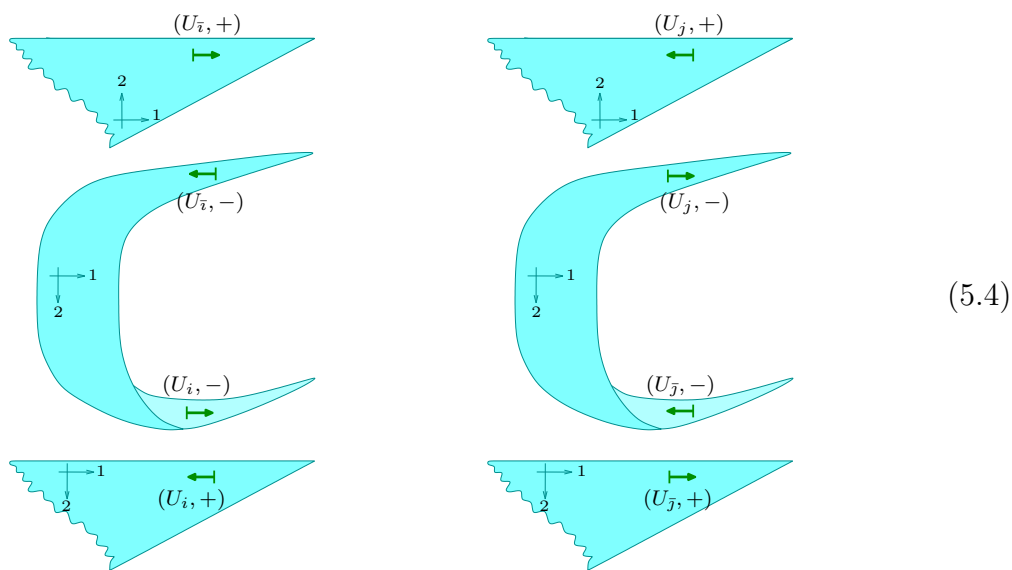
(5.2)

The two collars forming the subset  $\partial M_X \cap N_X$  of the boundary  $\partial M_X$  are indicated in colours. Note that by definition they coincide with the images  $f_i(A_\varepsilon)$  and  $f_j(A_\varepsilon)$  for  $f_i$  and  $f_j$  as introduced in (2.46). Zooming in on  $N_X$  results in the upper figure on the right hand side, which is then redrawn in wedge presentation in the lower figure.

It will be convenient, however, to slightly deform  $N_X$  in a region close to its boundary. Including also the ribbon graph, the resulting manifold, which we still denote by  $N_X$ , then looks as follows (in this picture, now the part  $\partial N_X^{(1)}$  of the boundary extends over both the inner cylindrical piece and the top and bottom parts):

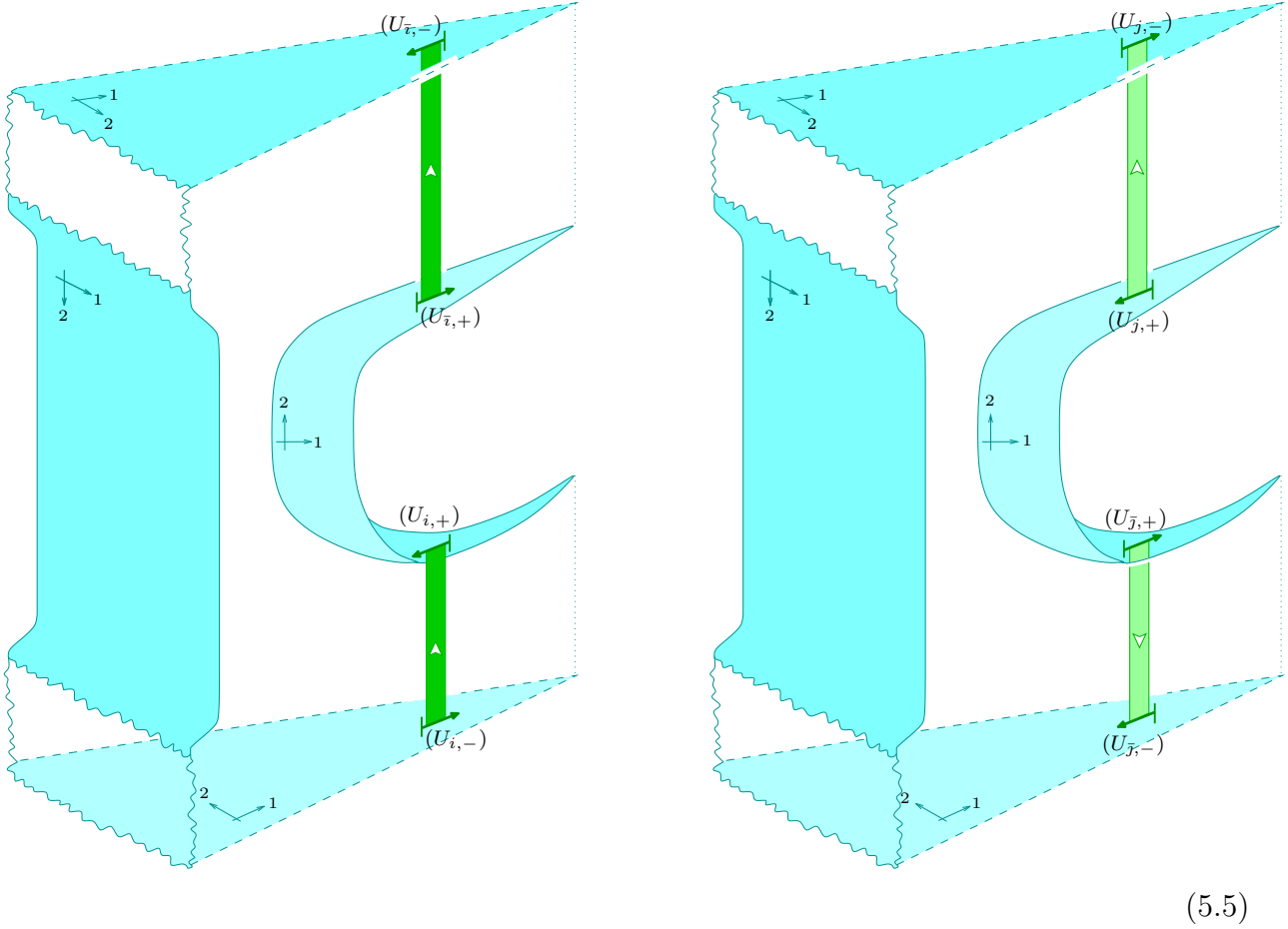


The relevant region of the extended surface  $Y_{ij}$  that was defined in (2.47) is embedded in two copies of  $\mathbb{R}^3$  in the following manner:<sup>6</sup>



<sup>6</sup> In each copy of  $\mathbb{R}^3$  there are two calottes and one sphere. Thus, in non-wedge representation, each of these surface fragments is a copy of the piece of two-manifold displayed in the rightmost figure of (2.19).

Next, we consider part of the cobordism<sup>7</sup> from  $Y_{ij}$  to  $\widehat{X}$ , used in defining  $\hat{g}_{f,i} \circ \hat{g}_{f,j}$ :

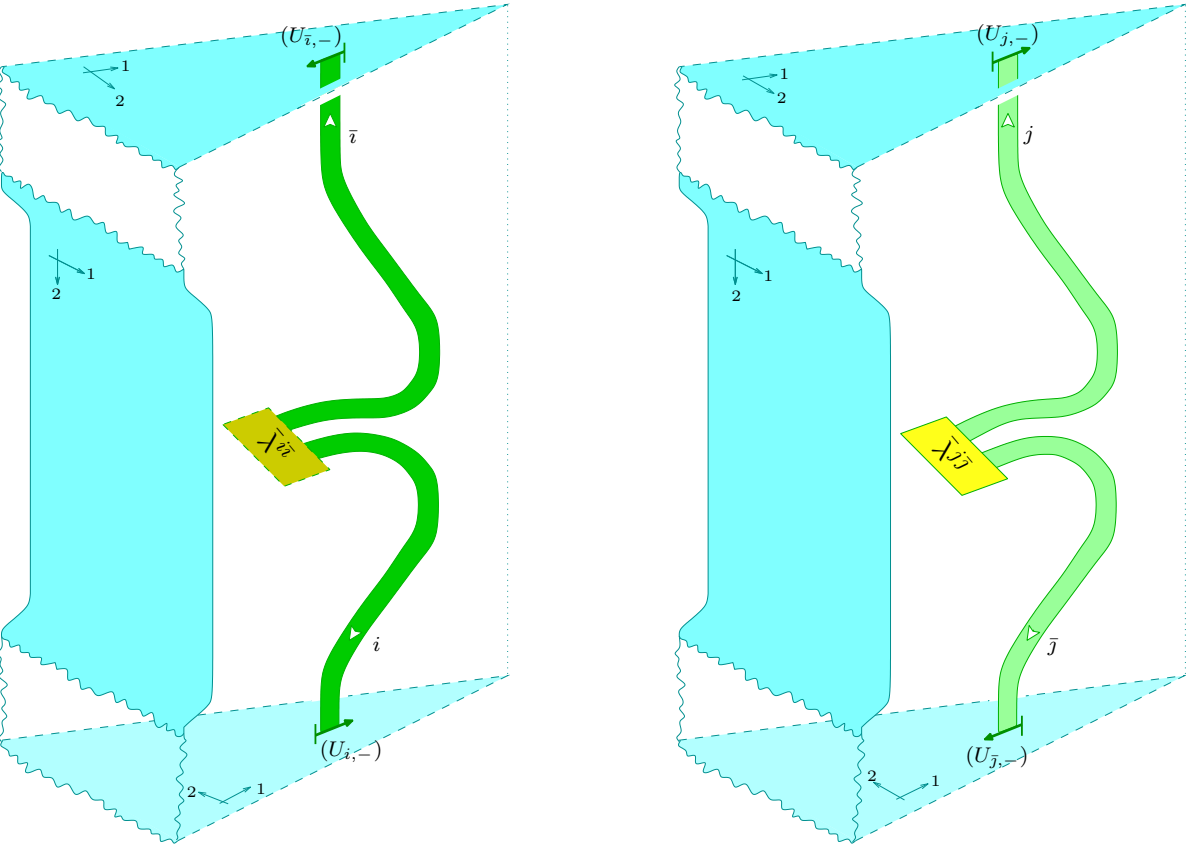


There are now ribbons running inside the cobordism, ending on the marked arcs on  $-Y_{ij}$ , with orientations as shown in the picture. The core orientation of each ribbon points away from the spherical boundary components. The two (‘outgoing’) cylindrical boundary components, which correspond to  $\partial N_X^{(2)}$  and  $\partial N_X^{(1)}$  in (5.3), respectively, have different orientation.

The gluing homomorphism  $G_{f,i,j}^{\text{bulk}}$  is the invariant of the cobordism that is obtained by gluing  $B_{i\bar{i}}^-$  and  $B_{j\bar{j}}^-$  to the (‘incoming’) spherical boundary components of (5.5), using the canonical identification of the spherical boundary components. The result is the following

<sup>7</sup> In non-wedge representation, this amounts to two copies of the three-manifold (2.20). The annular parts at the top and bottom, at which (2.20) is joined to the rest of the cobordism, correspond to the curly lines in (5.5).

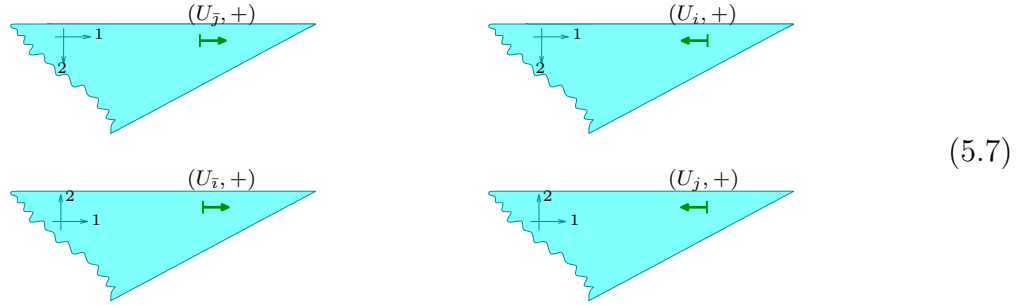
cobordism from  $\widehat{X}'_{ij}$  to  $\widehat{X}$  (recall that  $X'_{ij}$  is an abbreviation for  $\Gamma_{f,i,j,\alpha,\beta}^{\text{bulk}}(X)$ ):



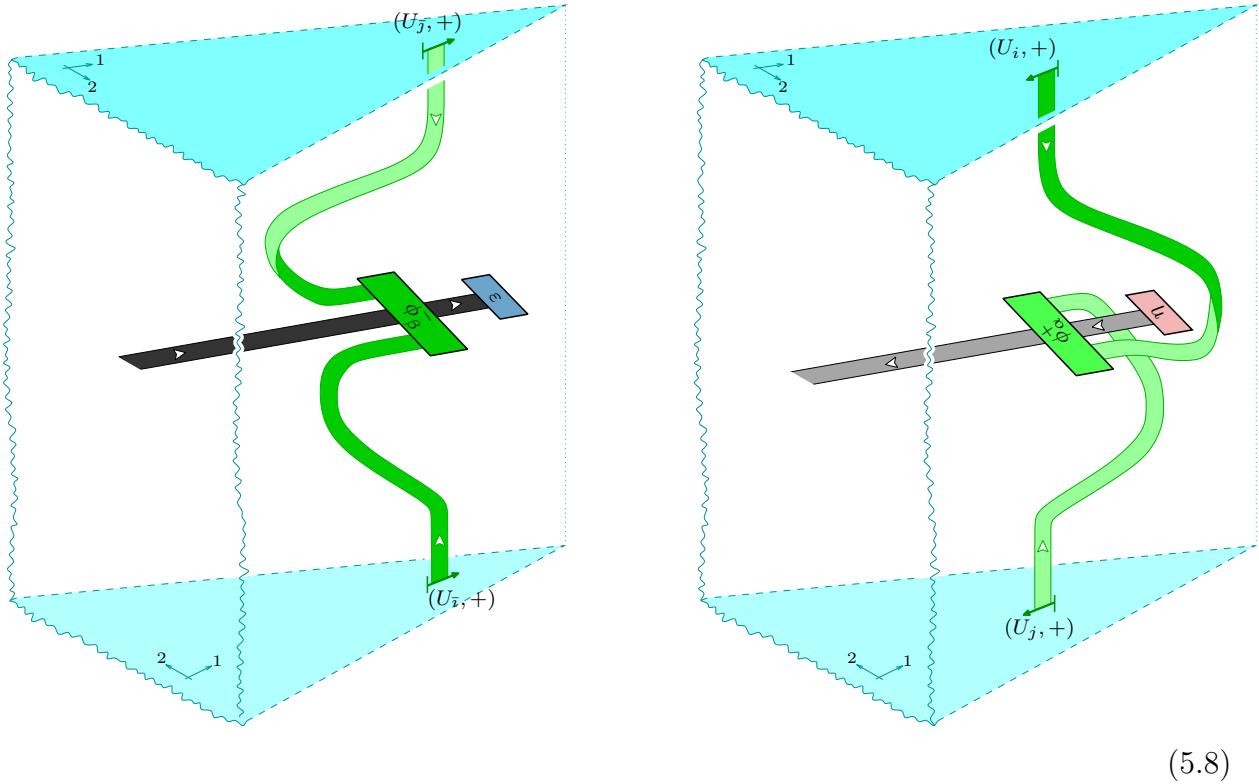
(5.6)

Of the connecting manifold  $M_{X'_{ij}}$ , the part of interest to us is a neighbourhood of the region where  $X'_{ij}$  is cut and pasted, or more precisely, small disks containing the bulk field insertions. We embed these disks in two copies of  $\mathbb{R}^3$  in the plane  $z = 3/2$ , centered at the point  $(0, 0, 3/2)$ , at which the insertion points  $p^\pm \in X$  are placed. The orientation of the first disk is the one inherited from the  $x$ - $y$ -plane passing through  $z$ , and a representative arc  $\gamma^-$  is aligned along the  $x$ -axis with the same orientation as the axis. The orientation and arc-orientation (for  $\gamma^+$ ) on the second disk are opposite to those of the first. On  $\widehat{X}'_{ij}$  each of the disks has two pre-images, at  $z = 1$  and  $z = 2$ , respectively. The marked arcs are labelled by  $(U_{i,+})$ ,  $(U_{j,+})$ ,  $(U_{i,-})$  and  $(U_{j,-})$ , respectively, and the surface- and

arc-orientations are as indicated in the following figure:



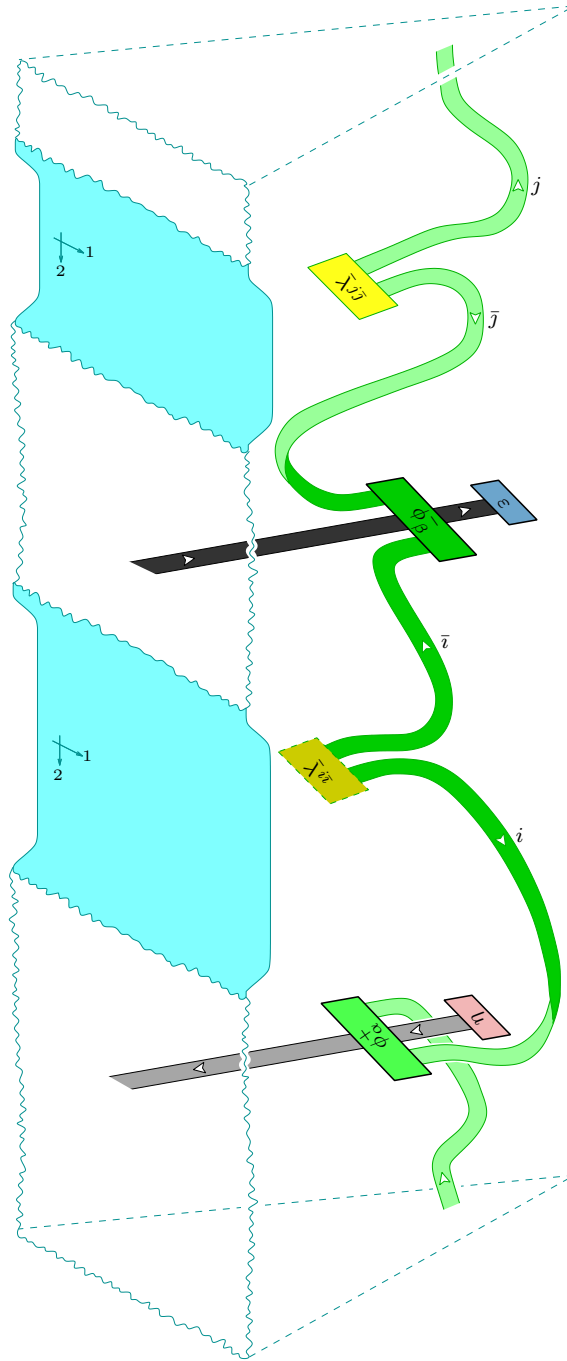
The relevant part of the connecting manifold  $M_{X'_{ij}}$  consists of two full cylinders, with the rest of  $M_{X'_{ij}}$  connected to the cylindrical parts of their boundaries:



The coupon in the piece of three-manifold in the left part of the figure is labelled by a bimodule morphism  $\phi_\beta^- \in \text{Hom}_{A|A}(U_{\bar{i}} \otimes^+ A \otimes^- U_j, A)$ , and the one in the right part by a bimodule morphism  $\phi_\alpha^+ \in \text{Hom}_{A|A}(U_i \otimes^+ A \otimes^- U_j, A)$ .

When using the canonical identification to glue  $M_{X'_{ij}}$  to the cobordism (5.6), the

resulting cobordism from  $\emptyset$  to  $\widehat{X}$  is



(5.9)

Here top and bottom are identified; for the coupons labelled by  $\phi_{\alpha}^{+}$  and  $\bar{\lambda}^{j\bar{j}}$  it is the white side that is facing upwards, while for the coupons labelled by  $\phi_{\beta}^{-}$  and  $\bar{\lambda}^{i\bar{i}}$  it is the black side. Again two of the Lagrangian subspaces coincide in each of the two Maslov indices relevant for the functoriality formula, so the latter cobordism is precisely the cobordism on the right hand side of the desired equality (2.50).

5.2. A SURGERY IDENTITY.

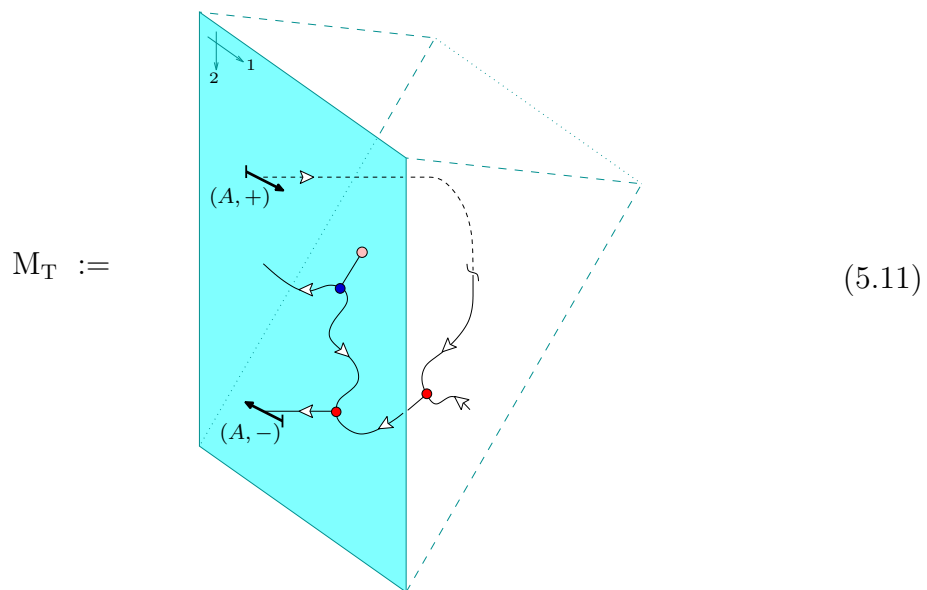
Having sorted out the situation of our interest at the geometrical level, we proceed to establish a few intermediate results in preparation of the proof. First, consider a tubular neighbourhood  $M_{ij,\alpha\beta}$  of all the vertical ribbons in figure (5.9), obtained by cutting along surface that in the presentation used in figure (5.9) is a vertical cylinder close to the displayed parts of the boundary. Orient its boundary  $\partial M_{ij,\alpha\beta}$  by the inward-pointing normal. This boundary is pierced at two arcs by  $A$ -ribbons; the directions of these arcs are given by the orientation induced from the ribbon orientation via the inward-pointing normal. The upper arc is labelled by  $(A, +)$ , and the lower one by  $(A, -)$ . With this prescription, and with the canonical choice of Lagrangian subspace (see (B.7)), the boundary becomes an extended surface, to be denoted by  $T_{A,A}$ , and  $M_{ij,\alpha\beta}$  a cobordism from  $\emptyset$  to  $T_{A,A}$ .

In blackboard framing we have

$M_{ij,\alpha\beta} =$  (5.10)

Next, define another cobordism  $M_T$  from  $\emptyset$  to  $T_{A,A}$  by taking  $M_T$  to be a solid torus with boundary  $T_{A,A}$ . However, referring to the graphical presentation in figure (5.10), while in  $M_{ij,\alpha\beta}$  a horizontal cycle is contractible, we choose  $M_T$  in such a manner that a vertical cycle is contractible. Note that with respect to  $M_T$  it is then not the canonical Lagrangian subspace that appears in  $T_{A,A}$ .

Place  $A$ -ribbons in  $M_T$  as indicated in the following figure:



(The  $A$ -ribbons entering on the front face and leaving the back face are connected, due to the identification of those two faces.)

5.3. PROPOSITION. *The cobordisms  $M_{ij,\alpha\beta}$  and  $M_T$  are related by*

$$Z(M_T, \emptyset, T_{A,A}) = \sum_{i,j,\alpha,\beta} \dim(U_i) \dim(U_j) (c_{i,j}^{\text{bulk}^{-1}})_{\beta\alpha} Z(M_{ij,\alpha\beta}, \emptyset, T_{A,A}). \quad (5.12)$$

Before proving this statement, we will need to establish two lemmas:

- The left side of (5.12) can be written as an expansion with respect to a basis of  $\mathcal{H}(T_{A,A})$ , and it is shown that the resulting summation can be restricted to the vectors  $Z(M_{ij,\alpha\beta}, \emptyset, T_{A,A})$ .
- By evaluating both sides on a basis of  $\text{Hom}(\mathcal{H}(T_{A,A}), \mathbb{C})$ , the expansion coefficients are shown to be those given in (5.12).

We first select a convenient basis of  $\text{Hom}(\mathbb{C}, \mathcal{H}(T_{A,A}))$  and introduce a certain cobordism  $P: T_{A,A} \rightarrow T_{A,A}$ . The basis of  $\text{Hom}(\mathbb{C}, \mathcal{H}(T_{A,A}))$  is provided by the invariants of the



cobordisms

$$L_{ij,\alpha\beta} := \text{Diagram} \quad (5.13)$$

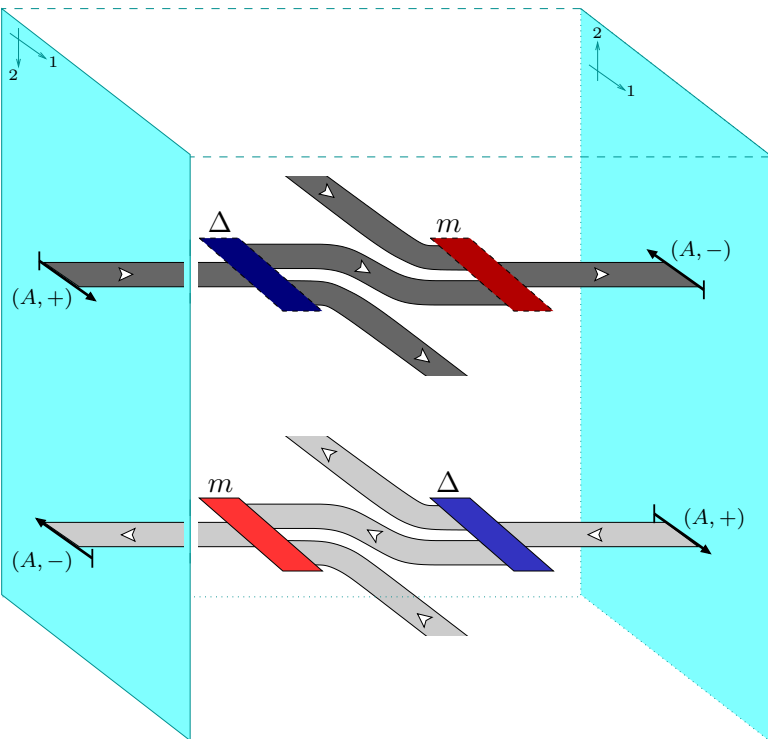
with  $\alpha$  and  $\beta$  running over a basis of  $\text{Hom}(U_i \otimes U_j, A)$  and of  $\text{Hom}(U_{\bar{i}} \otimes A \otimes U_{\bar{j}}, \mathbf{1})$ , respectively. It is not difficult to see that the collection of invariants of the cobordisms  $L_{ij,\alpha\beta}$ , for all values of  $i, j, \alpha, \beta$ , indeed forms a basis. By the general construction given in [Tu] (see lemma 2.1.3 in chapter IV), the space  $\mathcal{H}(\mathbb{T}_{A,A})$  is isomorphic to

$$\bigoplus_{i \in \mathcal{I}} \text{Hom}(\mathbf{1}, A^\vee \otimes U_i \otimes U_i^\vee \otimes A) \cong \bigoplus_{i,j \in \mathcal{I}} \text{Hom}(\mathbf{1}, A^\vee \otimes U_i \otimes U_j) \otimes_{\mathbb{C}} \text{Hom}(\mathbf{1}, U_j^\vee \otimes U_i^\vee \otimes A). \quad (5.14)$$

In the case of (5.13), the isomorphism is provided by first choosing bijections  $\text{Hom}(U_i \otimes U_j, A) \cong \text{Hom}(\mathbf{1}, A^\vee \otimes U_i \otimes U_j)$  and  $\text{Hom}(U_{\bar{i}} \otimes A \otimes U_{\bar{j}}, \mathbf{1}) \cong \text{Hom}(\mathbf{1}, U_j^\vee \otimes U_i^\vee \otimes A)$ . Then one uses these bijections to assign labels to the two larger coupons in (5.13) for each element of (5.14).

The cobordism  $P$  is obtained as follows. In the cylinder  $\mathbb{T}_{A,A} \times [0, 1]$  over  $\mathbb{T}_{A,A}$ , insert two straight  $A$ -ribbons that connect the marked arcs on  $\mathbb{T}_{A,A} \times \{0\}$  to those at  $\mathbb{T}_{A,A} \times \{1\}$ , as well as two  $A$ -ribbons in the interior running along one of the non-contractible cycles, joined to the straight  $A$ -ribbons by a coproduct on one side and a product on the other.

Thus

P = 

(5.15)

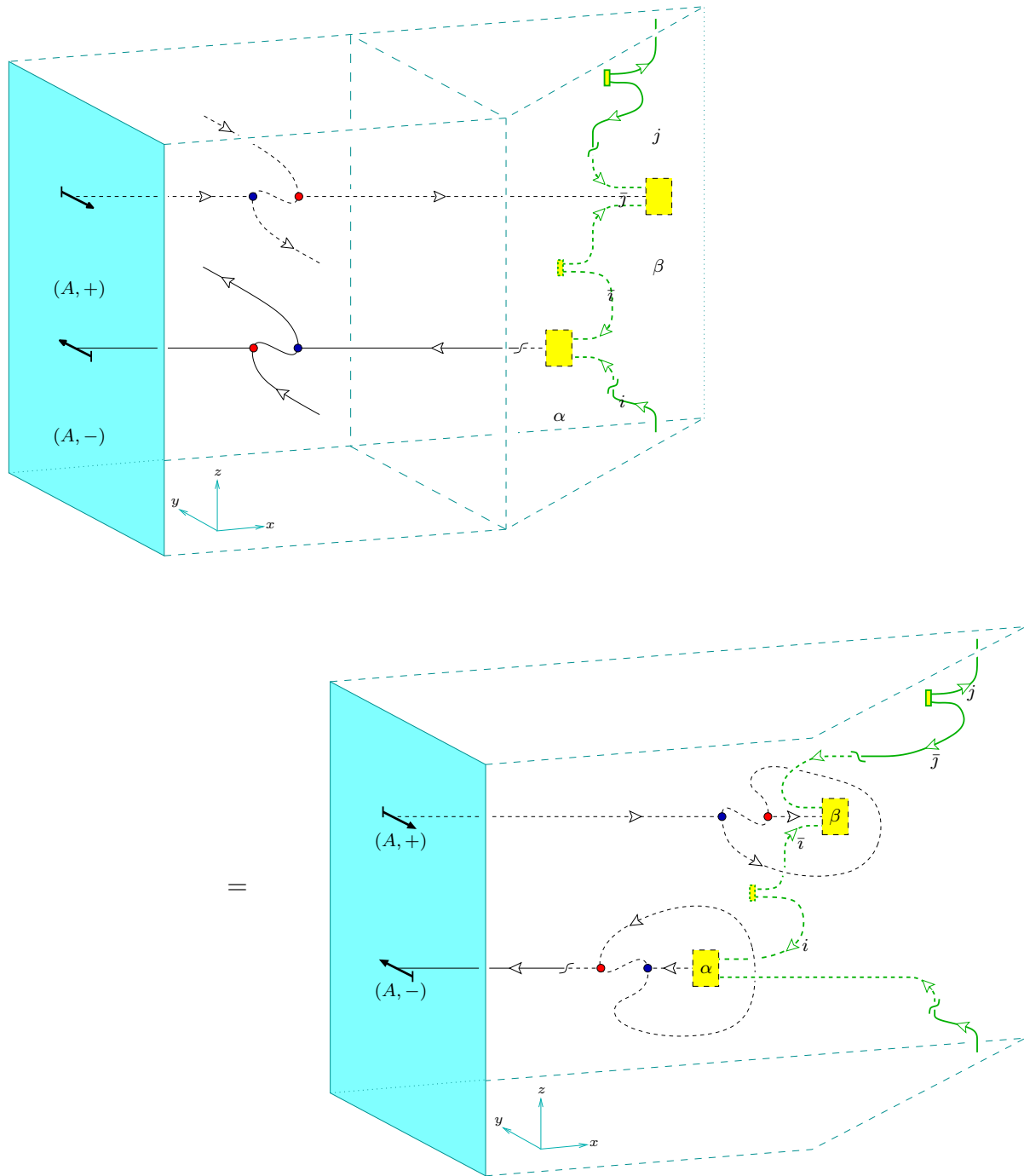
#### 5.4. LEMMA.

- (i)  $Z(P) \in \text{End}(\mathcal{H}(T_{A,A}))$  is a projector.
- (ii)  $Z(P)$  projects onto the subspace spanned by  $\{Z(M_{ij,\alpha\beta}, \emptyset, T_{A,A})1\}_{i,j,\alpha,\beta}$ , with  $M_{ij,\alpha\beta}$  the cobordisms introduced in (5.10).
- (iii) The invariants of the cobordisms  $P \circ M_T$  and  $M_T$  are equal,  $Z(P \circ M_T) = Z(M_T)$ .

PROOF. (i) That  $Z(P) \circ Z(P) = Z(P)$  follows easily by using associativity, coassociativity, specialness and the Frobenius property; compare the similar calculation in (I:5.36).

(ii) Consider the action of  $Z(P)$  on one of the basis elements  $Z(L_{ij,\alpha\beta})1 \in \mathcal{H}(T_{A,A})$ . The

ribbon graph for  $Z(P \circ L_{ij,\alpha\beta})$  can be deformed as follows.

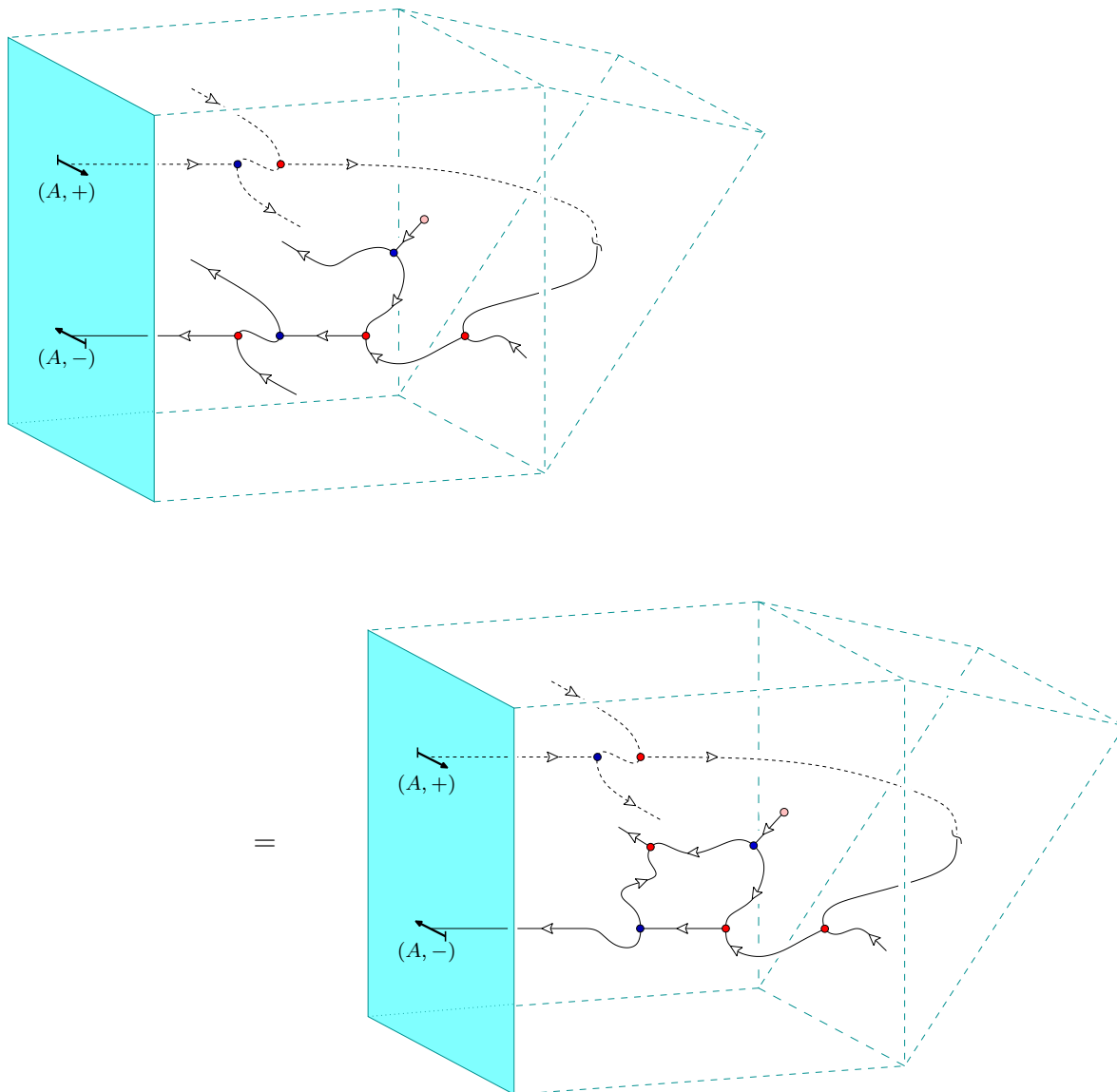


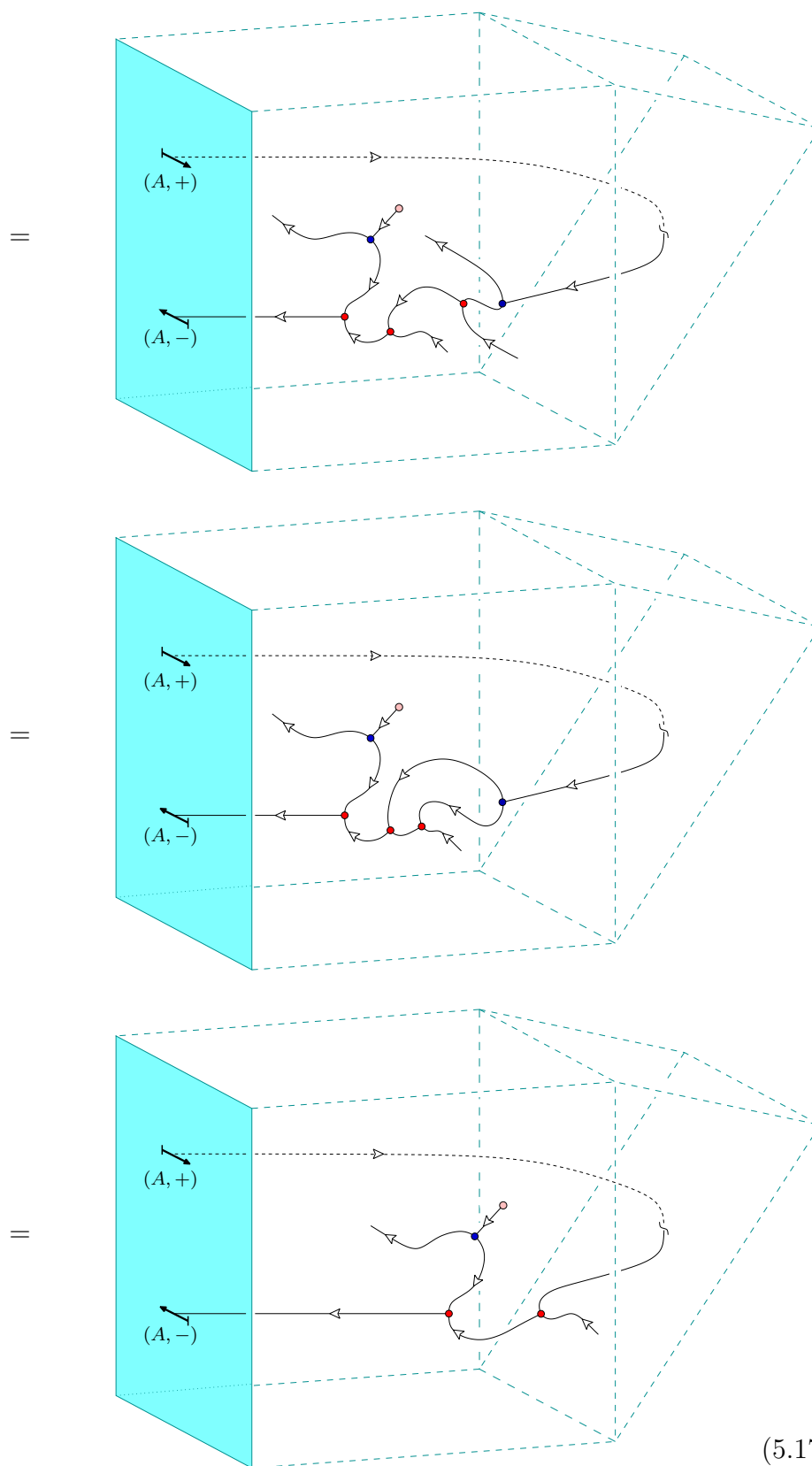
(5.16)

To see that this equality holds, notice that the figure on the right hand side is obtained from the left by a deformation: the  $A$ -ribbons parallel to the  $y$ -axis are moved to the right

until the ends join at the trivial cycle at the far right. The morphisms together with the encircling  $A$ -ribbons can now be recognised as local morphisms according to lemma D.2. Further, by combining proposition I:5.7 and lemma IV:2.2 one sees that bases for the corresponding spaces of local morphisms are provided by  $\phi_{(ij)\alpha} \in \text{Hom}_{A|A}(U_i \otimes^+ A \otimes^- U_j, A)$  and  $\phi_{(\bar{i}\bar{j})\beta} \in \text{Hom}_{A|A}(U_{\bar{i}} \otimes^+ A \otimes^- U_{\bar{j}}, A)$ . It follows that  $Z(P \circ L_{ij,\alpha\beta})$  can be expanded in terms of  $Z(M_{ij,\alpha\beta})$ , establishing that the image of  $Z(P)$  is contained in the subspace spanned by the vectors  $Z(M_{ij,\alpha\beta})$ .

(iii) The Frobenius property and specialness guarantee that the cobordism resulting from gluing  $P$  to  $M_T$  has the same invariant as  $M_T$ . In more detail, this is demonstrated by the following sequence of equalities:





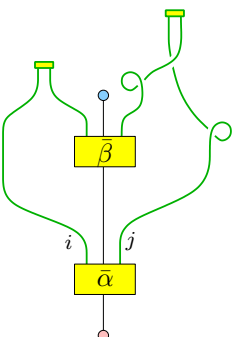
To see these equalities, one proceeds as follows. In the first step the Frobenius and associativity properties are employed to attach the ‘left-most’  $A$ -ribbon – i.e., the lower one coming from  $P$  that is piercing the front and back faces of the wedge (which are to be identified) – to the ribbons to its right (which come from  $M_T$ ). In the second step the loop that results from the first step is removed with the help of the Frobenius property, associativity, and specialness, and in addition the ‘upper’  $A$ -ribbon (the one coming from  $P$  that is entering and leaving the part of the manifold drawn in the upper part of the picture) is moved towards the region in which the previous manipulations took place, thereby now showing its white rather than black side. The third step consists in deforming the latter ribbon and using associativity and the Frobenius property. The last step is similar to the first two, first using associativity and Frobenius property, and then associativity and specialness to remove the resulting loop. ■

By lemma 5.4(ii),  $Z(M_T, \emptyset, T_{A,A})$  can be expanded in terms of the vectors  $\{Z(M_{ij,\alpha\beta}, \emptyset, T_{A,A})\}_{i,j,\alpha,\beta}$ . Accordingly we write

$$Z(M_T, \emptyset, T_{A,A}) = \sum_{i,j,\alpha,\beta} K_{ij,\alpha\beta} Z(M_{ij,\alpha\beta}, \emptyset, T_{A,A}) \quad (5.18)$$

with suitable coefficients  $K_{ij,\alpha\beta} \in \mathbb{C}$ . It remains to show that the expansion coefficients  $K_{ij,\alpha\beta}$  in a given basis coincide with the inverses of the structure constants of the two-point functions on the sphere in that same basis. We first observe

5.5. LEMMA. *The coefficients  $K_{ij,\alpha\beta}$  satisfy*

$$K_{ij,\alpha\beta} = S_{0,0} \left( \frac{\dim(U_i) \dim(U_j)}{\dim(A)} \right)^2 \quad (5.19)$$


PROOF. We start by verifying that the vector dual to  $Z(M_{ij,\alpha\beta}, \emptyset, T_{A,A})$  is given by the invariant of the cobordism

$$\tilde{M}_{ij,\alpha\beta} := \mathcal{N}$$

(5.20)

with  $\mathcal{N}$  a normalisation constant to be determined.

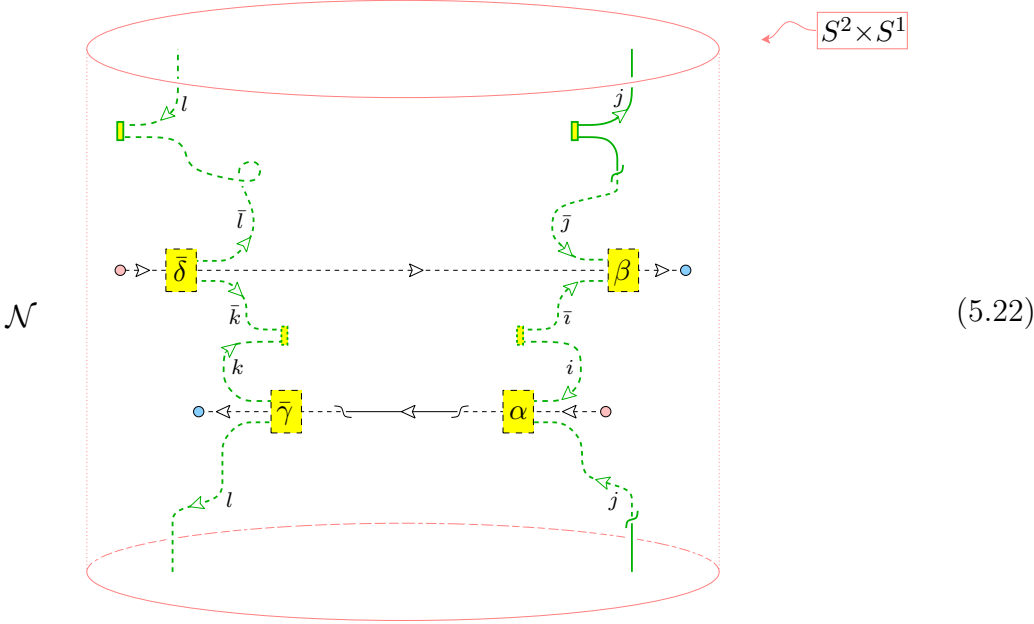
Thus  $\tilde{M}_{ij,\alpha\beta}$  is the same topological three-manifold as  $M_{ij,\alpha\beta}$ , but with opposite bulk- and boundary orientation; the ribbons are labelled by the same objects, but their cores are oriented differently. The coupons are now labelled by morphisms in  $\text{Hom}_{A|A}(A, U_i \otimes^+ A \otimes^- U_j)$  and in  $\text{Hom}_{A|A}(A, U_{\bar{i}} \otimes^+ A \otimes^- U_{\bar{j}})$ , respectively, and we choose bases  $\{\tilde{\phi}_\alpha^\pm\}$  that are dual to  $\{\phi_\alpha^\pm\}$  in the sense that

$= \delta_{\alpha,\beta}$

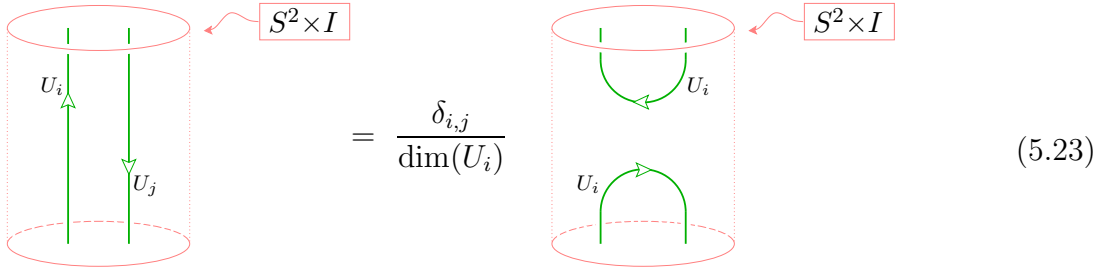
(5.21)

That this is possible follows from the presence of a non-degenerate pairing between the morphism spaces  $\text{Hom}(A, U_i \otimes A \otimes U_j)$  and  $\text{Hom}(U_i \otimes A \otimes U_j, A)$  (defined by the trace, see [Tu]), as is shown in appendix C.2. Gluing  $M_{ij,\alpha\beta}$  to  $\tilde{M}_{kl,\gamma\delta}$  via the canonical identification

of the boundaries results in the following ribbon graph:



Here  $S^2 \times S^1$  is drawn embedded in  $\mathbb{R}^3$ , with the  $S^1$  factor in vertical, direction, i.e. top and bottom are identified, and each horizontal plane is the stereographic image of an  $S^2$ . By using the identity





(which follows from dominance and  $\mathcal{H}(S^2, U_k) = \delta_{k,0}\mathbb{C}$ ) at four places in (5.22), we end up with the following ribbon graph:

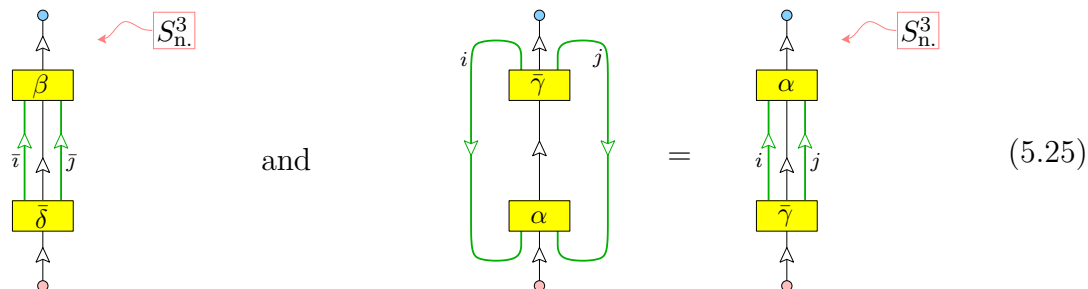
$$\frac{\mathcal{N} \delta_{i,k} \delta_{j,l}}{(\dim(U_i) \dim(U_j))^2}$$

$S^2 \times S^1$

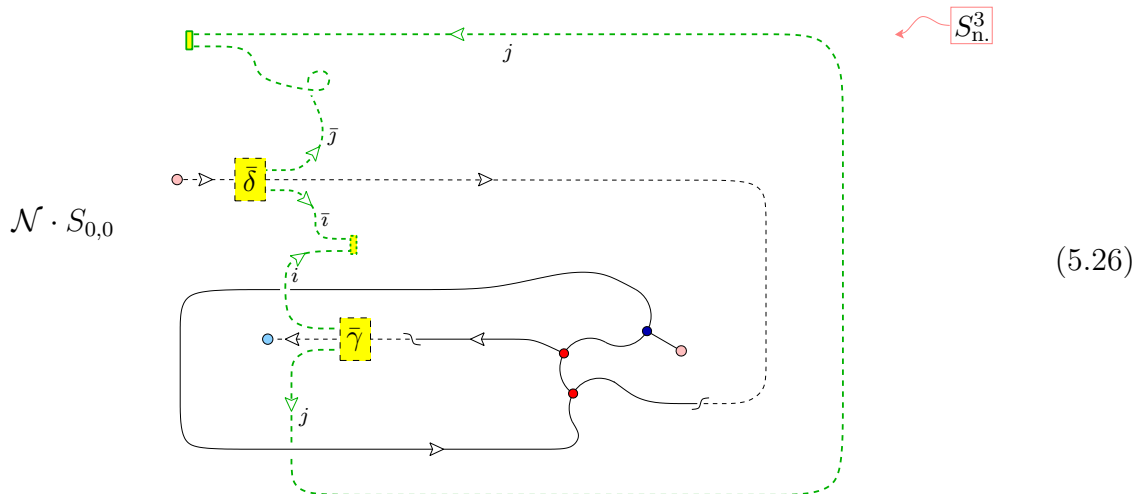
(5.24)

Here two components of the ribbon graph have been rotated such that the white side of the ribbons faces up. Next, using the identities (D.1), (D.2) and (D.19), one concludes that the value of the invariant corresponding to this cobordism evaluated on  $1 \in \mathbb{C}$  is given

by the product of the invariants of the following two graphs in <sup>8</sup>  $S^3$ :

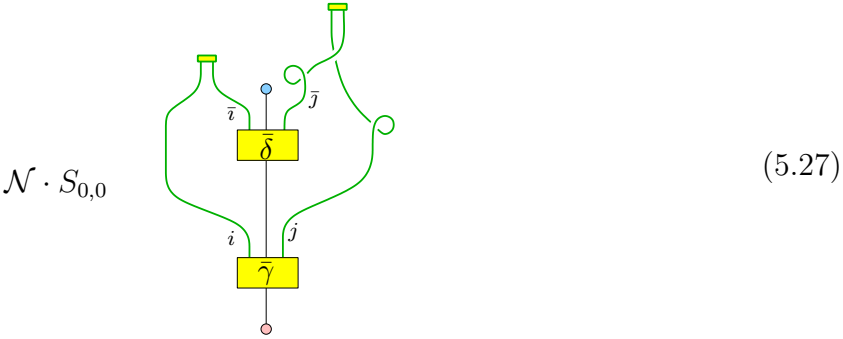


Since the respective basis elements are dual to each other, it follows that these numbers equal  $\dim(A) \delta_{\delta, \beta}$  and  $\dim(A) \delta_{\alpha, \gamma}$ , respectively. Hence the vectors  $\tilde{M}_{ij, \alpha\beta}$  are indeed dual to  $M_{ij, \alpha\beta}$ , and the value of the normalisation constant  $\mathcal{N}$  is  $(\dim(U_i) \dim(U_j) / \dim(A))^2$ . On the other hand, gluing  $\tilde{M}_{ij, \alpha\beta}$  to the cobordism  $M_T$  results in the ribbon graph



<sup>8</sup> The notation  $S_n^3$  used in the picture indicates that what is displayed is the graphical representation of the *normalised* invariant of a ribbon graph in the three-sphere. That is, for a ribbon graph  $R$  in  $S^3$  we define  $Z(S_n^3[R]) := Z(S^3[R]) / S_{0,0}$ . Denoting the empty ribbon graph by  $\emptyset$ , by the identity  $S_{0,0} = Z(S^3[\emptyset])$  this amounts to the normalisation  $Z(S_n^3[\emptyset]) = 1$ . This convention is also used explicitly in [FRSIV], while in [FRSI, FRSII, FRSIII] it is understood implicitly that  $S_n^3$  should be used instead of  $S^3$  (see section 5.1 of [FRSI]).

(the factor of  $S_{0,0}$  appears when passing from  $S^3$  to  $S_n^3$ ). This can be simplified by deformations and using (D.19), leading to



With  $\mathcal{N} = (\dim(U_i) \dim(U_j) / \dim(A))^2$ , this is precisely formula (5.19). ■

**PROOF OF PROPOSITION 5.3.** By equation (5.18), in order to establish (5.12) we need to show that

$$\dim(U_i) \dim(U_j) (c_{i,j}^{\text{bulk}})^{-1}_{\delta\alpha} = K_{ij,\alpha\delta}. \tag{5.28}$$

Lemma 5.5 provides a ribbon graph representation for  $K_{ij,\alpha\delta}$ . As an auxiliary calculation, place the ribbon graph in (5.19) together with the one for  $c_{ij,\alpha\beta}^{\text{bulk}}$  in (C.14) inside an  $S_n^3$  and sum over  $\alpha$ . In the graph defining  $c_{ij,\alpha\beta}^{\text{bulk}}$ , use the function  $f$  from (D.23) on the morphism  $\alpha$ , and similarly use the function  $g$  from (D.23) on the morphism  $\bar{\delta}$  in the graph defining  $K_{ij,\alpha\delta}$ . Using the matrix  $\Delta$  and its inverse, defined just

after lemma D.4, we find

$$\begin{aligned}
& \sum_{\alpha} \left( \text{Diagram 1} \right) = \sum_{\alpha} \left( \text{Diagram 2} \right) \\
& = \sum_{\alpha} \left( \text{Diagram 3} \right) = \sum_{\alpha, \gamma, \tau} \Delta_{\alpha\gamma} \Omega_{\delta\tau} \left( \text{Diagram 4} \right) \\
& = (\dim(A))^2 \sum_{\alpha, \gamma, \tau} \Delta_{\alpha\gamma} \Omega_{\delta\tau} \delta_{\beta, \gamma} \delta_{\alpha, \tau} = \frac{(\dim(A))^2}{\dim(U_i) \dim(U_j)} \delta_{\beta, \delta}.
\end{aligned} \tag{5.29}$$

Here in the first step the definitions (D.23) are used. For the left graph, this also involves a deformation, moving the thin coupons closer to the coupon labelled by  $\alpha$ . The second step is again a deformation of the left graph, followed by using the identity (D.19). The rest follows using (D.27) and (D.28).

This auxiliary calculation shows that

$$\sum_{\alpha} S_{0,0} c_{ij,\alpha\beta}^{\text{bulk}} \cdot \frac{1}{S_{0,0}} \left( \frac{\dim(A)}{\dim(U_i) \dim(U_j)} \right)^2 K_{ij,\alpha\delta} = \frac{\dim(A)^2}{\dim(U_i) \dim(U_j)} \delta_{\beta,\delta}. \tag{5.30}$$

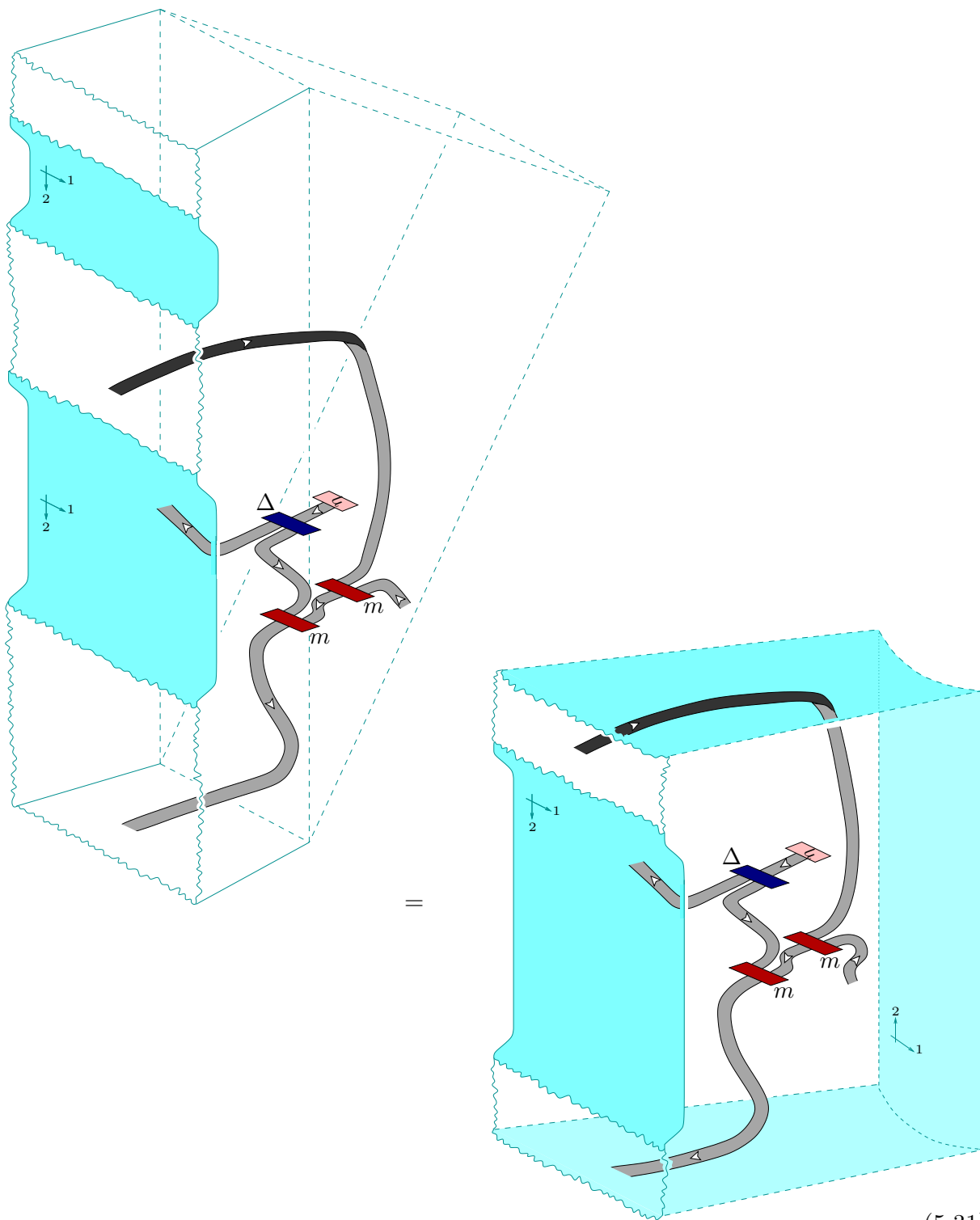
This establishes (5.28). ■

## 5.6. ORIENTED WORLD SHEETS.

We are now finally in a position to prove the bulk factorisation theorem.

**PROOF OF THEOREM 2.13.** By proposition 5.3, the sum on the right hand side of (2.50) can be replaced by the cobordism obtained from (5.9) by exchanging the tubular neighbourhood of the vertically running ribbons by  $M_T$ . Moreover, as illustrated in the following figure, the geometry of the relevant region of the three-manifold is precisely the

geometry of  $C(X)$ :



(5.31)

This proves the theorem. ■

### 5.7. UNORIENTED WORLD SHEETS.

The proof of theorem 2.14 is identical to that of theorem 2.13.

A property of the unoriented bulk factorisation not present in the oriented one is the following. With every embedding  $f: A_\varepsilon \rightarrow X$  we obtain another embedding  $\tilde{f}: A_\varepsilon \rightarrow X$  by setting  $\tilde{f}(x, y, z) := f(x, -y, z)$ , which results in the opposite local orientation of  $X$  on the image of  $A_\varepsilon$ . By theorem 2.14, both  $f$  and  $\tilde{f}$  give factorisation identities for the correlators. These identities can be related by a change of the local orientation that enters the definition of a bulk field (see definition IV:3.6 or appendix B.4). Such a change of local orientation is immaterial only because  $\tilde{A}$  is a Jandl algebra.

## A. Algebras in modular tensor categories

### A.1. MODULAR TENSOR CATEGORIES AND GRAPHICAL CALCULUS.

A *ribbon category* [Ka, chap. XIV.3] is a strict monoidal category endowed with duality, braiding, and twist, which are the following families of morphisms: A (right) *duality* on a strict monoidal category  $\mathcal{C}$  associates to every  $U \in \mathcal{O}bj(\mathcal{C})$  an object  $U^\vee \in \mathcal{O}bj(\mathcal{C})$ , called the (right-) dual of  $U$ , and morphisms

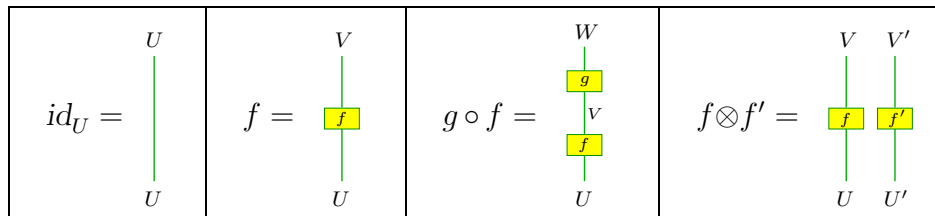
$$b_U \in \text{Hom}(\mathbf{1}, U \otimes U^\vee), \quad d_U \in \text{Hom}(U^\vee \otimes U, \mathbf{1}), \quad (\text{A.1})$$

and to every morphism  $f \in \text{Hom}(U, Y)$  the morphism

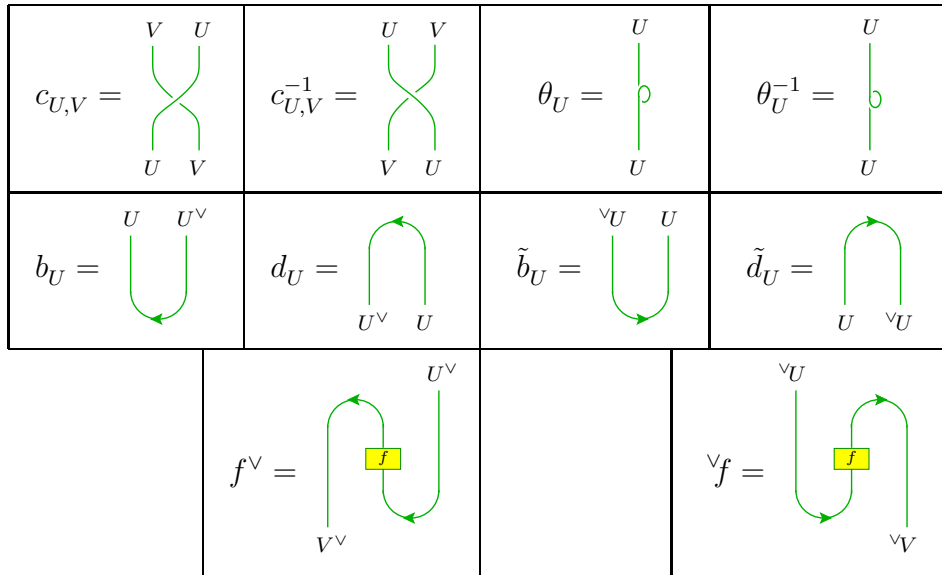
$$f^\vee := (d_Y \otimes id_{U^\vee}) \circ (id_{Y^\vee} \otimes f \otimes id_{U^\vee}) \circ (id_{Y^\vee} \otimes b_U) \in \text{Hom}(Y^\vee, U^\vee). \quad (\text{A.2})$$

A *braiding* on  $\mathcal{C}$  is a family of isomorphisms  $c_{U,V} \in \text{Hom}(U \otimes V, V \otimes U)$ , one for each pair of objects  $U, V \in \mathcal{O}bj(\mathcal{C})$ , and a *twist* is a family of isomorphisms  $\theta_U$ , one for each  $U \in \mathcal{O}bj(\mathcal{C})$ . These morphisms are subject to various axioms, which are analogous to properties of ribbons in  $S^3$  and correspondingly can be conveniently visualized through a graphical calculus as introduced in [JS] (see e.g. also [Ka, Mj]).

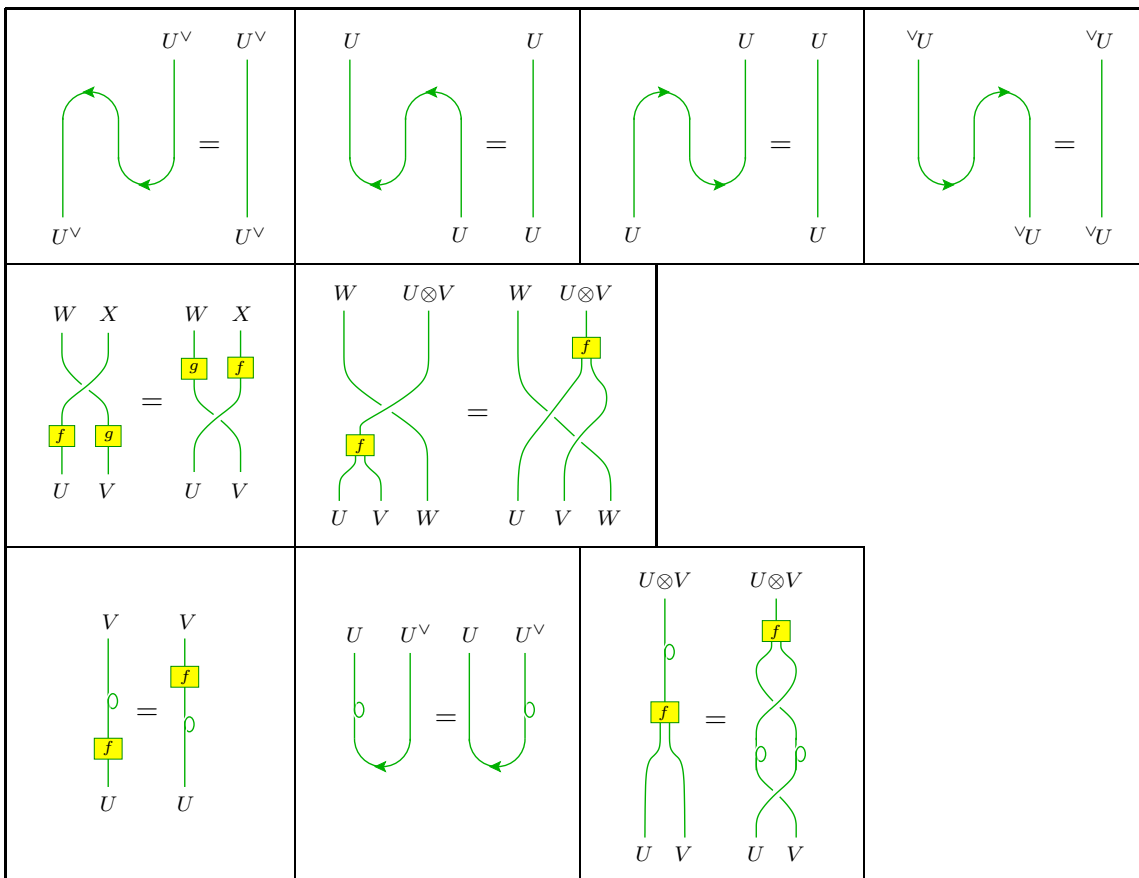
With the convention that pictures are read from bottom to top, the graphical notation for identity morphisms and for general morphisms and their composition and tensor product looks as follows:



The next pictures show the structural morphisms of a ribbon category: the braiding, twist, and left and right dualities, as well as the definition of the (left and right) dual of a morphism. (A ribbon category has automatically also a left duality, with left dual objects  ${}^\vee U := U^\vee$  and left duality morphisms  $\tilde{b}_U$  and  $\tilde{d}_U$ . It is in fact sovereign, i.e. the left and right dualities coincide both on objects and on morphisms. Also, lines labelled by the monoidal unit  $\mathbf{1}$  are not drawn – owing to strictness they are ‘invisible’.)



With these conventions, the axioms of a ribbon category – the properties of dualities, functoriality and tensoriality of the braiding, functoriality of the twist, and compatibility of the twist with duality and with braiding – look as follows.



A *modular tensor category* [Tu] is a  $\mathbb{C}$ -linear semisimple abelian ribbon category with simple monoidal unit and with a finite number of isomorphism classes of simple objects in which the braiding is maximally non-symmetric. The latter property means that the numerical  $|\mathcal{I}| \times |\mathcal{I}|$ -matrix  $s = (s_{U_i, U_j})_{i, j \in \mathcal{I}}$  with entries

$$s_{U_i, U_j} := \text{tr}(c_{U_i, U_j} c_{U_j, U_i}) \in \mathbb{C} \quad (\text{A.3})$$

is non-degenerate. Here we have identified the one-dimensional  $\mathbb{C}$ -vector space  $\text{Hom}(\mathbf{1}, \mathbf{1})$  with  $\mathbb{C}$  and have chosen a set  $\{U_i \mid i \in \mathcal{I}\}$  of representatives of the finitely many isomorphism classes of simple objects of  $\mathcal{C}$ . Also, as representative of the class of the tensor unit  $\mathbf{1}$  we choose  $\mathbf{1}$  itself and denote the corresponding element of the label set  $\mathcal{I}$  by 0, i.e. write  $\mathbf{1} = U_0$ .

Instead of  $s$ , one often also uses the matrix  $S := S_{0,0} s$  that is scaled by the number  $S_{0,0} := (\sum_i \dim(U_i)^2)^{-1/2}$ . One then has  $\dim(U_i) \equiv \text{tr}(id_{U_i}) = s_{U_i, U_0} = S_{i,0}/S_{0,0}$ .

## A.2. THREE-DIMENSIONAL TFT FROM MODULAR TENSOR CATEGORIES.

Next we briefly state our conventions for three-dimensional topological field theory; for more details see e.g. [Tu, BK, KRT] or section I:2. Given a modular tensor category  $\mathcal{C}$ , the construction of [Tu] allows one to obtain a three-dimensional TFT, that is, a projective monoidal functor from a geometric category  $\mathcal{G}_{\mathcal{C}}$  to  $\mathcal{Vect}_{\mathbb{C}}$ , the category of finite-dimensional complex vector spaces.

The geometric category  $\mathcal{G}_{\mathcal{C}}$  has extended surfaces as objects and homotopy classes of cobordisms between extended surfaces as morphisms. An *extended surface*  $E$  consists of the following data:

- A compact oriented two-dimensional manifold with empty boundary, also denoted by  $E$ .
- A finite (unordered) set of marked points – that is, of quadruples  $(p_a, [\gamma_a], V_a, \varepsilon_a)$ , where the  $p_a \in E$  are mutually distinct points of the surface  $E$  and  $[\gamma_a]$  is a germ of arcs<sup>9</sup>  $\gamma_a: [-\delta, \delta] \rightarrow E$  with  $\gamma_a(0) = p_a$ . Furthermore,  $V_a \in \text{Obj}(\mathcal{C})$ , and  $\varepsilon_a \in \{\pm 1\}$  is a sign.
- A Lagrangian subspace  $\lambda \subset H_1(E, \mathbb{R})$ .

A morphism  $E \rightarrow E'$  is an *extended cobordism*  $M$  (or rather a homotopy class thereof), consisting of the following data:

- A compact oriented three-manifold, also denoted by  $M$ , such that  $\partial M = (-E) \sqcup E'$ . Here  $-E$  is obtained from  $E$  by reversing its 2-orientation and replacing any marked point  $(p, [\gamma], U, \varepsilon)$  by  $(p, [\tilde{\gamma}], U, -\varepsilon)$  with  $\tilde{\gamma}(t) = \gamma(-t)$ . The boundary  $\partial M$  of a cobordism is oriented according to the inward-pointing normal.

---

<sup>9</sup> By a *germ of arcs* we mean an equivalence class  $[\gamma]$  of continuous embeddings  $\gamma$  of intervals  $[-\delta, \delta] \subset \mathbb{R}$  into the extended surface  $E$ . Two embeddings  $\gamma: [-\delta, \delta] \rightarrow E$  and  $\gamma': [-\delta', \delta'] \rightarrow E$  are equivalent iff there is a positive  $\varepsilon < \delta, \delta'$  such that the restrictions of  $\gamma$  and  $\gamma'$  to the interval  $[-\varepsilon, \varepsilon]$  are equal.



- A ribbon graph inside  $M$  such that for each marked point  $(p, [\gamma], U, \varepsilon)$  of  $(-E) \sqcup E'$  there is a ribbon ending on  $(-E) \sqcup E'$ .

The notion of a ribbon graph is reviewed in section I:2.3; the allowed ways for a ribbon to end on an arc are shown explicitly in (IV:3.1).

Composition in  $\mathcal{G}_C$  is defined by glueing, the identity morphism from  $E$  to  $E$  is the cylinder  $E \times [0, 1]$ , and the tensor product is given by disjoint union of objects and cobordisms.

Starting from a modular tensor category  $\mathcal{C}$ , one can construct a projective monoidal functor  $(Z, \mathcal{H}): \mathcal{G}_C \rightarrow \mathcal{Vect}_C$  [Tu, Theorem IV.6.6]. Here  $\mathcal{H}$  denotes the action of the functor on objects, i.e.  $\mathcal{H}(E)$  is a finite-dimensional  $\mathbb{C}$ -vector space, and  $Z$  denotes the action on morphisms, such that  $Z(M, E, E')$  is a linear map from  $\mathcal{H}(E)$  to  $\mathcal{H}(E')$ . The pair  $(Z, \mathcal{H})$  is only a projective functor in the sense that

$$Z'(M' \circ M) = \kappa^\mu Z'(M') \circ Z'(M), \tag{A.4}$$

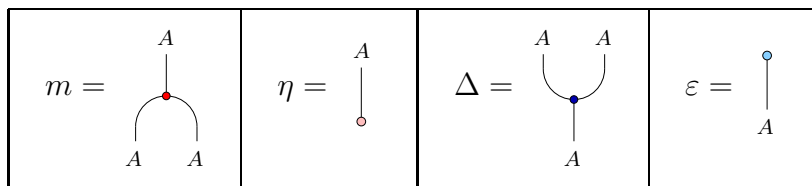
where  $M: E \rightarrow E'$ ,  $M': E' \rightarrow E''$  are extended cobordisms,  $\kappa = S_{0,0} \sum_j \theta_j^{-1} \dim(U_j)^2$ , and  $\mu$  is an integer computed from the Lagrangian subspaces in  $E$ ,  $E'$  and  $E''$  via Maslov indices; for details see [Tu, chap. IV.7] or [FFFS2, section 2.7].

### A.3. ALGEBRAS.

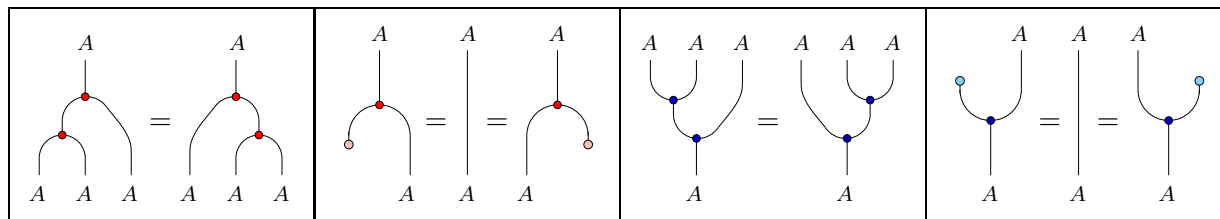
A (unital associative) *algebra*  $A$  in a monoidal category  $\mathcal{C}$  is a triple  $(A, m, \eta)$  consisting of an object  $A$  of  $\mathcal{C}$  and morphisms  $m \in \text{Hom}(A \otimes A, A)$  and  $\eta \in \text{Hom}(\mathbf{1}, A)$  that satisfy

$$m \circ (m \otimes id_A) = m \circ (id_A \otimes m) \quad \text{and} \quad m \circ (\eta \otimes id_A) = id_A = m \circ (id_A \otimes \eta). \tag{A.5}$$

(What we call an algebra here is often, in particular in [Ma], referred to as a monoid.) Analogously, a (counital coassociative) *coalgebra* in  $\mathcal{C}$  is a triple  $(A, \Delta, \varepsilon)$  consisting of an object  $A$  and morphisms  $\Delta \in \text{Hom}(A, A \otimes A)$  and  $\varepsilon \in \text{Hom}(A, \mathbf{1})$  obeying coassociativity and counit properties that amount to reversing the arrows in the associativity and unit properties. We depict the structural morphisms of a (co)algebra as follows.



The associativity of the product, unit property, coassociativity of the coproduct, and counit property are then given by the following diagrams.



A *Frobenius algebra* in a monoidal category  $\mathcal{C}$  is a quintuple  $(A, m, \eta, \Delta, \varepsilon)$  such that  $(A, m, \eta)$  is an algebra and  $(A, \Delta, \varepsilon)$  is a coalgebra, with the two structures related by

$$(id_A \otimes m) \circ (\Delta \otimes id_A) = \Delta \circ m = (m \otimes id_A) \circ (id_A \otimes \Delta), \quad (\text{A.6})$$

which says that the coproduct  $\Delta$  is a morphism of  $A$ -bimodules. In the special case that  $\mathcal{C}$  is the category of complex vector spaces, this definition of Frobenius algebra is equivalent to more familiar ones as an algebra with a nondegenerate invariant bilinear form or as an algebra that is isomorphic to its dual as a (left or right) module over itself.

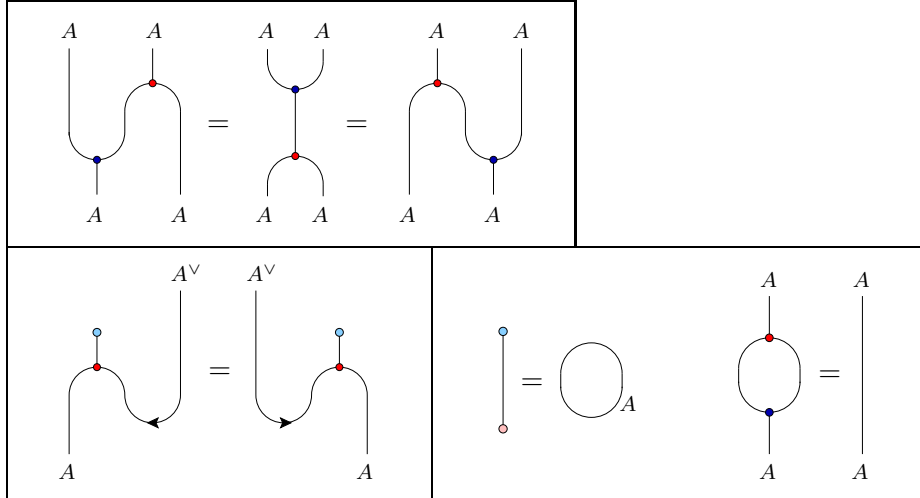
A Frobenius algebra in a monoidal category with left and right dualities is called *symmetric* iff the two morphisms

$$[(\varepsilon \circ m) \otimes id_{A^\vee}] \circ (id_A \otimes b_A) \quad \text{and} \quad [id_{A^\vee} \otimes (\varepsilon \circ m)] \circ (\tilde{b}_A \otimes id_A) \quad (\text{A.7})$$

in  $\text{Hom}(A, A^\vee)$ , which by the Frobenius property are in fact isomorphisms, are equal. A Frobenius algebra in a monoidal category is called *special* iff

$$\varepsilon \circ \eta = \beta_1 id_1 \quad \text{and} \quad m \circ \Delta = \beta_A id_A \quad (\text{A.8})$$

for non-zero numbers  $\beta_1$  and  $\beta_A$ . For a symmetric special Frobenius algebra  $A$  one has  $\beta_1 \beta_A = \dim(A)$ ; we normalise  $\varepsilon$  and  $\Delta$  such that  $\beta_1 = \dim(A)$  and  $\beta_A = 1$ . In pictures, the defining properties of a symmetric special Frobenius algebra look as follows.



A *reversion* on an algebra  $A = (A, m, \eta)$  is an endomorphism  $\sigma \in \text{Hom}(A, A)$  that is an algebra anti-homomorphism and squares to the twist, i.e.

$$\sigma \circ \sigma = \theta_A, \quad \sigma \circ m = m \circ c_{A,A} \circ (\sigma \otimes \sigma), \quad \sigma \circ \eta = \eta. \quad (\text{A.9})$$

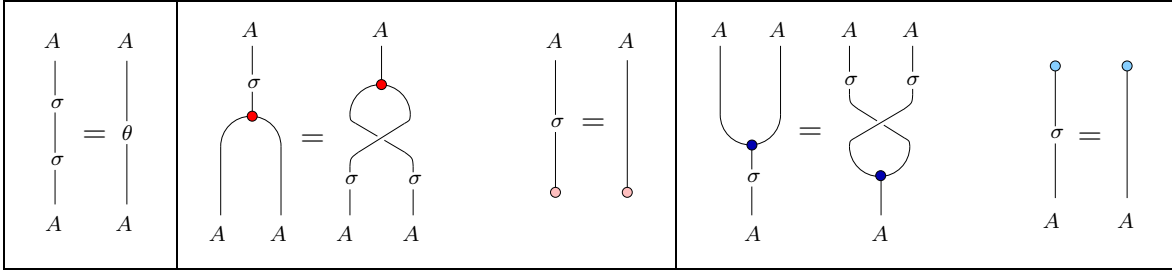
If  $A$  is also a coalgebra, then in addition

$$\Delta \circ \sigma = (\sigma \otimes \sigma) \circ c_{A,A} \circ \Delta \quad \text{and} \quad \varepsilon \circ \sigma = \varepsilon \quad (\text{A.10})$$

must hold in order for  $\sigma$  to be a reversion. We [FRSII] call a symmetric special Frobenius algebra with reversion a *Jandl algebra*; for a Jandl algebra  $\tilde{A} = (A, m, \eta, \Delta, \varepsilon, \sigma)$  the properties (A.10) are actually a consequence of the properties (A.9).

Given two reversions  $\sigma_1$  and  $\sigma_2$  on an algebra  $A$ , the morphism  $\omega = \sigma_1^{-1} \circ \sigma_2$  is an algebra automorphism of  $A$ . Conversely, all possible reversions on an algebra  $A$  can be obtained by composing a single reversion  $\sigma_0$  with algebra automorphisms  $\omega$  of  $A$ . More precisely, for  $\sigma$  a reversion on  $A$ ,  $\omega \circ \sigma$  is again a reversion iff  $\omega \circ \sigma \circ \omega = \sigma$ .

Gratically, the conditions (A.9) and (A.10) look as follows.

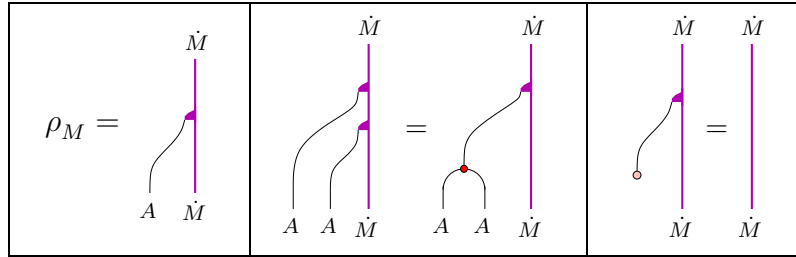


#### A.4. MODULES.

A *left module* over an algebra  $A$  is a pair  $M = (\dot{M}, \rho)$  consisting of an object  $\dot{M}$  of  $\mathcal{C}$  and a morphism  $\rho \equiv \rho_M \in \text{Hom}(A \otimes \dot{M}, \dot{M})$  that satisfies

$$\rho \circ (m \otimes id_{\dot{M}}) = \rho \circ (id_A \otimes \rho) \quad \text{and} \quad \rho \circ (\eta \otimes id_{\dot{M}}) = id_{\dot{M}}. \quad (\text{A.11})$$

In pictures,



Analogously one defines a right  $A$ -module  $(\dot{M}, \varrho)$ . An  $A$ -*bimodule* is a triple  $X = (\dot{X}, \rho, \varrho)$  such that  $(\dot{X}, \rho)$  is a left  $A$ -module and  $(\dot{X}, \varrho)$  a right  $A$ -module and such that the left and right actions commute,

$$\rho \circ (id_A \otimes \varrho) = \varrho \circ (\rho \otimes id_A). \quad (\text{A.12})$$

We denote by

$$\begin{aligned} \text{Hom}_A(N, M) &= \{f \in \text{Hom}(\dot{N}, \dot{M}) \mid f \circ \rho_N = \rho_M \circ (id_A \otimes f)\} \quad \text{and} \\ \text{Hom}_{A|A}(B, C) &= \{f \in \text{Hom}(\dot{B}, \dot{C}) \mid f \circ \rho_B = \rho_C \circ (id_A \otimes f), f \circ \varrho_B = \varrho_C \circ (f \otimes id_A)\} \end{aligned} \quad (\text{A.13})$$

the subspaces of morphisms in  $\mathcal{C}$  that intertwine the left action of  $A$  on the left modules  $N$  and  $M$ , and the left and right actions on the bimodules  $B$  and  $C$ , respectively.

Owing to associativity,  $A$  is a bimodule over itself. If  $\mathcal{C}$  is braided, then for any  $A$ -bimodule  $X$  and any two objects  $U, V$  of  $\mathcal{C}$  one endow the object  $U \otimes X \otimes V$  with several structures of an  $A$ -bimodule. In particular there is an  $A$ -bimodule structure on  $U \otimes A \otimes V$ , which we denote by  $U \otimes^+ A \otimes^- V$ , for which the left and right actions of  $A$  are defined by

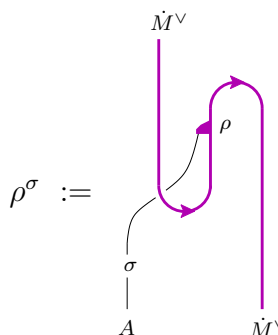
$$\rho := c_{U,A}^{-1} \otimes id_V \quad \text{and} \quad \varrho := id_U \otimes c_{A,V}^{-1}, \quad (\text{A.14})$$

respectively.

If  $M$  is a module over a Jandl algebra  $\tilde{A}$ , the presence of the reversion  $\sigma$  allows one to define for any left  $A$ -module  $M$  a left  $A$ -module structure  $M^\sigma$  on the object dual to  $M$ :

$$M^\sigma := (\tilde{M}^\vee, \rho^\sigma) \quad (\text{A.15})$$

with



$$\rho^\sigma := \quad (\text{A.16})$$

The assignment  $M \mapsto M^\sigma$  yields a ( $\sigma$ -dependent) duality endofunctor on the category left  $A$ -modules, whose square is equivalent to the identity functor.

## B. The assignment $X \mapsto C(X)$

The formulation and the proof of modular invariance and of factorisation require a precise definition of all correlators of a full rational CFT. In the TFT approach, this is achieved by representing each correlator as the invariant of a suitable ribbon graph in a three-manifold, which specifies the correlator as an element in the relevant space of conformal blocks. This construction is summarised below; for more details, as well as motivations, we refer to the papers [FRSI, FRSII, FRSIV] in which the construction was developed. To be precise, in our exposition we follow closely [FRSIV], which introduced a few minor modifications (summarised in section IV:3.1) as compared to [FRSI, FRSII].

The basic ingredients of the construction are as follows. As explained in section B.1, a world sheet  $X$  is a compact two-dimensional manifold with a finite number of field insertions, and to each such world sheet there is associated an extended surface  $\hat{X}$ , a compact oriented surface with a finite number of marked points. The CFT correlator  $C(X)$  that corresponds to a world sheet  $X$  is defined as

$$C(X) := Z(M_X, \emptyset, \hat{X})1 \in \mathcal{H}(\hat{X}) \quad (\text{B.1})$$

where  $M_X$ , the *connecting manifold*, is a cobordism to be defined in sections B.1 and B.3.

For the rest of this section we select once and for all a modular tensor category  $\mathcal{C}$ , as well as

- a symmetric special Frobenius algebra  $A$  in  $\mathcal{C}$ , in case we wish to describe a conformal field theory on oriented surfaces only, respectively
- a Jandl algebra  $\tilde{A}$  in  $\mathcal{C}$ , in case we wish to include also unoriented world sheets.

The details of the construction depend on whether  $X$  is oriented or unoriented. Still, in the sequel we treat oriented and unoriented world sheets simultaneously. In the parts relevant to both cases we refer to the algebra  $A$ , while in the parts applicable to the unoriented case alone we refer to the algebra  $\tilde{A}$ .

### B.1. THE WORLD SHEET.

Oriented and unoriented world sheets are defined as follows.

**B.2. DEFINITION.** (i) *An unoriented world sheet  $X$  is a compact two-dimensional topological manifold, also denoted by  $X$  (which may have non-empty boundary and may be non-orientable), together with a finite, unordered set of marked points and an orientation  $\text{or}(\partial X)$  of its boundary.*

*A marked point is either*

- *a bulk insertion, that is, a tuple  $\Phi = (i, j, \phi, p, [\gamma], \text{or}_2(p))$ , where  $i, j \in \mathcal{I}$ ,  $\phi \in \text{Hom}_{\tilde{A}|\tilde{A}}(U_i \otimes^+ \tilde{A} \otimes^- U_j, \tilde{A})$ ,  $p \in X \setminus \partial X$ ,  $[\gamma]$  is an arc-germ with  $\gamma(0) = p$  and  $\text{or}_2(p)$  is an orientation of a neighbourhood of  $p \in X$ .*
- *a boundary insertion, that is, a tuple  $\Psi = (M, N, U, \psi, p, [\gamma])$ , where  $M, N$  are left  $\tilde{A}$ -modules,  $U \in \text{Obj}(\mathcal{C})$ ,  $\psi \in \text{Hom}_{\tilde{A}}(M \otimes U, N)$ ,  $p \in \partial X$  and  $[\gamma]$  is an arc-germ with  $\gamma(0) = p$ . There has to exist a representative  $\gamma$  of  $[\gamma]$  that is a subset of  $\partial X$ .*

*No two bulk or boundary insertions are allowed to be located at the same point of  $X$ . If two boundary insertions  $\Psi_1 = (M_1, N_1, U, \psi_1, p_1, [\gamma_1])$  and  $\Psi_2 = (M_2, N_2, B, \psi_2, p_2, [\gamma_2])$  are adjacent and  $\Psi_1$  comes “after”  $\Psi_2$  with respect to  $\text{or}(\partial X)$ , i.e. pictorially,*

(B.2)

*then we require  $N_1 = M_2$ . If there is a connected component of  $\partial X$  without boundary insertions, it gets labelled by a left  $\tilde{A}$ -module.*

(ii) *An oriented world sheet  $X$  is an unoriented world sheet  $X$  together with an orientation  $\text{or}_2(X)$  of  $X$ . For a bulk insertion  $\Phi = (i, j, \phi, p, [\gamma], \text{or}_2(p))$ ,  $\text{or}_2(p)$  is required to agree with  $\text{or}_2(X)$ . Also,  $\text{or}_2(X)$  induces an orientation of  $\partial X$  via the inward pointing normal, which is required to agree with  $\text{or}(\partial X)$ .*

The machinery of TFT is to be applied to *extended surfaces*. An extended surface  $E$  is a closed compact two-dimensional manifold with a finite number of marked points and a choice of Lagrangian subspace  $\lambda \subset H_1(E, \mathbb{R})$ . A marked point on  $E$  is a quadruple

$(p, [\gamma], U, \varepsilon)$  with  $p \in E$ ,  $[\gamma]$  an arc germ centered at  $p$ ,  $U$  an object of  $\mathcal{C}$ , and  $\varepsilon \in \{\pm\}$ . The *double*  $\widehat{X}$  of a world sheet  $X$  is an extended surface; as a topological surface,  $\widehat{X}$  is the total space of the orientation bundle over  $X$  modulo an identification of the two points of the fiber over any boundary point,

$$\widehat{X} := Or(X)/\sim \quad \text{with} \quad (x, \text{or}_2) \sim (x, -\text{or}_2) \quad \text{for} \quad x \in \partial X. \quad (\text{B.3})$$

Thus points of  $\widehat{X}$  are equivalence classes  $[x, \text{or}_2]$ . By construction  $\widehat{X}$  is oriented.

The *connecting manifold*  $M_X$  of  $X$  is defined as a topological three-manifold by

$$M_X := (\widehat{X} \times [-1, 1])/\sim \quad \text{with} \quad ([x, \text{or}_2], t) \sim ([x, -\text{or}_2], -t). \quad (\text{B.4})$$

Points on  $M_X$  are equivalence classes  $[[x, \text{or}_2], t] =: [x, \text{or}_2, t]$ . There is a natural embedding

$$\iota : X \rightarrow M_X, \quad x \mapsto [x, \pm \text{or}_2, 0] \quad (\text{B.5})$$

of the world sheet in the connecting manifold, as well as a projection

$$\pi : M_X \rightarrow X, \quad [x, \text{or}_2, t] \mapsto x. \quad (\text{B.6})$$

We equip  $M_X$  with the orientation that is induced by the orientation of  $\widehat{X}$  together with the standard orientation of the interval. By construction,  $\partial M_X = \widehat{X}$ , where the orientation of the boundary is induced by the inward-pointing normal.

The construction of the connecting manifold provides naturally a Lagrangian subspace of the first homology group with real coefficients of the double:

$$\lambda := \text{Ker } f_* \quad (\text{B.7})$$

with  $f: \widehat{X} = \partial M_X \rightarrow M_X$  the inclusion map and  $f_*$  the induced map  $H_1(\widehat{X}, \mathbb{R}) \rightarrow H_1(M_X, \mathbb{R})$ . (An alternative definition of Lagrangian subspace is given in lemma 3.5 of [FFFS2], compare also theorem 5.1.1 of [Qu]; its relation to the present one is explained in remark 3.1 of [FRS II].)

Field insertions on the world sheet  $X$  yield marked points on  $\widehat{X}$ . Each boundary field insertion  $\Psi = (M, N, V, \psi, p, [\gamma])$  gives rise to a single marked point  $(\tilde{p}, [\tilde{\gamma}], V, +)$  with  $\tilde{p} = [p, \pm \text{or}_2(p)]$ . To define  $[\tilde{\gamma}]$ , note that any representative  $\gamma$  of the class  $[\gamma]$  has a restriction to  $\partial X$ , i.e. one has  $\gamma([-\delta, \delta]) \subset \partial X$  for a suitable  $\delta > 0$ . This restriction provides a unique pre-image on  $\widehat{X}$ , and then we set  $\tilde{\gamma} := [\gamma, \pm \text{or}_2]$  for the restriction of any representative  $\gamma$  of  $[\gamma]$ .

Each bulk field insertion  $(i, j, \phi, p, [\gamma], \text{or}_2)$  gives two marked points on  $\widehat{X}$ ,  $(\tilde{p}_i, [\tilde{\gamma}_i], U_i, +)$  and  $(\tilde{p}_j, [\tilde{\gamma}_j], U_j, +)$ , with  $\tilde{p}_i = [p, \text{or}_2(p)]$ ,  $\tilde{p}_j = [p, -\text{or}_2(p)]$ , and  $\tilde{\gamma}_i = [\gamma, \text{or}_2(\gamma)]$ ,  $\tilde{\gamma}_j = [\gamma, -\text{or}_2(\gamma)]$ .

### B.3. THE RIBBON GRAPH.

Next, we provide  $M_X$  with a ribbon graph  $R$ , turning it into a cobordism  $M_X[R]$  of extended surfaces. The construction of the ribbon graph involves a number of arbitrary choices, in particular that of a triangulation  $T$ ; denote the resulting ribbon graph by  $R_T$ . It turns out that the linear map  $Z(M_X[R_T]): \mathbb{C} \rightarrow \mathcal{H}(\hat{X})$  is independent of all these choices. In steps (i)–(ix) below, we will always think of  $X$  as embedded in  $M_X$  via  $\iota_X$ .

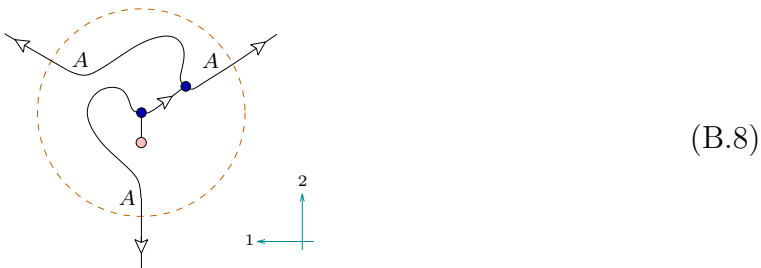
(i) Choose a triangulation  $T$  of  $X$  that has two- or three-valent vertices and faces with an arbitrary number of edges<sup>10</sup> – Choice #1.

The choice of  $T$  is subject to the following conditions.

- The boundary  $\partial X$  is covered by edges of  $T$ .
- Two-valent vertices in  $T$  occur precisely at the marked points of  $X$ .
- For a bulk insertion at  $p$  with arc germ  $[\gamma]$ , there has to be a representative  $\gamma$  of  $[\gamma]$  such that  $\gamma$  is covered by edges of  $T$  (see e.g. figure (IV:4.26))

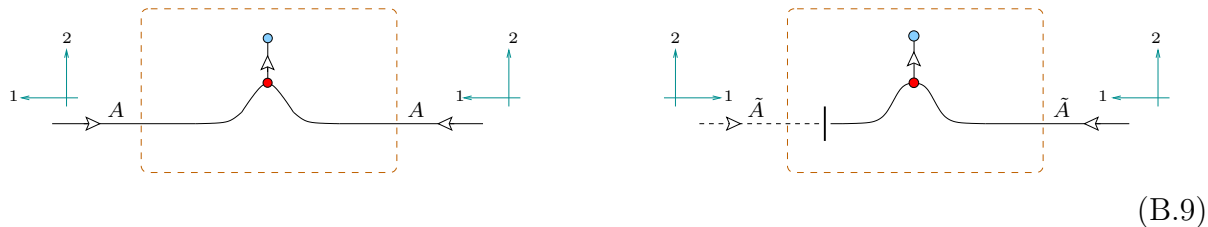
(ii) At each three-valent vertex  $v$  of  $T$  in the interior of  $X$  choose an orientation of a small neighbourhood of  $v$ . If  $X$  is an oriented world sheet, choose  $\text{or}_2(X)$  at each vertex; if  $X$  is an unoriented world sheet, this is a genuine choice – Choice #2.

(iii) On each three-valent vertex  $v$  in the interior of  $X$  place the following fragment of ribbon graph with three outgoing  $A$ -ribbons,



such that the orientation around  $v$  as chosen in (ii) agrees with the one indicated in the figure. There are three possibilities to do this (rotating the graph) – Choice #3.

(iv) On each edge of  $T$  which does not lie on  $\partial X$ , place one of the following two fragments of ribbon graph such that the local orientation around the two vertices connected by the edge agrees with the one indicated in the figure:



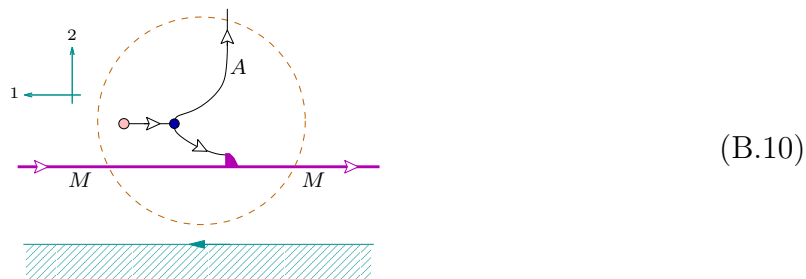
<sup>10</sup> Thus  $T$  is actually the dual of what is commonly referred to as a triangulation.

In each case this is possible in two ways – Choice #4. Note that the situation on the right hand side of (B.9) can occur only for unoriented world sheets. Accordingly, the ribbon graph has been labelled by  $\tilde{A}$  and involves explicitly the reversion (contained in the definition of the vertical bar in the figure, see figure (II:3.4); the dashed-line notation refers to the “black” side of a ribbon, see figure (II:3.3)).

(v) The edges on the boundary  $\partial X$  get labelled by left  $A$ -modules as follows. If an edge  $e$  of  $T$  lies on a connected component of  $\partial X$  without field insertion, it gets labelled by the  $A$ -module assigned to that boundary component (recall definition B.2 (i)). Otherwise,  $e$  lies between two (not necessarily distinct) boundary insertions. In this case it gets labelled by  $N_1 = M_2$ , using the convention in figure (B.2).

(vi) On each edge on the boundary  $\partial X$  labelled by  $M$  place a ribbon also labelled by  $M$ . A small neighbourhood of  $\partial X$  can be oriented using the orientation of  $\partial X$  and the inward pointing normal. The orientations of the ribbon core and surface have to be opposite to those of  $\partial X$  and  $X$ , respectively.

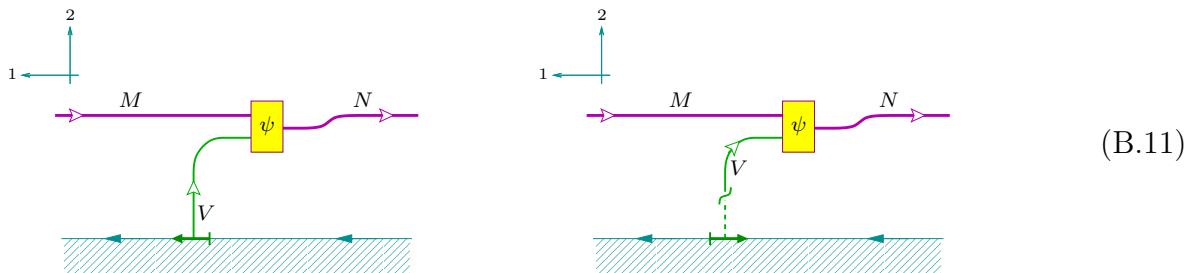
(vii) On each three-valent vertex on the boundary  $\partial X$  place ribbon graph fragment



(B.10)

such that bulk and boundary orientation indicated in the figure agree with those of  $X$ . Here  $M$  is the label of the two edges lying on the boundary  $\partial X$ , as assigned in (v) (they have the same label by construction). Shown in (B.10) is a horizontal section of the connecting manifold as displayed in figure (IV:3.12). Correspondingly the lower boundary in (B.10) is that of  $M_X$  while the ribbons  $M$  are placed on the boundary of  $X$  as embedded in  $M_X$ . The arrow on the boundary in (B.10) indicates the orientation of  $\partial X$  (transported to  $\partial M_X$  along the preferred intervals).

(viii) Let  $v \in \partial X$  be a two-valent vertex of  $T$  and let  $\Psi = (M, N, V, \psi, p, [\gamma])$  be the corresponding boundary insertion. At  $v$  place one of the two ribbon graph fragments

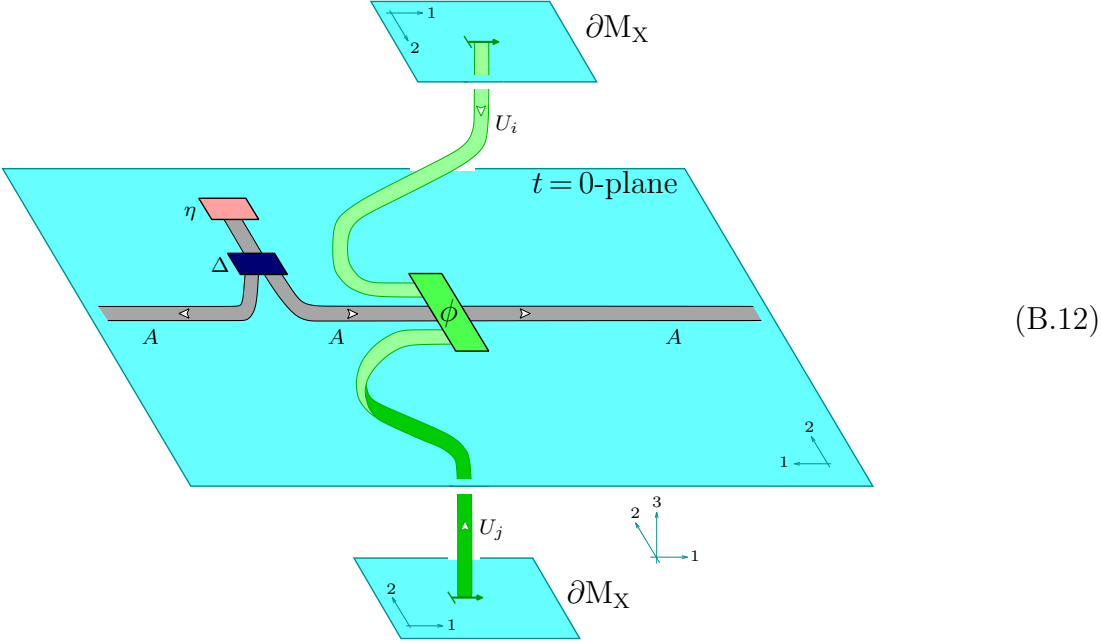


(B.11)



depending on the relative orientation of the arc-germ  $[\gamma]$  and the boundary  $\partial X$ , and such that bulk and boundary orientation indicated in the figure agree with those of  $X$ .

(ix) Let  $v$  be a two-valent vertex of  $T$  in the interior of  $X$  and let  $\Phi = (i, j, \phi, p, [\gamma], \text{or}_2(p))$  be the corresponding bulk insertion. Place the following fragment of ribbon graph at  $v$ :



This is done in such a way that the 2-orientation in the  $t=0$ -plane and the orientations of the arcs on  $\partial M_X$  are as indicated in the figure. (In the picture, the  $A$ -ribbons are viewed white side up).

Using the various properties of the category  $\mathcal{C}$  and of the algebra  $A$  (respectively,  $\tilde{A}$ ), one shows that the invariants of ribbon graphs arising from different choices in the prescription are the same. For choices #2–#4 this is explained in detail in [FRSI, FRSII]. Specifically, for choice #2 see sections II:3.1, IV:3.2 and IV:3.3, for choice #3 see section I:5.1, and for choice #4 sections I:5.1 and II:3.1. Regarding independence of the triangulation (choice #1), the corresponding argument has been indicated in [FRSI] (see (I:5.11) and (I:5.12)); the details are supplied in this paper in propositions 3.2 and 3.9 as part of the proof of modular invariance.

This completes the prescription for the ribbon graph in  $M_X$ . As already stated, the CFT correlator  $C(X)$  (standing for  $C_A$  or  $C_{\tilde{A}}$ , depending on whether we deal with the oriented or unoriented case) corresponding to the world sheet  $X$  (and algebra  $A$ , respectively  $\tilde{A}$ , in  $\mathcal{C}$ ), is  $C(X) = Z(M_X, \emptyset, \hat{X})1$ .

**B.4. EQUIVALENT LABELLINGS OF UNORIENTED WORLD SHEETS.**

Not all labellings of boundary conditions, boundary fields and bulk fields as described in definition B.2 lead to distinct correlators (i.e. to different vectors in  $\mathcal{H}(\hat{X})$ ). For example,

if two  $A$ -modules  $M$  and  $M'$  are isomorphic, then labelling a boundary condition by  $M$  or  $M'$  leads to the same correlator.

For unoriented world sheets, there is a less trivial relation between labellings of fields and boundary conditions which involves the change of the local orientation  $\text{or}_1$  of the boundary and the local orientation  $\text{or}_2$  around bulk insertions. To describe these equivalent labellings we need some additional ingredients.

For  $\tilde{A}$  a Jandl algebra and  $M$  a left  $\tilde{A}$ -module,  $M^\sigma$  will denote the conjugate left  $\tilde{A}$ -module as defined in (II:2.26). We will need, for any object  $V$  of  $\mathcal{C}$  and any two left  $\tilde{A}$ -modules  $M$  and  $N$ , a linear map  $s: \text{Hom}_{\tilde{A}}(M \otimes V, N) \rightarrow \text{Hom}_{\tilde{A}}(N^\sigma \otimes V, M^\sigma)$ ;  $s$  is given by

$$s(\psi) := \begin{array}{c} \begin{array}{c} M^\vee \\ \downarrow \\ \text{---} \\ \downarrow \\ \psi \\ \downarrow \\ N^\vee \end{array} \\ \text{---} \\ \downarrow \\ V \end{array} \quad (\text{B.13})$$

As has been shown in lemma IV:3.2, this is indeed a map of  $\tilde{A}$ -module morphisms. We also need, for any two objects  $U$  and  $V$  of  $\mathcal{C}$ , the vector space isomorphism

$$\omega_{UV}^{\tilde{A}}: \text{Hom}_{\tilde{A}\tilde{A}}(U \otimes^+ \tilde{A} \otimes^- V, \tilde{A}) \rightarrow \text{Hom}_{\tilde{A}\tilde{A}}(V \otimes^+ \tilde{A} \otimes^- U, \tilde{A}) \quad (\text{B.14})$$

defined as

$$\omega_{UV}^{\tilde{A}}(\phi) := \begin{array}{c} \tilde{A} \\ \downarrow \\ \sigma \\ \downarrow \\ \phi \\ \downarrow \\ \sigma^{-1} \\ \downarrow \\ V \quad \tilde{A} \quad U \end{array} \quad (\text{B.15})$$

It is shown in lemma IV:3.5 that  $\omega_{UV}^{\tilde{A}}$  is indeed a map of bimodule morphisms and that  $\omega_{VU}^{\tilde{A}} \circ \omega_{UV}^{\tilde{A}} = \text{id}$ .

Let now  $X$  be an unoriented world sheet and  $B$  be a connected component of  $\partial X$ . Passing along  $B$  in the direction opposite to  $\text{or}(\partial X)$  we obtain a list of labels for that boundary component

$$(M_1, \dots, M_{n'}; \Psi_1, \dots, \Psi_n; \text{or}_1), \quad (\text{B.16})$$

where  $M_1, \dots, M_{n'}$  are left  $\tilde{A}$ -modules,  $\Psi_k = (M_k, M_{k+1}, V_k, \psi_k, p_k, [\gamma_k])$  are boundary fields and  $\text{or}_1$  is the orientation of  $B$  induced by that of  $\partial X$ . The module  $M_k$  labels the segment of the boundary between the insertion points  $p_k$  and  $p_{k+1}$ . If  $n = 0$ , then  $n' = 1$ ; otherwise  $n' = n$ . Denote by  $X'$  the world sheet obtained by labelling the boundary component  $B$  not by (B.16) but by a different tuple  $(M'_1, \dots, M'_{n'}; \Psi'_1, \dots, \Psi'_{n'}; \text{or}'_1)$ . The following conditions guarantee that  $C_{\tilde{A}}(X) = C_{\tilde{A}}(X')$ .

- (i)  $\text{or}'_1 = \text{or}_1$ , and for every  $k \in \{1, 2, \dots, n\}$ ,  $V'_k = V_k$ ,  $[\gamma'_k] = [\gamma_k]$ , and there exist isomorphisms  $\varphi_k \in \text{Hom}_{\tilde{A}}(M'_k, M_k)$  such that

$$\psi_k = \varphi_{k+1} \circ \psi'_k \circ (\varphi_k^{-1} \otimes \text{id}_{V_k}). \quad (\text{B.17})$$

- (ii)  $\text{or}'_1 = -\text{or}_1$ , and for every  $k \in \{1, 2, \dots, n\}$ ,  $V'_k = V_{n-k}$ ,  $[\gamma'_k] = [\gamma_{n-k}]$ , and there exist isomorphisms  $\varphi_k \in \text{Hom}_{\tilde{A}}(M'_k, M_{n'-k+1}^\sigma)$  such that

$$s(\psi_{n-k}) = \begin{cases} \varphi_{k+1} \circ \psi'_k \circ (\varphi_k^{-1} \otimes \text{id}_{V'_k}) & \text{if } \text{or}'_1 = \text{or}(\gamma'_k), \\ \varphi_{k+1} \circ \psi'_k \circ (\varphi_k^{-1} \otimes \theta_{V'_k}) & \text{if } \text{or}'_1 = -\text{or}(\gamma'_k). \end{cases} \quad (\text{B.18})$$

Similarly, let  $\Phi = (i, j, \phi, p, [\gamma], \text{or}_2)$  be a bulk insertion of  $X$  and let  $X'$  the world sheet obtained by replacing the bulk field  $\Phi$  with

$$\Phi' = (j, i, \omega_{U_i U_j}^{\tilde{A}}(\phi), p, [\gamma], -\text{or}_2(p)), \quad (\text{B.19})$$

so that in particular the local orientation around the insertion point  $p$  is reversed. In this case one also finds  $C_{\tilde{A}}(X) = C_{\tilde{A}}(X')$ .

The equivalences for the bulk and boundary labellings outlined above are established in sections IV:3.2 and IV:3.3.

## C. Two-point correlators

In this appendix the two-point correlators on the disk and on the sphere are calculated, and it is shown that they are non-degenerate. In both cases the world sheet will be endowed with an orientation. When considering a disk or sphere without orientation, i.e. correlators  $C_{\tilde{A}}$ , then of the global orientation we retain just the local orientations around the field insertions, as well as for the boundary circle in the case of the disk.

### C.1. THE TWO-POINT CORRELATOR ON THE DISK.

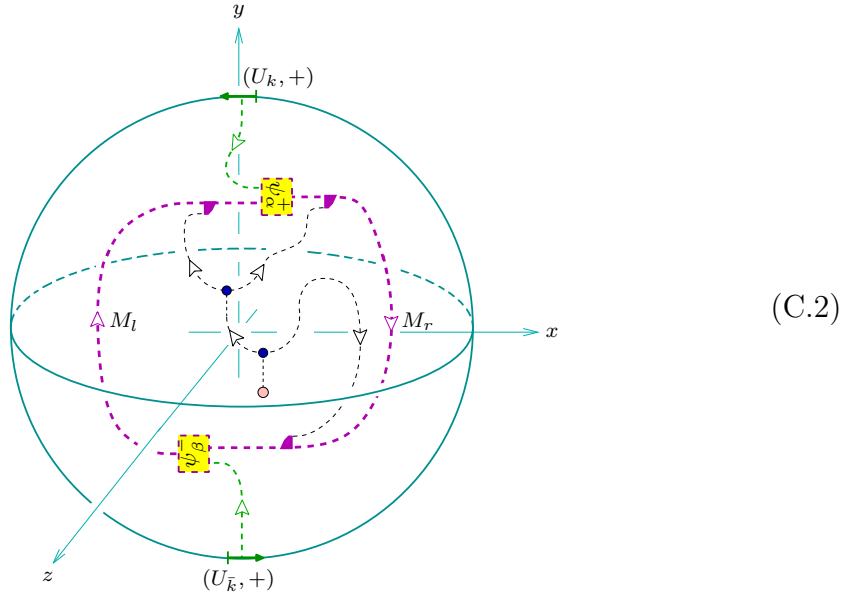
Here we present some properties of the correlator of two boundary fields on the disk, which enter the proof of boundary factorisation. The relevant world sheet is

$$X = D \equiv D(M_l, M_r, k, \psi_\alpha^+, \psi_\beta^-), \quad (\text{C.1})$$

as displayed in figure (2.22), with  $\psi_\alpha^+$  and  $\psi_\beta^-$  denoting elements of  $\text{Hom}_A(M_l \otimes U_k, M_r)$  and  $\text{Hom}_A(M_r \otimes U_{\bar{k}}, M_l)$ , respectively. Our aim is to obtain a ribbon graph that determines

the structure constants  $c_{M_l, M_r, k, \psi_\alpha^+, \psi_\beta^-}^{\text{bnd}}$  that are defined by formula (2.26). This is done by composing both sides of (2.26) with the cobordism  $\overline{B}_{k\bar{k}}^+ : \mathcal{H}(\widehat{D}) \rightarrow \emptyset$  that is defined as being dual to  $B_{k\bar{k}}^+$  in the sense that  $Z(\overline{B}_{k\bar{k}}^+) \circ Z(B_{k\bar{k}}^+)1 = 1$ .

The connecting manifold  $M_D$  is a three-ball, with boundary  $\partial M_D \cong \partial B_{k\bar{k}}^+$ . It contains an annular ribbon running along  $\iota(\partial D)$ , which in the region  $x < 0$  is labelled by the  $A$ -module  $M_l$ , and in the region  $x > 0$ , by  $M_r$ , the two parts being separated by coupons centered at  $p^+ = (0, 1, 0)$  and at  $p^- = -p^+$  and labelled by  $\psi_\alpha^+$  and  $\psi_\beta^-$ , respectively. In addition, to the coupon centered at  $p^+$  there is also attached a ribbon labelled by  $U_k$ , which ends on the marked arc  $\gamma^+$  on  $\partial M_D$  labelled by  $(U_k, +)$ . Similarly, to the other coupon there is attached a ribbon labelled by  $U_{\bar{k}}$ , ending on the other marked arc  $\gamma^-$  with label  $(U_{\bar{k}}, +)$ . Orientations and core-orientations of all ribbons are determined by the general prescription. We choose a minimal triangulation of  $\iota(D)$ , consisting of three edges ending on  $\iota(\partial D)$  at the points  $(-\cos \frac{2\pi a}{3}, \sin \frac{2\pi a}{3}, 0)$  with  $a = 0, 1, 2$ , and one vertex at  $(0, 0, 0)$ . This triangulation is covered by a combination of  $A$ -ribbons and coupons as explained in appendix B.3. The ‘white sides’ of all ribbons and coupons face the negative  $z$ -direction. Thus  $M_D$  looks as follows:



The various properties of  $A$  and its modules allow for a complete removal of the  $A$ -ribbons. This can be done as follows. First, the  $A$ -ribbon pointing down is moved upwards along  $M_r$ , and when approaching the next  $A$ -ribbon, the representation property is invoked. Coassociativity and specialness then remove that ribbon completely. The remaining  $A$ -ribbon is removed by first using the intertwining property of  $\psi_\alpha^+$ , then the representation property, and finally specialness and once more the representation unit property. Thus we arrive at the graph in (C.2), but with all  $A$ -ribbons removed; gluing  $\overline{B}_{k\bar{k}}^+$  to this

three-manifold then gives the graph (turned upside down with respect to (C.2))

$$(C.3)$$

(Recall from footnote 8 that the symbol  $S_n^3$  indicates the normalised invariant of a ribbon graph in  $S^3$ .) On the other hand, gluing  $\overline{B}_{k\bar{k}}^+$  to the right hand side of (2.26) we simply get

$$(C.4)$$

To proceed, it is convenient to rewrite the result in terms of elements of the morphism spaces  $\text{Hom}^{(P)}(U_{\bar{k}}, M_r^V \otimes M_l)$  and  $\text{Hom}^{(P)}(M_r^V \otimes M_l, U_{\bar{k}})$ , as defined in section 4.2. The isomorphisms (4.14) and (4.16) allow for an interpretation of the graph (C.3) as  $\text{tr}(e_\alpha \circ f_\beta)$ , or graphically,

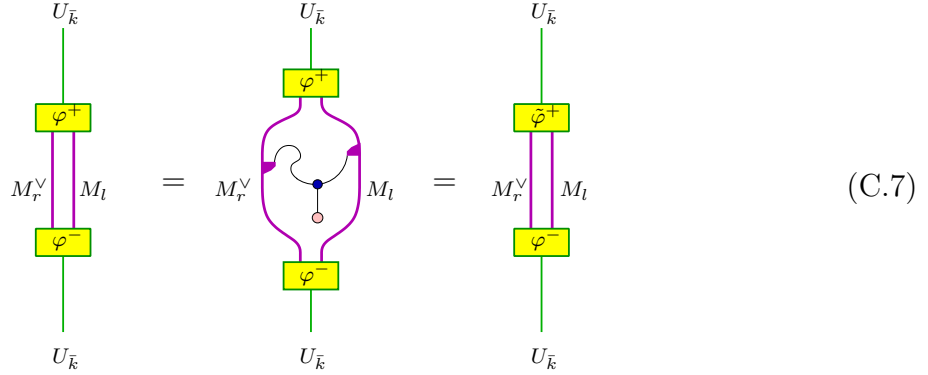
$$(C.5)$$

The morphisms  $e_\alpha$  and  $f_\beta$  are related to  $\psi_\alpha^+$  and  $\psi_\beta^-$  in the manner described in section 4.2.

Whenever the spaces  $\text{Hom}(U, V \otimes W)$  and  $\text{Hom}(V \otimes W, U)$  are non-zero for a simple object  $U$ , then the bilinear form  $\Lambda$  on  $\text{Hom}(U, V \otimes W) \times \text{Hom}(V \otimes W, U)$  defined by

$$(C.6)$$

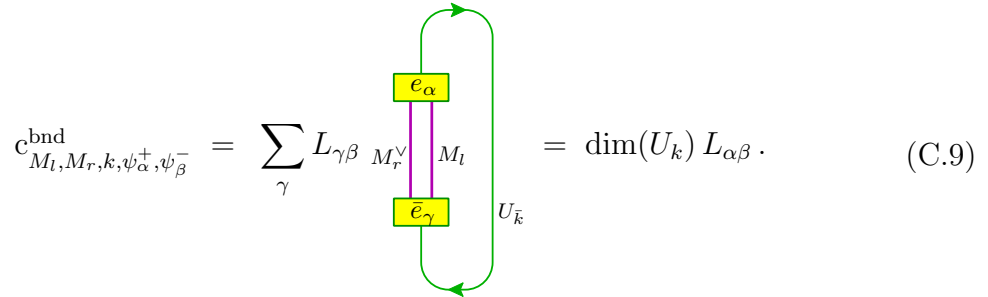
is non-degenerate (see e.g. [Tu]). We apply this result to the case  $U = U_{\bar{k}}$ ,  $V = \dot{M}_r^\vee$  and  $W = \dot{M}_l$ . Then the restriction of  $\Lambda$  to the subspace  $\text{Hom}^{(P)}(U_{\bar{k}}, M_r^\vee \otimes M_l) \times \text{Hom}^{(P)}(M_r^\vee \otimes M_l, U_{\bar{k}})$  is still non-degenerate. To see this, we note that for any object  $U$  and  $A$ -modules  $M$  and  $N$  we have  $P_{MN} \circ \varphi = \varphi$  for all  $\varphi \in \text{Hom}^{(P)}(M \otimes N, U)$ , and  $\psi \circ P_{MN} = \psi$  for all  $\psi \in \text{Hom}^{(P)}(U, M \otimes N)$ , and that the maps from  $\text{Hom}(M \otimes N, U)$  to  $\text{Hom}^{(P)}(M \otimes N, U)$  and from  $\text{Hom}(U, M \otimes N)$  to  $\text{Hom}^{(P)}(U, M \otimes N)$  that are obtained by composition with  $P_{MN}$  from the left and right, respectively, are surjective. As a consequence, for any two morphisms  $\varphi^- \in \text{Hom}^{(P)}(U_{\bar{k}}, M_r^\vee \otimes M_l)$  and  $\varphi^+ \in \text{Hom}(M_r^\vee \otimes M_l, U_{\bar{k}})$ , we have the equalities  $\varphi^+ \circ \varphi^- = \varphi^+ \circ (P_{M_r^\vee M_l} \circ \varphi^-) = \tilde{\varphi}^+ \circ \varphi^-$  with  $\tilde{\varphi}^+ := \varphi^+ \circ P_{M_r^\vee M_l}$ . In pictures,



Thus indeed  $\Lambda$  is non-degenerate also on these subspaces. As a consequence, given a basis  $\{e_\alpha\}$  of  $\text{Hom}^{(P)}(M_r^\vee \otimes M_l, U_{\bar{k}})$ , we can choose a dual basis  $\{\bar{e}_\beta\}$  of  $\text{Hom}^{(P)}(U_{\bar{k}}, M_r^\vee \otimes M_l)$ , such that  $\Lambda(e_\alpha, \bar{e}_\beta) = \delta_{\alpha,\beta}$ . Define the invertible square matrix  $L \equiv L(M_l, M_r, k)$  by

$$f_\beta =: \sum_{\gamma} L_{\gamma\beta} \bar{e}_\gamma. \quad (\text{C.8})$$

Let now  $\{\psi_\alpha^+\}$  and  $\{\psi_\beta^-\}$  denote bases of  $\text{Hom}_A(M_l \otimes U_k, M_r)$  and  $\text{Hom}_A(M_r \otimes U_{\bar{k}}, M_l)$ , respectively. Using the isomorphisms (4.14) and (4.16), we then get



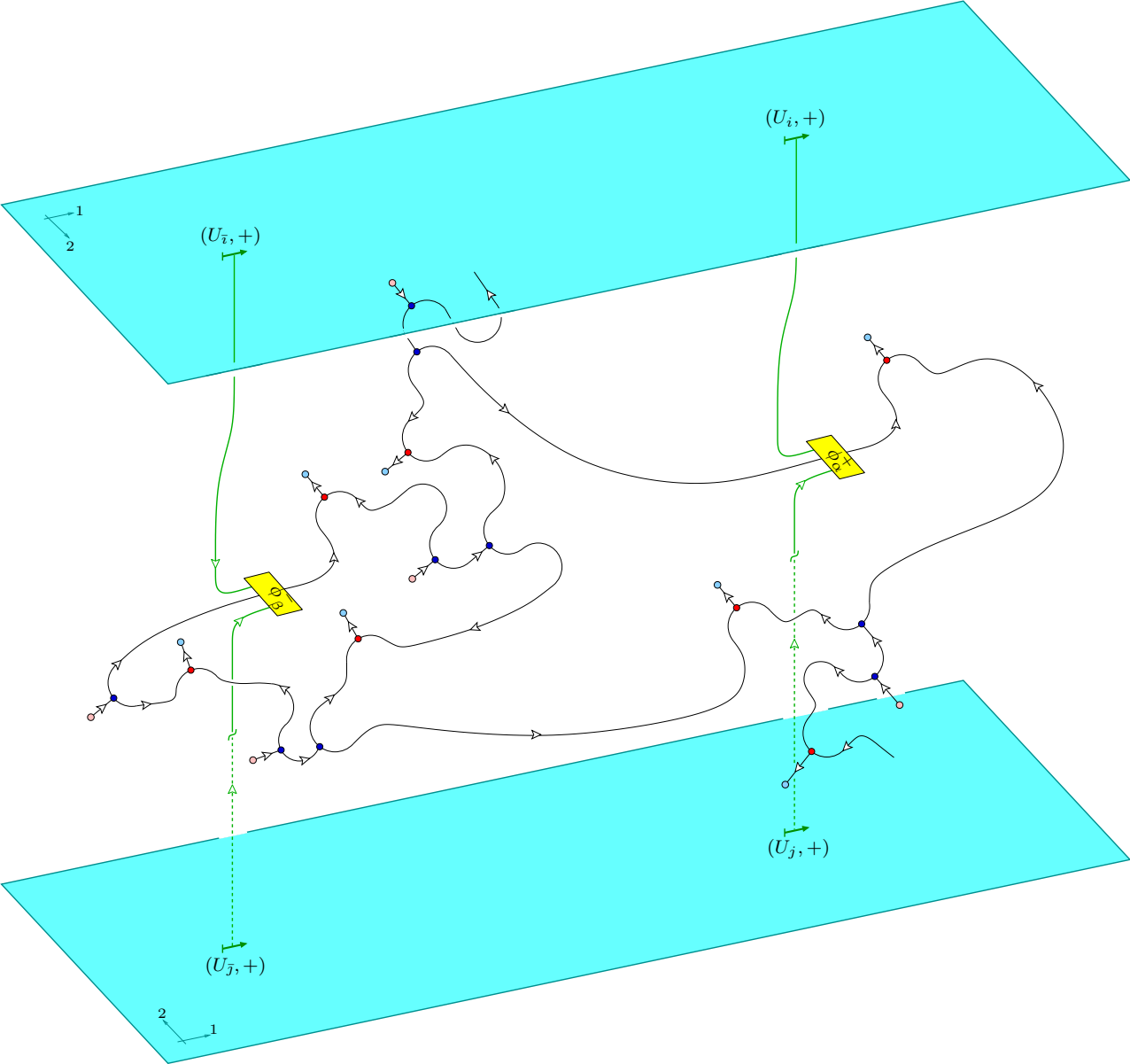
In particular, the matrix  $c_{M_l, M_r, k}^{\text{bnd}}$  is invertible.

## C.2. THE TWO-POINT CORRELATOR ON THE SPHERE.

Here we present the ribbon graph whose invariant gives the structure constants for the two-point correlator of bulk fields on the sphere  $S^2$ . We start with the world sheet

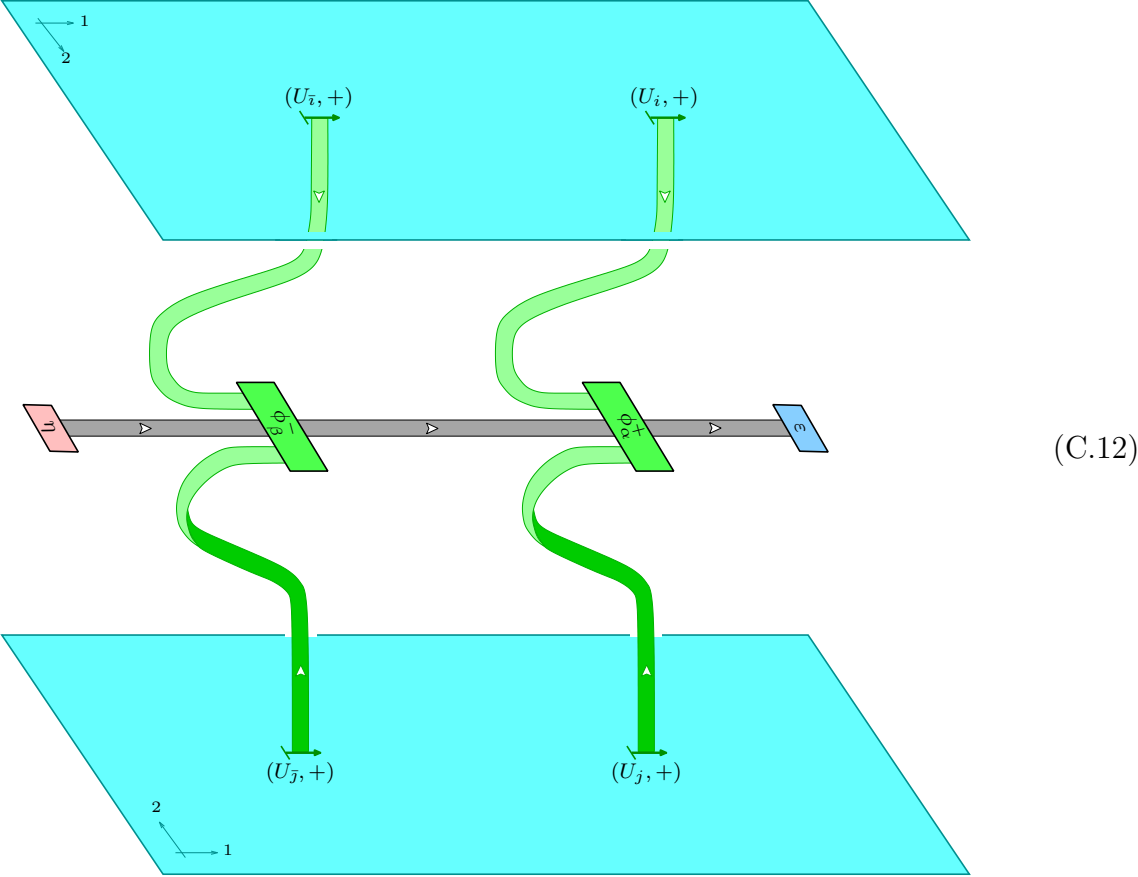
$$X = S \equiv S(i, j, \phi_\alpha^+, \phi_\beta^-) \quad (\text{C.10})$$

as defined in section 2.11. Its double  $\hat{S}$  is the disconnected sum of two spheres with two marked arcs each, differing in the labels of marked arcs and surface orientation. The identification of  $\hat{S}$  with  $S^2_{(2)} \sqcup S^2_{(2)}$  uses the map  $(x, y, z) \mapsto (x, -y, z)$  on one of the components. The connecting manifold  $M_S$  is embedded in  $\mathbb{R}^3$  as a cylinder over  $S^2_{(2)}$  centered at the origin. The parameter  $t$  in the construction of the connecting manifold is then identified with the distance from the origin, such that the boundary component carrying the marked points  $(U_j, +)$  and  $(U_{\bar{j}}, +)$  is located at  $t=1$ , while the component carrying  $(U_i, +)$  and  $(U_{\bar{i}}, +)$  resides at  $t=2$ . Straightening a part of the spherical shell to the plane, the connecting manifold is illustrated as



(C.11)

To insert  $A$ -ribbons in the embedded world sheet, we have chosen a triangulation in the following way. One edge runs along the equator of  $\iota(S)$ . Starting at the equator, another edge runs along a great circle through the coupon labelled by  $\phi_\alpha^+$  and continues until it hits the equator again. Similarly, for an edge running through the other coupon, but the start and end points on the equator are translated a small distance, so as to avoid four-valent vertices. This triangulation is covered by  $A$ -ribbons. In the picture, the two loose ends of  $A$ -ribbons are identified. A neater picture is obtained by using the specialness, symmetry and Frobenius properties of  $A$ , together with the intertwining properties of the bimodule morphisms; this allows us to remove a large portion of the covered triangulation. To simplify the picture further, the identity (D.19) is used. These manipulations result in



To determine the structure constants  $(c_{i,j}^{\text{bulk}})_{\alpha\beta}$  in (2.41), we compose the cobordism  $M_S$



with  $\overline{B}_{i\bar{i}}^+ \sqcup \overline{B}_{j\bar{j}}^+$ . The resulting cobordism is

$$\frac{1}{S_{0,0}} \text{ (Diagram) } \quad (\text{C.13})$$

Applying the same procedure also on the right hand side of (2.41), we arrive at the result

$$c_{ij,\alpha\beta}^{\text{bulk}} = \frac{1}{S_{0,0}} \text{ (Diagram) } \quad (\text{C.14})$$

for the structure constants of the bulk two-point correlator.

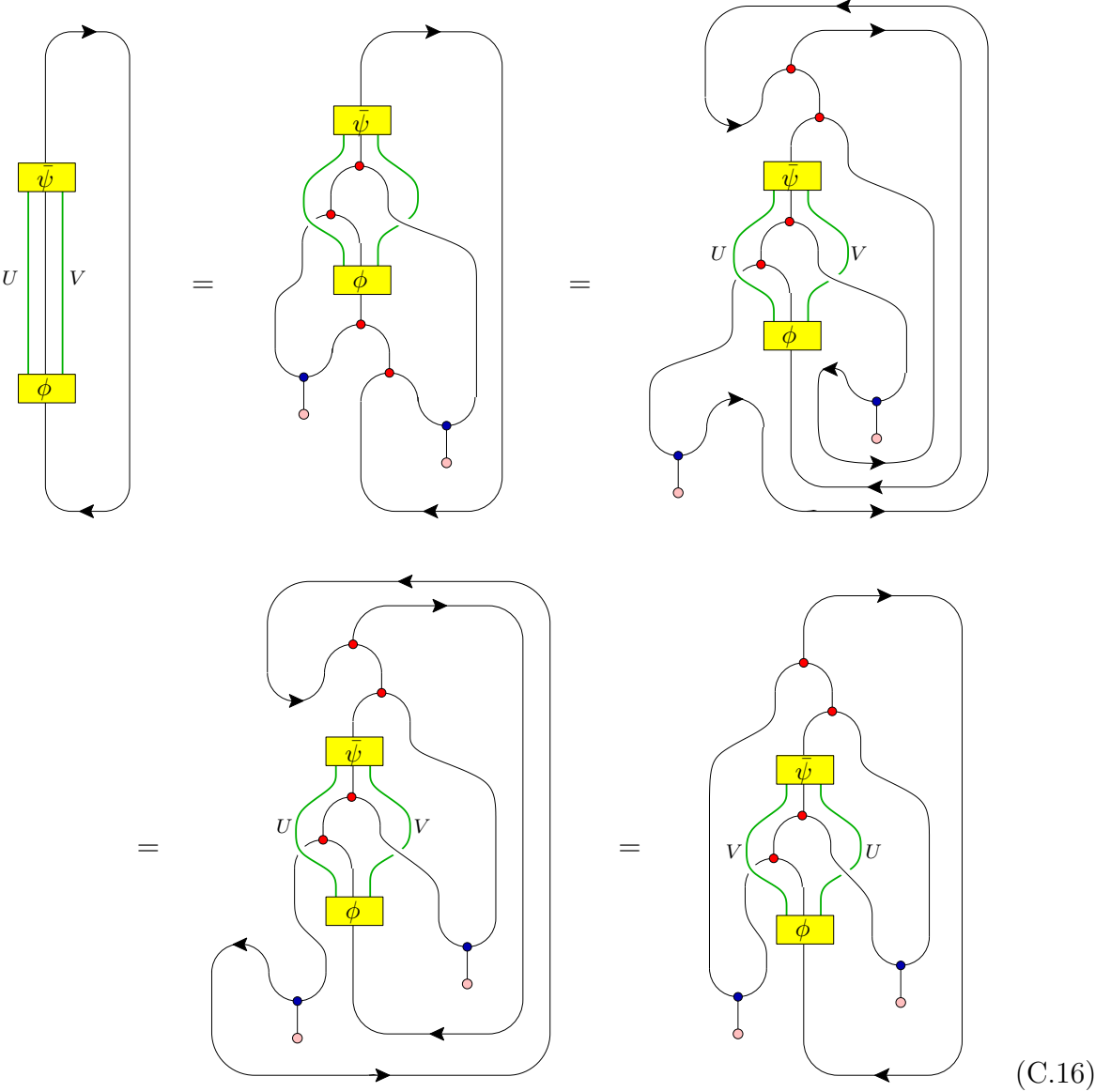
**C.3. LEMMA.** *The matrix  $c_{i,j}^{\text{bulk}}$  is non-degenerate.*

**PROOF.** The proof is similar to the proof of non-degeneracy for the two-point correlator on the disk. First, by setting

$$\text{tr}(\bar{\psi} \circ \varphi) =: \Lambda(\bar{\psi}, \varphi) \dim(A) \quad (\text{C.15})$$

for any  $\bar{\psi} \in \text{Hom}(U \otimes A \otimes V, A)$  and  $\varphi \in \text{Hom}(A, U \otimes A \otimes V)$ , we obtain a non-degenerate pairing  $\Lambda$  of the vector spaces  $\text{Hom}(A, U \otimes A \otimes V)$  and  $\text{Hom}(U \otimes A \otimes V, A)$ . To see that the restriction of  $\Lambda$  to the subspaces  $\text{Hom}_{A|A}(U \otimes^+ A \otimes^- V, A)$  and  $\text{Hom}_{A|A}(A, U \otimes^+ A \otimes^- V)$  is non-degenerate as well, take  $\varphi$  to be a bimodule morphism and consider the pairing with an arbitrary  $\bar{\psi}$ . The bimodule property allows for the insertion of a projector, and taking the trace of the composed morphisms allows to move the projector to the other

morphism. This is shown in the following picture:



Thus indeed  $\Lambda$  restricts non-degenerately to the bimodule morphisms. By using the identities (D.5) and (D.6), together with associativity, specialness and symmetry, it follows easily that  $\text{tr}(\bar{\psi} \circ \varphi) = \varepsilon \circ \bar{\psi} \circ \varphi \circ \eta$  when  $\varphi$  and  $\bar{\psi}$  are bimodule morphisms. This relates  $\Lambda$  to the graph (C.14), and hence  $c_{i,j}^{\text{bulk}}$  is non-degenerate. ■

### D. Some properties of (bimodule) morphisms

Here we list a few useful properties of some morphisms – mainly morphisms of  $A$ -bimodules – that appear in the proof of bulk factorisation and in the discussion of the two-point correlator on  $S^2$ .

First, the following results follow immediately by deformation of the graphs:

$$= 1 \tag{D.1}$$

and

$$= \theta_i^{-1} \circ \theta_i = 1. \tag{D.2}$$

Next we state

**D.1. LEMMA.** *Every  $\phi \in \text{Hom}_{A|A}(U \otimes^+ A \otimes^- V, A)$  satisfies*

- (i)  $\phi = m \circ (\phi \otimes id_A) \circ (id_U \otimes \eta \otimes c_{A,V}),$
  - (ii)  $\phi = m \circ (id_A \otimes \phi) \circ (c_{U,A} \otimes \eta \otimes id_V),$
  - (iii)  $\phi = ((\varepsilon \circ \phi \circ (id_U \otimes m \otimes id_V)) \otimes id_A) \circ (id_{U \otimes A} \otimes c_{A,V}^{-1} \otimes id_A) \circ (id_{U \otimes A \otimes V} \otimes (\Delta \circ \eta)),$
  - (iv)  $\phi = (id_A \otimes ((\varepsilon \circ \phi \circ (id_U \otimes m \otimes id_V)) \circ (id_A \otimes c_{U,A}^{-1} \otimes id_{A \otimes V})) \circ ((\Delta \circ \eta) \otimes id_{U \otimes A \otimes V}).$
- $$\tag{D.3}$$

*Analogous properties hold for  $\psi \in \text{Hom}_{A|A}(A, U \otimes^+ A \otimes^- V)$ .*

**PROOF.** (i, ii): Using the defining properties of  $\eta$  and the intertwining properties of  $\phi$  we have

$$\tag{D.4}$$

(iii, iv): Similarly, with the help of the counit and Frobenius properties one gets

(D.5)

The corresponding relations for  $\psi \in \text{Hom}_{A|A}(A, U \otimes^+ A \otimes^- V)$  follow analogously:

(D.6)

and

(D.7) ■

Applying these identities to coupons in the connecting manifold that are labelled by the respective bimodule morphisms, one can effectively move  $A$ -ribbons from one side of the coupon to the other and thereby substantially reduce the total number of ribbons in the connecting manifold (not counting the resulting ‘short’  $A$ -ribbons that directly connect a unit or co-unit coupon to coupons for bimodule morphisms).

For convenience, we also list a few special consequences of lemma D.1. Their proofs are elementary, involving essentially the same moves as the proof of the lemma, combined

with the symmetry of  $A$ .

Diagrammatic equation (D.8) showing transformations of a box labeled  $\phi$  with four legs labeled  $U, A, V, A$ . The sequence of diagrams is as follows:
 

- Diagram 1: Box  $\phi$  with legs  $U, A, V, A$ . A red dot is on the top  $A$  leg, and a blue dot is on the top  $U$  leg. Green lines connect the bottom  $U$  and  $V$  legs to the red dot.
- Diagram 2: Box  $\phi$  with legs  $U, A, V, A$ . A red dot is on the top  $A$  leg, and a blue dot is on the top  $U$  leg. A black line connects the top  $U$  leg to the red dot.
- Diagram 3: Box  $\phi$  with legs  $U, A, V, A$ . A red dot is on the top  $A$  leg, and a blue dot is on the top  $U$  leg. A black line connects the top  $U$  leg to the red dot, and another black line connects the red dot to the top  $A$  leg.
- Diagram 4: Box  $\phi$  with legs  $U, A, V, A$ . A red dot is on the top  $A$  leg, and a blue dot is on the top  $U$  leg. A black line connects the top  $U$  leg to the red dot, and another black line connects the red dot to the top  $U$  leg.
- Diagram 5: Box  $\phi$  with legs  $U, A, V, A$ . A red dot is on the top  $A$  leg, and a blue dot is on the top  $U$  leg. A black line connects the top  $U$  leg to the red dot, and another black line connects the red dot to the top  $A$  leg.

(D.8)

Diagrammatic equation (D.9) showing transformations of a box labeled  $\phi$  with four legs labeled  $A, U, A, V$ . The sequence of diagrams is as follows:
 

- Diagram 1: Box  $\phi$  with legs  $A, U, A, V$ . A red dot is on the top  $A$  leg, and a blue dot is on the top  $U$  leg. Green lines connect the bottom  $A$  and  $V$  legs to the red dot.
- Diagram 2: Box  $\phi$  with legs  $A, U, A, V$ . A red dot is on the top  $A$  leg, and a blue dot is on the top  $U$  leg. A black line connects the top  $U$  leg to the red dot.
- Diagram 3: Box  $\phi$  with legs  $A, U, A, V$ . A red dot is on the top  $A$  leg, and a blue dot is on the top  $U$  leg. A black line connects the top  $U$  leg to the red dot, and another black line connects the red dot to the top  $A$  leg.
- Diagram 4: Box  $\phi$  with legs  $A, U, A, V$ . A red dot is on the top  $A$  leg, and a blue dot is on the top  $U$  leg. A black line connects the top  $U$  leg to the red dot, and another black line connects the red dot to the top  $U$  leg.

(D.9)

Diagrammatic equation (D.10) showing transformations of a box labeled  $\psi$  with four legs labeled  $U, V, A, A$ . The sequence of diagrams is as follows:
 

- Diagram 1: Box  $\psi$  with legs  $U, V, A, A$ . A red dot is on the top  $A$  leg, and a blue dot is on the top  $U$  leg. Green lines connect the bottom  $U$  and  $V$  legs to the red dot.
- Diagram 2: Box  $\psi$  with legs  $U, V, A, A$ . A red dot is on the top  $A$  leg, and a blue dot is on the top  $U$  leg. A black line connects the top  $U$  leg to the red dot.
- Diagram 3: Box  $\psi$  with legs  $U, V, A, A$ . A red dot is on the top  $A$  leg, and a blue dot is on the top  $U$  leg. A black line connects the top  $U$  leg to the red dot, and another black line connects the red dot to the top  $A$  leg.
- Diagram 4: Box  $\psi$  with legs  $U, V, A, A$ . A red dot is on the top  $A$  leg, and a blue dot is on the top  $U$  leg. A black line connects the top  $U$  leg to the red dot, and another black line connects the red dot to the top  $U$  leg.

(D.10)

Diagrammatic equation (D.11) showing transformations of a box labeled  $\psi$  with four legs labeled  $U, V, A, A$ . The sequence of diagrams is as follows:
 

- Diagram 1: Box  $\psi$  with legs  $U, V, A, A$ . A red dot is on the top  $A$  leg, and a blue dot is on the top  $U$  leg. Green lines connect the bottom  $U$  and  $V$  legs to the red dot.
- Diagram 2: Box  $\psi$  with legs  $U, V, A, A$ . A red dot is on the top  $A$  leg, and a blue dot is on the top  $U$  leg. A black line connects the top  $U$  leg to the red dot.
- Diagram 3: Box  $\psi$  with legs  $U, V, A, A$ . A red dot is on the top  $A$  leg, and a blue dot is on the top  $U$  leg. A black line connects the top  $U$  leg to the red dot, and another black line connects the red dot to the top  $A$  leg.
- Diagram 4: Box  $\psi$  with legs  $U, V, A, A$ . A red dot is on the top  $A$  leg, and a blue dot is on the top  $U$  leg. A black line connects the top  $U$  leg to the red dot, and another black line connects the red dot to the top  $U$  leg.

(D.11)

(D.12)

(D.13)

(D.14)

(D.15)

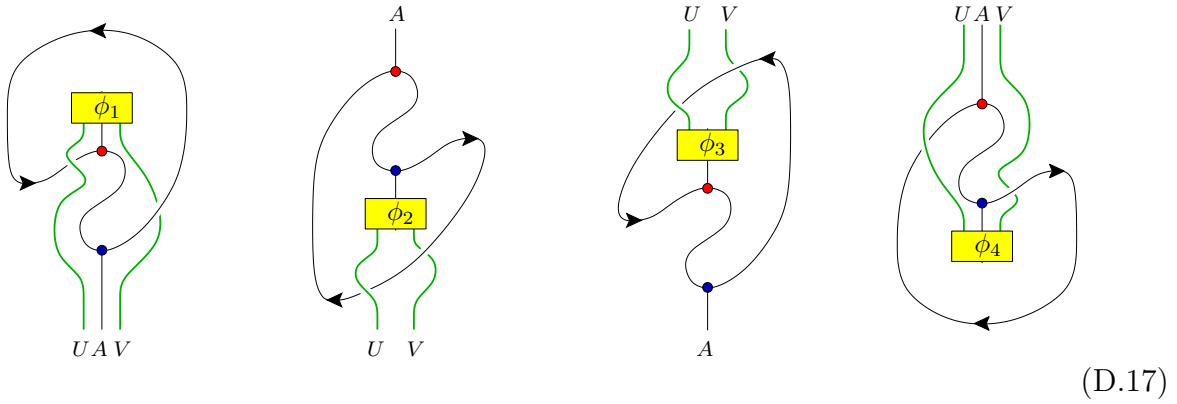
Recall from definition I:5.5 that a morphism  $\phi \in \text{Hom}(A \otimes U, V)$  is called a *local* morphism iff  $\phi \circ P_U = \phi$ , with  $P_U$  the idempotent defined in (I:5.34). Similarly, a morphism  $\phi \in \text{Hom}(V, A \otimes U)$  is called local iff  $P_U \circ \phi = \phi$ . Further, we can use the dualities of  $\mathcal{C}$  to obtain isomorphisms

$$\begin{aligned} \text{Hom}(A \otimes X, Y) &\cong \text{Hom}(Y^\vee \otimes A \otimes X, \mathbf{1}) \cong \text{Hom}(A, Y \otimes X^\vee) \quad \text{and} \\ \text{Hom}(Y, A \otimes X) &\cong \text{Hom}(\mathbf{1}, Y^\vee \otimes A \otimes X) \cong \text{Hom}(Y \otimes X^\vee, A). \end{aligned} \tag{D.16}$$

We refer to a morphism that via these isomorphisms is mapped to a local morphism in  $\text{Hom}(A \otimes X, Y)$  and  $\text{Hom}(Y, A \otimes X)$  again as being local. Local morphisms satisfy

properties analogous to those of bimodule morphisms given above (compare proposition I:5.7). Here we are interested in the following particular case.

**D.2. LEMMA.** *For  $\phi_1, \phi_2, \phi_3, \phi_4$  arbitrary morphisms in the vector spaces  $\text{Hom}(U \otimes A \otimes V, \mathbf{1})$ ,  $\text{Hom}(U \otimes V, A)$ ,  $\text{Hom}(A, U \otimes V)$  and  $\text{Hom}(\mathbf{1}, U \otimes A \otimes V)$ , respectively, the following morphisms are local morphisms in the respective spaces:*

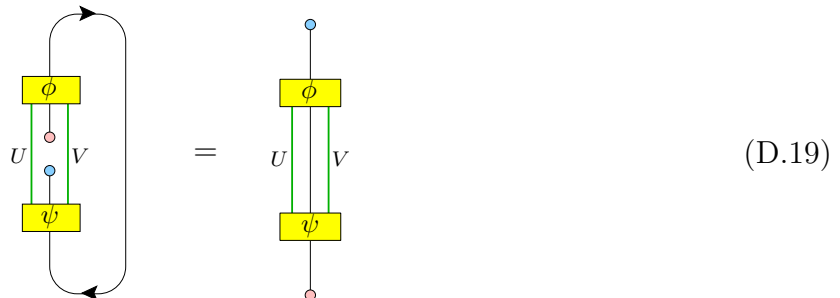


**PROOF.** The statement is a straightforward consequence of the fact that the morphisms corresponding to the closed  $A$ -loops in these pictures are idempotents, just as  $P_U$  in (I:5.34). The required manipulations are very similar to those in the proof of proposition I:5.7, and we refrain from spelling the out explicitly. ■

**D.3. LEMMA.** *For any pair of morphisms  $\phi \in \text{Hom}_{A|A}(U \otimes^+ A \otimes^- V, A)$  and  $\psi \in \text{Hom}_{A|A}(A, U \otimes^+ A \otimes^- V)$  we have*

$$\text{tr}(\phi \circ (\text{id}_U \otimes (\eta \circ \varepsilon) \otimes \text{id}_V) \circ \psi) = \varepsilon \circ \phi \circ \psi \circ \eta. \tag{D.18}$$

*Graphically,*



PROOF. The following equalities hold:

$$= \quad = \quad = \quad = \quad (D.20)$$

The first step follows from lemma D.1(iii) and the first identity in (D.6), the second step uses the unit property and symmetry, and the final equality follows by the unit, counit and Frobenius properties. ■

Next we define two linear maps

$$f: \text{Hom}_{A|A}(U_i \otimes^+ A \otimes^- U_j, A) \rightarrow \text{Hom}_{A|A}(A, U_i \otimes^+ A \otimes^- U_j) \quad (D.21)$$

and

$$g: \text{Hom}_{A|A}(A, U_i \otimes^+ A \otimes^- U_j) \rightarrow \text{Hom}_{A|A}(U_i \otimes^+ A \otimes^- U_j, A) \quad (D.22)$$

by

$$:= \quad := \quad := \quad (D.23)$$

D.4. LEMMA. *The functions  $f$  and  $g$  satisfy*

$$g \circ f = \frac{1}{\dim(U_i) \dim(U_j)} \text{id}_{\text{Hom}_{A|A}(U_i \otimes^+ A \otimes^- U_j, A)} \quad \text{and} \quad (D.24)$$

$$f \circ g = \frac{1}{\dim(U_i) \dim(U_j)} \text{id}_{\text{Hom}_{A|A}(A, U_i \otimes^+ A \otimes^- U_j)},$$

PROOF. The composition  $g \circ f$  applied to a bimodule morphism  $\phi$  gives



$$(D.25)$$

where the small coupons stand for the morphisms  $\lambda_{i\bar{i}}$  and  $\bar{\lambda}^{i\bar{i}}$  (respectively  $\lambda_{j\bar{j}}$  and  $\bar{\lambda}^{j\bar{j}}$ ) which were defined in (2.25). Since  $U_i$  and  $U_j$  are simple objects, we have

$$(D.26)$$

for some scalars  $\mu_i$  and  $\nu_j$ . By taking the trace on both sides of the equalities, simple manipulations show  $\mu_i = \dim(U_i)^{-1} = \nu_j$ . Similar manipulations give the result for  $f \circ g$ . ■

It is useful to express this lemma in terms of specific bases. Let us select bases  $\{\phi_\alpha^{ij}\}$  of  $\text{Hom}_{A|A}(U_i \otimes^+ A \otimes^- U_j, A)$  and  $\{\bar{\phi}_\alpha^{ij}\}$  of  $\text{Hom}_{A|A}(A, U_i \otimes^+ A \otimes^- U_j)$  that are dual in the sense of (5.21). Define matrices  $\Delta$  and  $\Omega$  by

$$f(\phi_\alpha^{ij}) = \sum_\gamma \Delta_{\alpha\gamma} \bar{\phi}_\gamma^{ij}, \quad g(\bar{\phi}_\alpha^{ij}) = \sum_\gamma \Omega_{\alpha\gamma} \phi_\gamma^{ij}. \quad (D.27)$$

In terms of these matrices, lemma D.4 takes the form

$$\sum_\gamma \Delta_{\alpha\gamma} \Omega_{\gamma\beta} = \sum_\gamma \Omega_{\alpha\gamma} \Delta_{\gamma\beta} = \frac{1}{\dim(U_i) \dim(U_j)} \delta_{\alpha,\beta}, \quad (D.28)$$

thus showing that  $\dim(U_i) \dim(U_j) \Omega = \Delta^{-1}$ .

## References

- [BK] B. Bakalov and A.A. Kirillov, *Lectures on Tensor Categories and Modular Functors* (American Mathematical Society, Providence 2001)
- [BS] M. Bianchi and A. Sagnotti, *Open strings and the relative modular group*, Phys. Lett. B 231 (1989) 389–396
- [CL] J.L. Cardy and D.C. Lewellen, *Bulk and boundary operators in conformal field theory*, Phys. Lett. B 259 (1991) 274–278
- [FFFS1] G. Felder, J. Fröhlich, J. Fuchs, and C. Schweigert, *Conformal boundary conditions and three-dimensional topological field theory*, Phys. Rev. Lett. 84 (2000) 1659–1662 [[hep-th/9909140](#)]
- [FFFS2] G. Felder, J. Fröhlich, J. Fuchs, and C. Schweigert, *Correlation functions and boundary conditions in RCFT and three-dimensional topology*, Compos. Math. 131 (2002) 189–237 [[hep-th/9912239](#)]
- [FPS] D. Fioravanti, G. Pradisi, and A. Sagnotti, *Sewing constraints and non-orientable strings*, Phys. Lett. B 321 (1994) 349–354 [[hep-th/9311183](#)]
- [FB] E. Frenkel and D. Ben-Zvi, *Vertex Algebras and Algebraic Curves*, second edition (American Mathematical Society, Providence, 2004) [[www.math.berkeley.edu/~frenkel/BOOK](#)]
- [FFRS] J. Fröhlich, J. Fuchs, I. Runkel, and C. Schweigert, *Correspondences of ribbon categories*, Adv. Math. 199 (2006) 192–329 [[math.CT/0309465](#)]
- [FRS 0] J. Fuchs, I. Runkel, and C. Schweigert, *Conformal correlation functions, Frobenius algebras and triangulations*, Nucl. Phys. B 624 (2002) 452–468 [[hep-th/0110133](#)]
- [FRS I] J. Fuchs, I. Runkel, and C. Schweigert, *TFT construction of RCFT correlators I: Partition functions*, Nucl. Phys. B 646 (2002) 353–497 [[hep-th/0204148](#)]
- [FRS II] J. Fuchs, I. Runkel, and C. Schweigert, *TFT construction of RCFT correlators II: Unoriented world sheets*, Nucl. Phys. B 678 (2004) 511–637 [[hep-th/0306164](#)]
- [FRS III] J. Fuchs, I. Runkel, and C. Schweigert, *TFT construction of RCFT correlators III: Simple currents*, Nucl. Phys. B 694 (2004) 277–353 [[hep-th/0403157](#)]
- [FRS IV] J. Fuchs, I. Runkel, and C. Schweigert, *TFT construction of RCFT correlators IV: Structure constants and correlation functions*, Nucl. Phys. B 715 (2005) 539–638 [[hep-th/0412290](#)]

- [FHK] M. Fukuma, S. Hosono, and H. Kawai, *Lattice topological field theory in two dimensions*, Commun. Math. Phys. 161 (1994) 157–175 [hep-th/9212154]
- [JS] A. Joyal and R. Street, *The geometry of tensor calculus, I*, Adv. Math. 88 (1991) 55–112
- [Ka] C. Kassel, *Quantum Groups* (Springer Verlag, New York 1995)
- [KRT] C. Kassel, M. Rosso, and V. Turaev, *Quantum Groups and Knot Invariants* (Soc. Math. de France, Paris 1997)
- [KM] V. Karimipour and A. Mostafazadeh, *Lattice topological field theory on non-orientable surfaces*, J. Math. Phys. 38 (1997) 49–66 [hep-th/9508041]
- [Le] D.C. Lewellen, *Sewing constraints for conformal field theories on surfaces with boundaries*, Nucl. Phys. B 372 (1992) 654–682
- [Ma] S. Mac Lane, *Categories for the Working Mathematician* (Springer Verlag, New York 1971)
- [Mj] S. Majid, *Foundations of Quantum Group Theory* (Cambridge University Press, Cambridge 1995)
- [Qu] F. Quinn, *Group categories and their field theories*, Geom. and Topol. Monogr. 2 (1998) 407–453 [math.GT/9811047]
- [S1] H. Sonoda, *Sewing conformal field theories*, Nucl. Phys. B 311 (1988) 401–416
- [S2] H. Sonoda, *Sewing conformal field theories 2*, Nucl. Phys. B 311 (1988) 417–432
- [Tu] V.G. Turaev, *Quantum Invariants of Knots and 3-Manifolds* (de Gruyter, New York 1994)
- [TV] V.G. Turaev and O. Viro, *State sum invariants of 3-manifolds and quantum 6j-symbols*, Topology 31 (1992) 865–902

*Fachbereich Mathematik, Universität Hamburg Schwerpunkt Algebra und Zahlentheorie, and Zentrum für mathematische Physik, Bundesstraße 55, D-20 146 Hamburg*

*Institutionen för fysik, Karlstads Universitet, Universitetsgatan 5, S-651 88 Karlstad*

*Max-Planck-Institut für Gravitationsphysik, Albert-Einstein-Institut, Am Mühlenberg 1, D-14 476 Golm*

*Fachbereich Mathematik, Universität Hamburg Schwerpunkt Algebra und Zahlentheorie, and Zentrum für mathematische Physik, Bundesstraße 55, D-20 146 Hamburg*

Email: jens.fjelstad@kau.se  
 jfuchs@fuchs.tekn.kau.se  
 ingo.runkel@kcl.ac.uk  
 schweigert@math.uni-hamburg.de